Figure 4-74. Sediment from south quadrant of tank after Test #1.

Figure 4-75. SEM overview image, magnified 40 times, of a Test #1, Day 30, sediment sample.

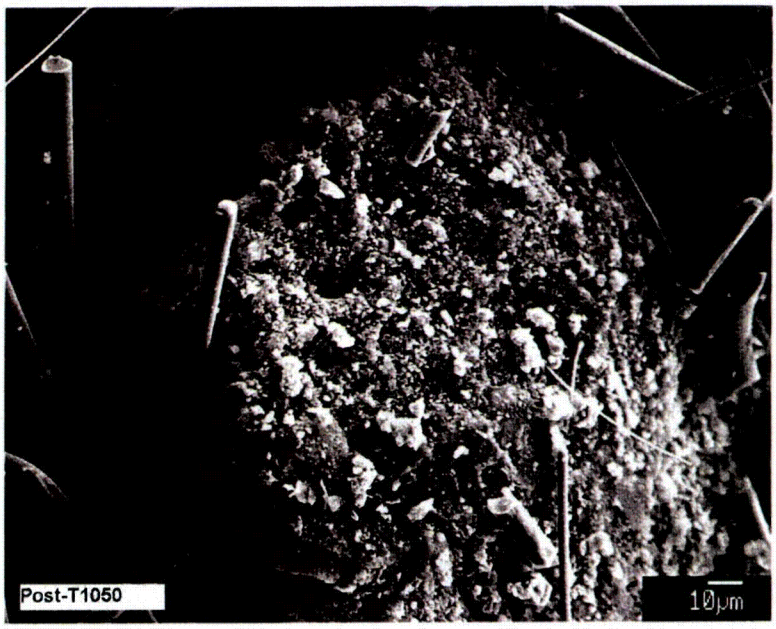

Figure 4-76. SEM image with a higher magnification on a Test #1, Day 30, sediment sample.

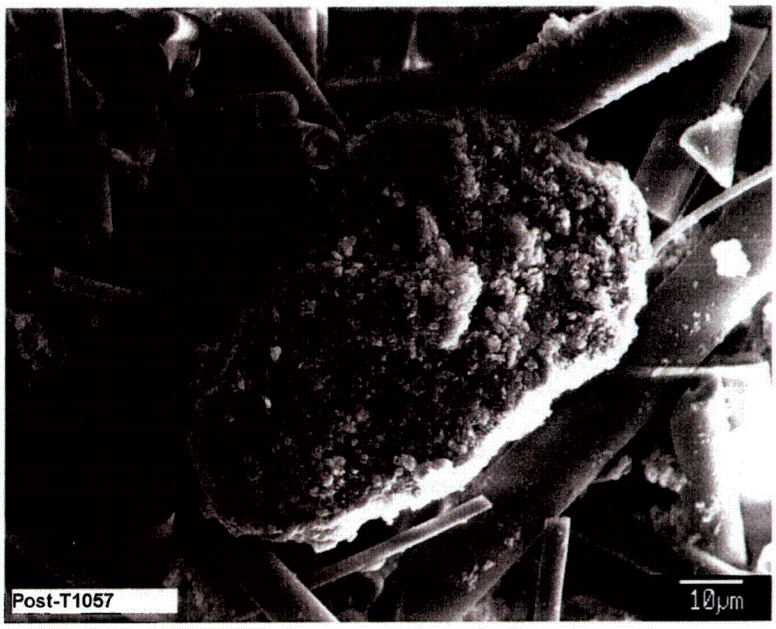

Figure 4-77. SEM image, magnified 1000 times, of a Test #1, Day 30, sediment sample.

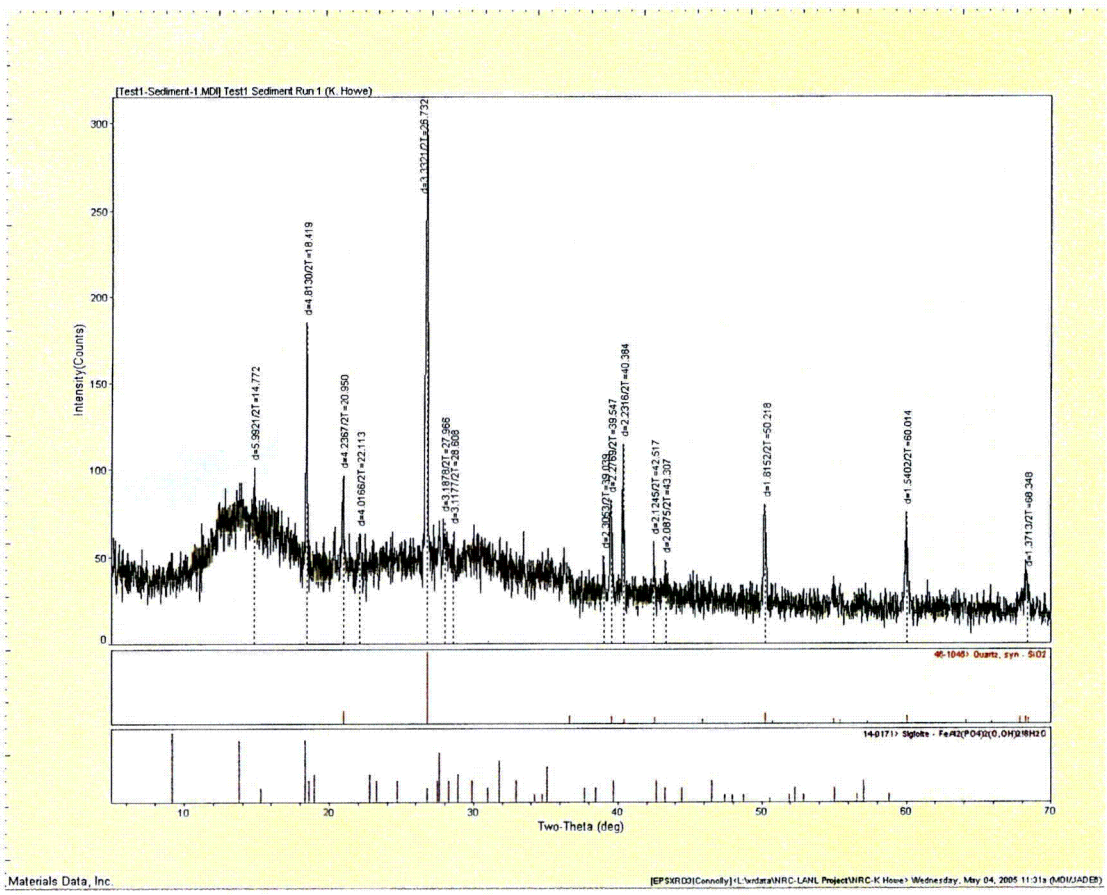

Figure 4-78. XRD result on a Test #1, Day 30, mixed-sediment sample.

4.3.2. Test #2 Sediment

In Test #2, the latent debris and crushed concrete material were observed to settle completely on the bottom of the tank over the course of several days. This particulate, in combination with fugitive fiberglass debris, forms the basic substrate of the sediment layer recovered from the tank at the end of Test #2. A total of 256 g of wet sediment was recovered from the tank following the test. Figure 4-79 shows a photo of a Test #2, Day 30, sediment sample, which is composed of particulate deposits and fiberglass debris. Figures 4-80, 4-81, and 4-82 show SEM images and EDS spectra of Test #2 sediment samples. Because of the heterogeneous nature of the sediment, this sediment is likely composed of corrosion products, concrete debris, dirt, and fiberglass. As in Test #1, the highest elemental content of the Test #2 sediment was silicon (Table 4-6), which likely came from the fiberglass debris. The ratio of dry to moist sediment mass was determined to be 0.5, which is consistent with the ratio found for the Test #1 sediment.

Figure 4-79. Picture of a Test #2, Day 30, sediment sample.

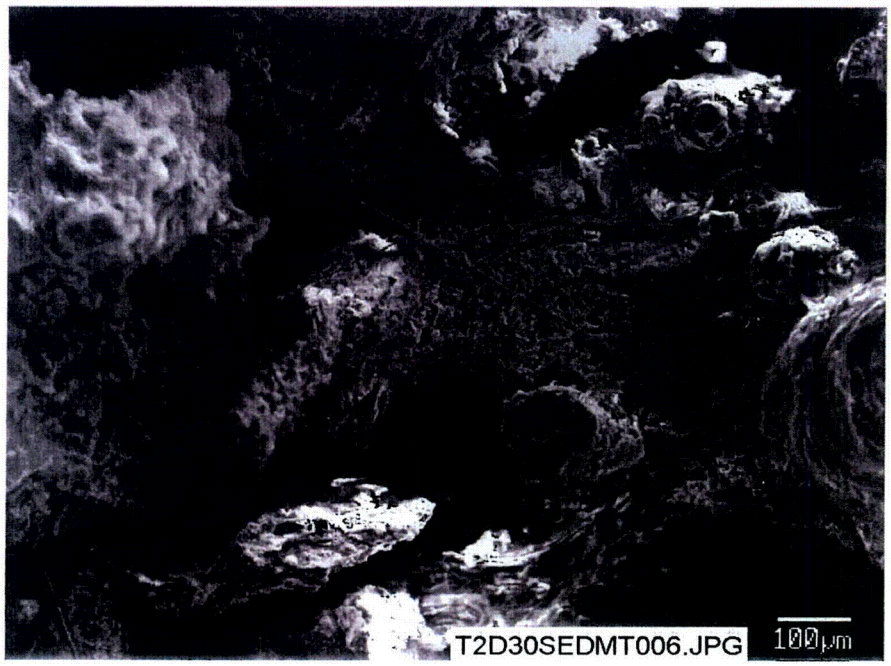

Figure 4-80. SEM image of a Test #2, Day 30, sediment sample.

Figures 4-81 and 4-82 provide a higher magnification and an EDS spectrum of the same Test #2 sediment shown in Figure 4-80. Underlying fibers are visible in this image, and the dominant elemental constituents of the particulate deposits are oxygen, magnesium, phosphorus, calcium, aluminum, silicon, carbon, and zinc. The XRD result of Test #2 sediment is shown in Figure 4-83. Again, the presence of quartz is consistent with the fiberglass debris in the sediment.

Figure 4-81. Higher-magnification SEM image of a Test #2, Day 30, sediment sample.

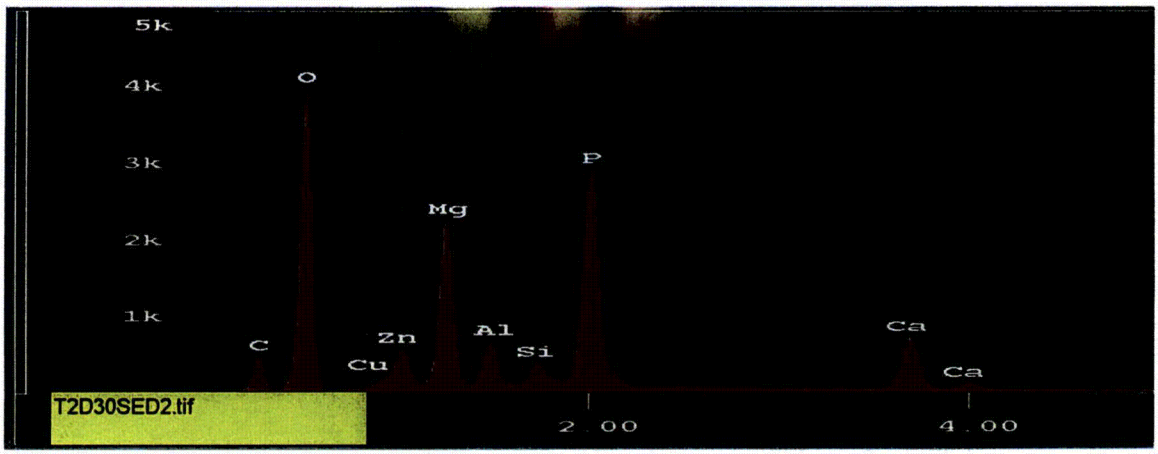

Figure 4-82. EDS counting spectrum for the porously structured material shown in Figure 4-81.

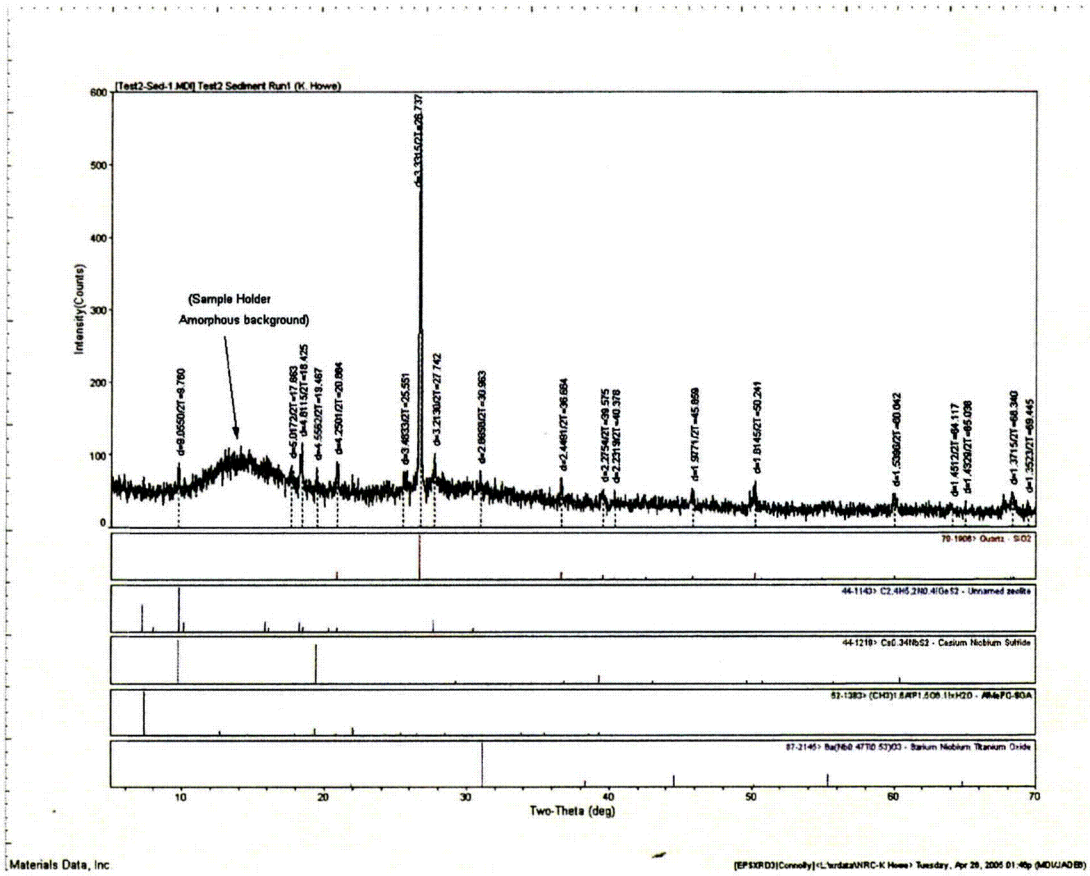

Figure 4-83. XRD results for Test #2, Day 30, mixed sediment.

Test #3 Sediment

Eighty percent of the fiberglass was replaced by cal-sil in Test #3. As a result, the cal-sil debris contributed significantly to the sediment, as shown in Figure 4-84, which is a photograph of the Test #3 sediment extracted from the bottom of the tank. The pink and yellow particles seen in the sediment correspond to baked and unbaked cal-sil. Over 78 kg of wet sediment were recovered

from the tank following the test (approximately 20 kg of dry cal-sil dust was initially added to the tank).

ESEM/EDS results for pink and yellow sediment are shown in Figures 4-85, 4-86, 4-87, and 4-88. No significant difference was found regarding the composition of the pink and yellow sediments; both of them were composed mainly of oxygen, silicon, calcium, aluminum, sodium, magnesium, iron, boron, and carbon. Comparing the EDS results of the yellow and pink sediment with the unbaked and baked cal-sil samples, respectively, both yellow and pink sediments are of higher content of oxygen. Since the yellow and pink sediments from Test #3 were analyzed with ESEM (the sediment samples were wet), and the unbaked and baked cal-sil samples were dry and analyzed with the probe SEM, the higher oxygen content in the sediment samples was likely from water.

Figure 4-84. Sediment removed from the tank after Test #3.

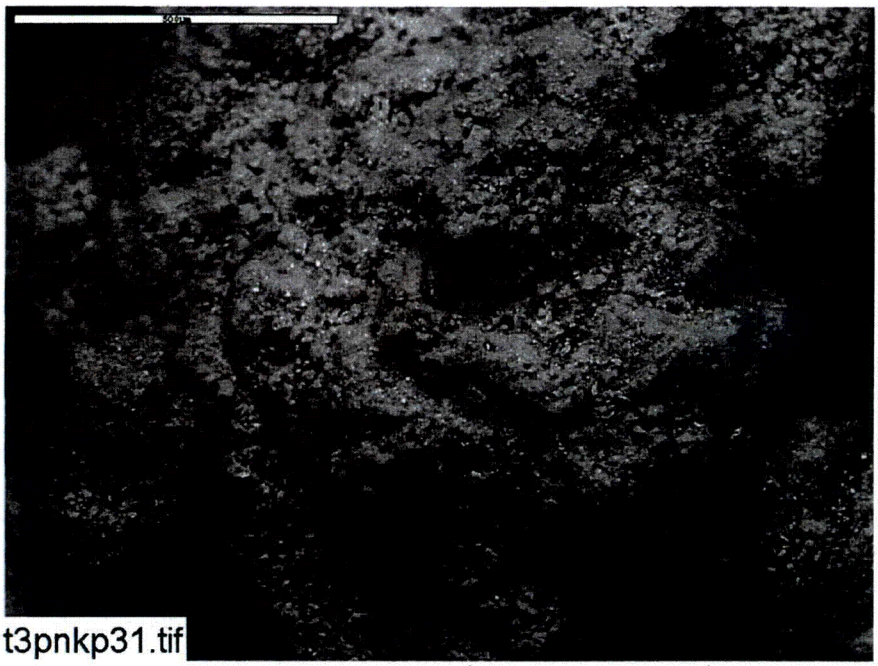

Figure 4-85. ESEM image of a Test #3, Day 30, pink sediment, magnified 100 times. (t3pnkp31, 5/6/05)

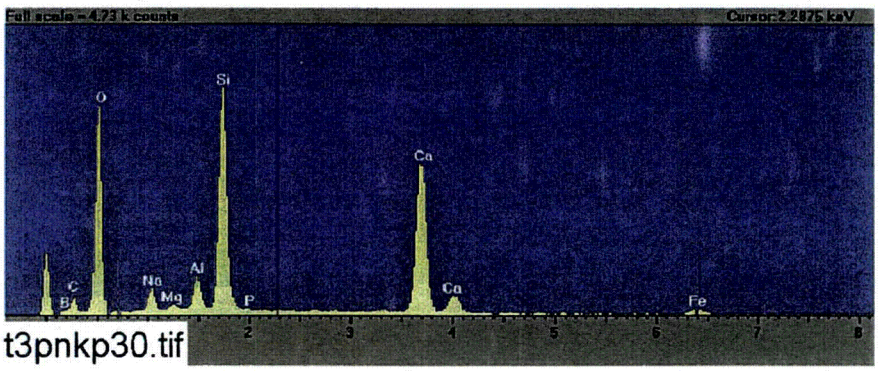

Figure 4-86. EDS counting spectrum for the pink sediment shown in Figure 4-85. (t3pnkp30, 5/6/05)

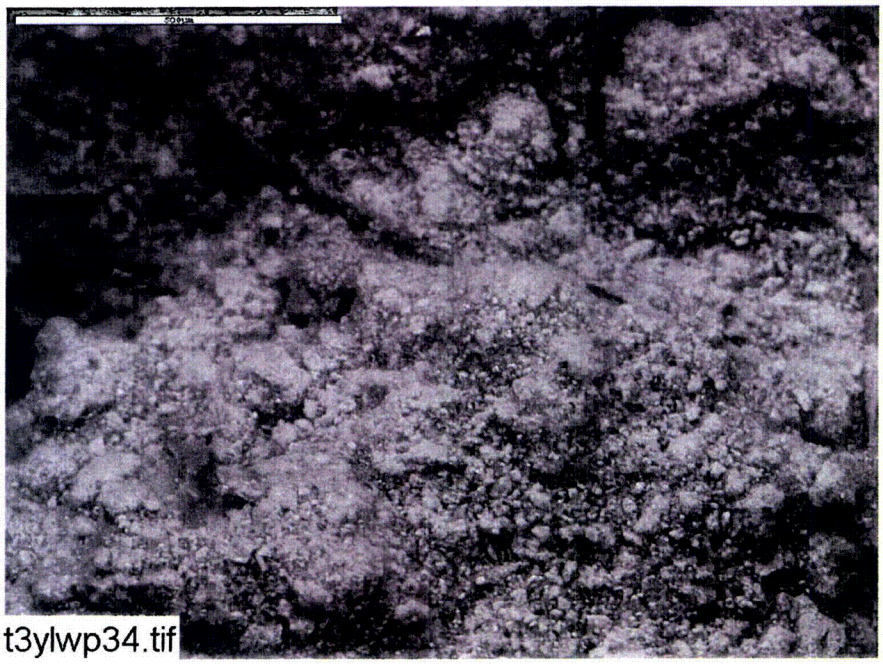

Figure 4-87. ESEM image of a Test #3, Day 30, yellow sediment, magnified 100 times. (t3ylwp34, 5/6/05)

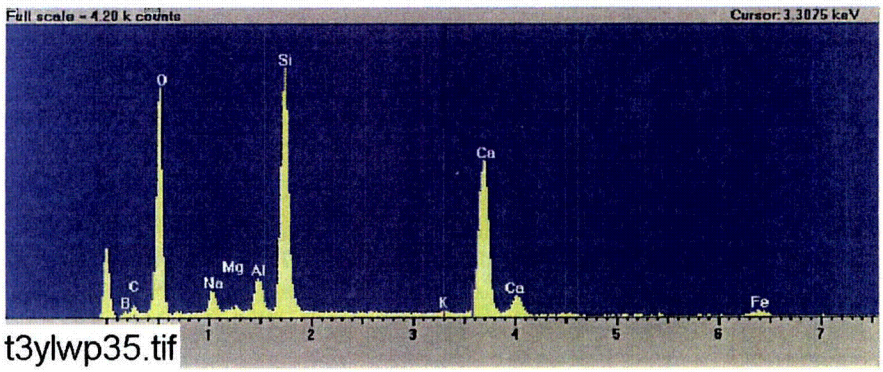

Figure 4-88. EDS counting spectrum for the particles shown in Figure 4-87. (t3ylwp35, 5/6/05)

The XRD results in Figure 4-89 indicate the sediment contained crystalline calcite ($CaCO_3$), tobermorite [$Ca_{2.25}(Si_3O_{7.5}(OH)_{1.5})(H_2O)$, and $Ca_4(Si_6O_{15}(OH)_2)(H_2O)_5$], which is consistent with the XRD results of unused baked and unused unbaked cal-sil samples (see Section 4.2.2). This result suggests that cal-sil debris contributed greatly to the sediment of Test #3, including both unbaked and baked cal-sil. It should be noted that other deposits, such as fiberglass debris and corrosion products, may also be present in the sediment.

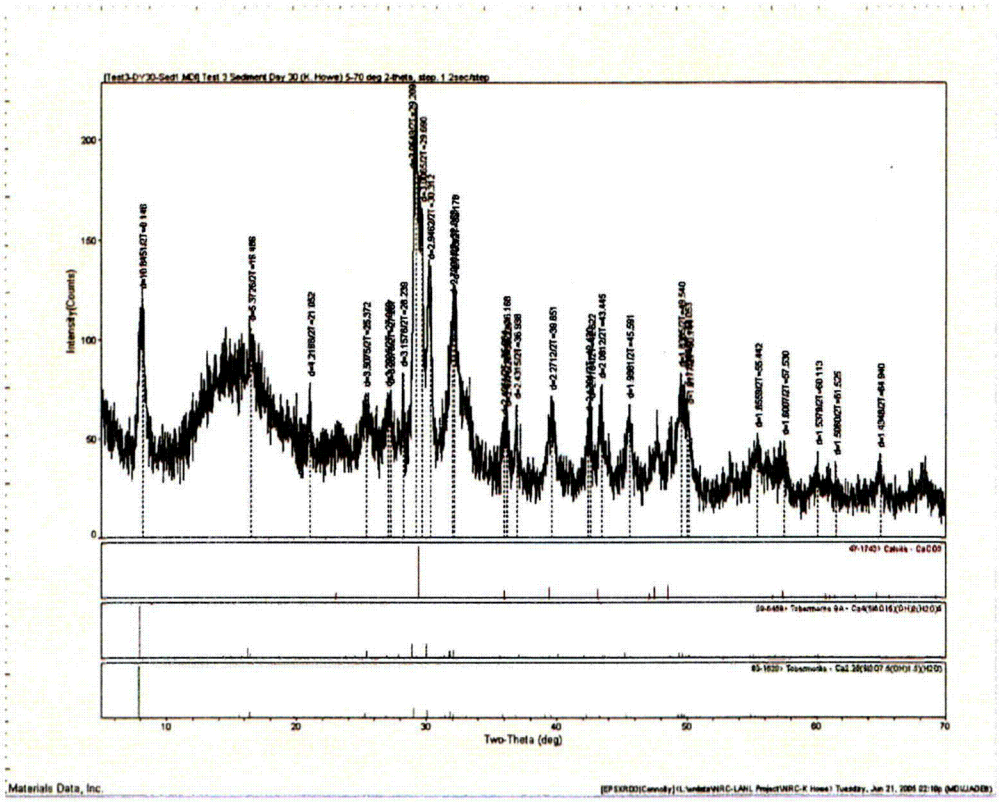

Figure 4-89. XRD results for the Test #3, Day 30, mixed sediment.

Test #4 Sediment

As in Test #3, 80% of the fiberglass was replaced by cal-sil in Test #4. Over 86 kg of wet sediment were recovered from the tank following the test (approximately 20 kg of dry cal-sil dust was initially added to the tank). Figure 4-90 shows a photograph of the sediment, which appears to be composed mainly of cal-sil debris. The SEM/EDS and XRD analysis provided information on the morphology and composition of Test #4 sediments, as shown in Figures 4-91, 4-92, 4-93, and 4-94. EDS results show that more than 84% of the sediment was composed of silicon, calcium, and oxygen. Similarly, the XRF results in Table 4-6 show that Si and Ca are the major elements in the composition of the sediment (oxygen is not detectable by XRF), plus small amounts of Na, Al, Fe, and Mg.

Based on the XRD results in Figure 4-94, the sediment sample contained crystalline substances of tobermorite [$Ca_{2.25}(Si_3O_{7.5}(OH)_{1.5})(H_2O)$ and $Ca_4(Si_6O_{15}(OH)_2)(H_2O)_5$], as well as calcite ($CaCO_3$), which were also in the unused unbaked or unused baked cal-sil samples. Considering the collective evidence from the EDS, XRF, and XRD analyses, it is likely that the sediment was composed of a significant amount of cal-sil debris, including both baked and unbaked cal-sil. It should be noted that other deposits, such as fiberglass debris and corrosion products, may also be present in the sediment.

Figure 4-90. Sediment removed from the tank after Test #4.

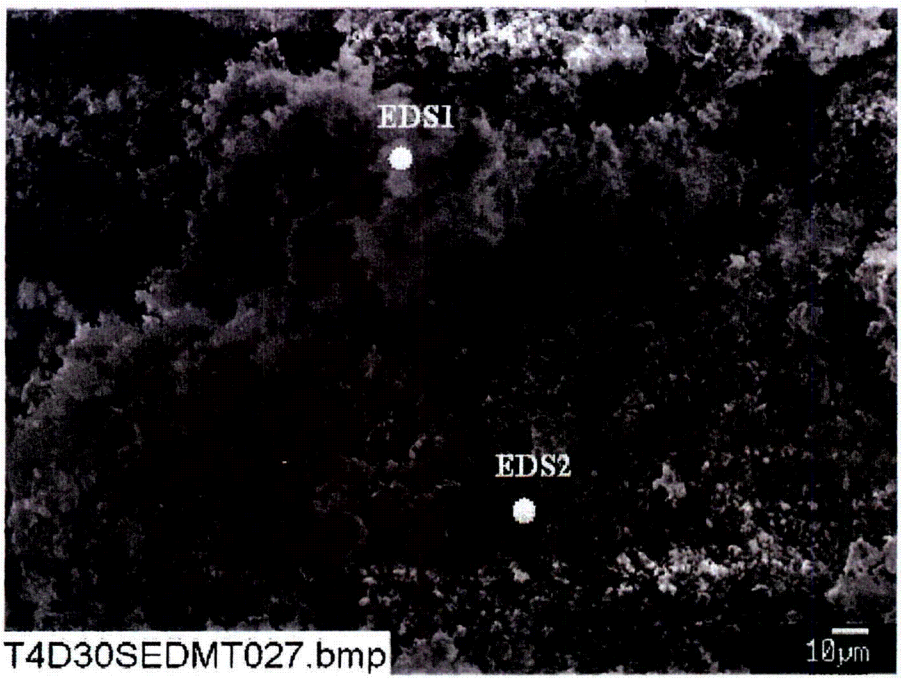

Figure 4-91. Annotated SEM image, magnified 500 times, for a Test #4, Day 30, sediment sample at the bottom of the tank. (T4D30SEDMT027.bmp)

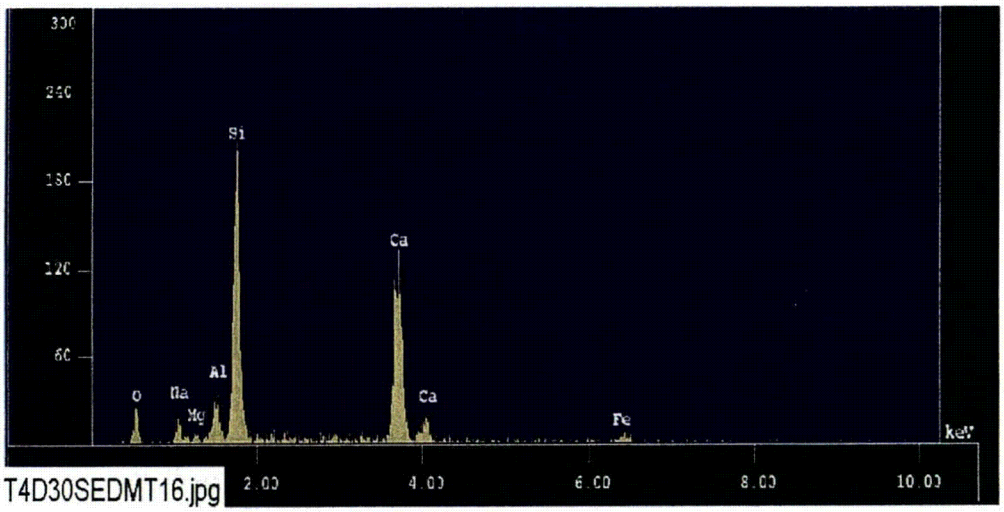

Figure 4-92. EDS counting spectrum for the white snow-like deposits (EDS1) shown in Figure 4-91. (T4D30SEDMT16.jpg)

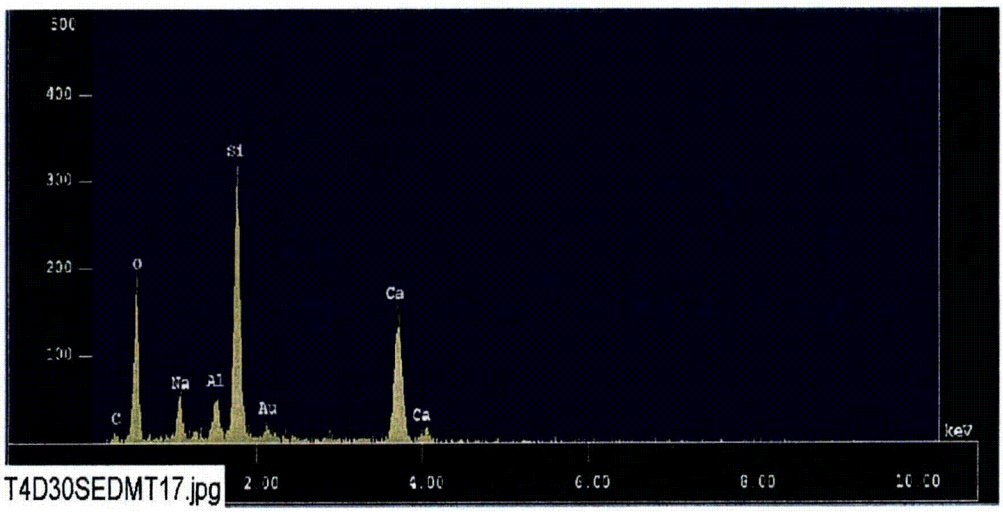

Figure 4-93. EDS counting spectrum for the dark deposits (EDS2) shown in Figure 4-91. (T4D30SEDMT17.jpg)

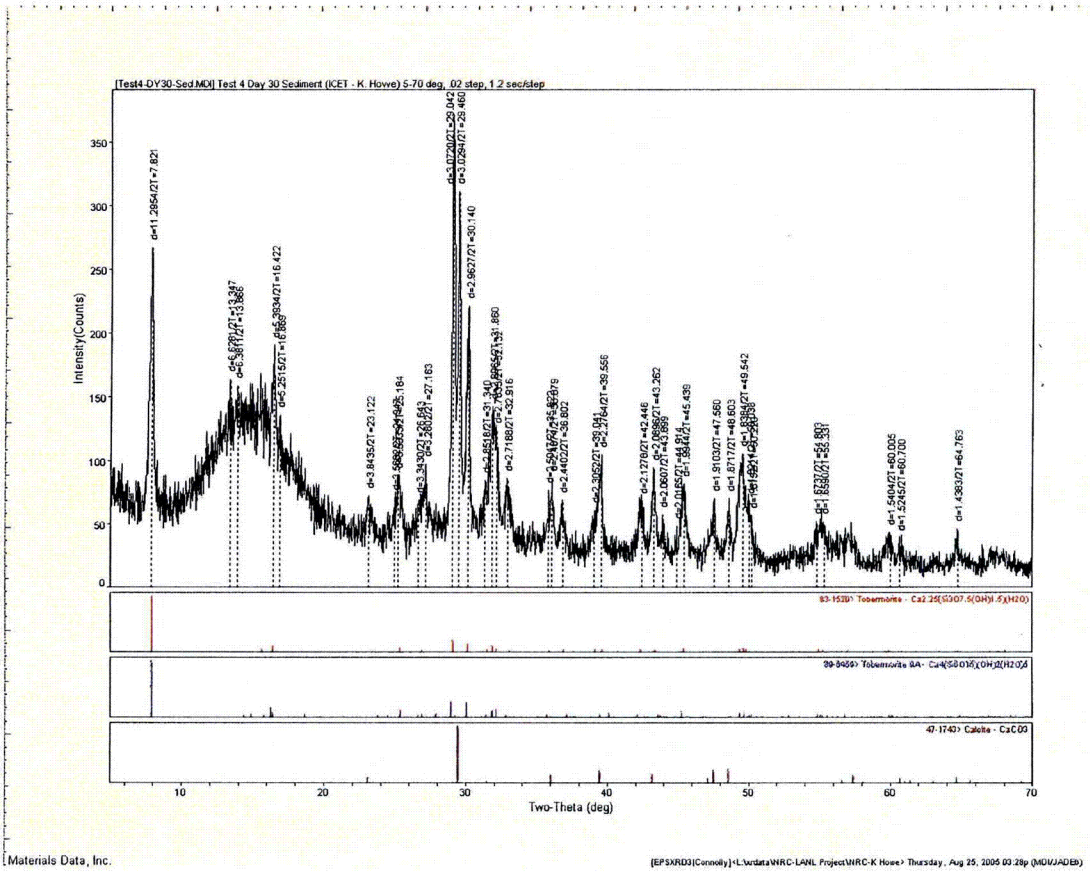

Figure 4-94. XRD results for the possible matching crystalline substances in the Test #4, Day 30, sediment.

Test #5 Sediment

Similar to Test #1 and Test #2, fiberglass was the only insulation material used in Test #5. The least amount (only 89 g) of wet sediment was recovered from the tank following the test. Figure 4-95 is a photograph of the sediment from Test #5, which shows a significant amount of fiberglass debris. The SEM image in Figure 4-96 also indicates a large amount of fiberglass debris, mixed with a few particulate deposits in the sediment. The particulate deposit is composed of silicon, aluminum, oxygen, carbon, sodium, and magnesium, as shown in Figure 4-97. The particulate deposits may originate from the corrosion products, dirt, and chemical precipitates. Consistent with the photograph and SEM images, the XRF results show that silicon was 29.8% of the total mass of the dried sediments, as shown in Table 4-6.

In addition, the XRD result in Figure 4-98 indicates the presence of quartz crystal in the sediment. The quartz likely derived from the fiberglass debris, which is consistent with the Tests #1 and #2 sediment. It should be noted that the XRD result also shows the possible crystalline match of cobalt and uranium compounds in the sediment. However, cobalt and uranium were not likely to be present. The XRD signature corresponding to these compounds likely results from the heterogeneous nature of the sediment and are not part of the sediment composition.

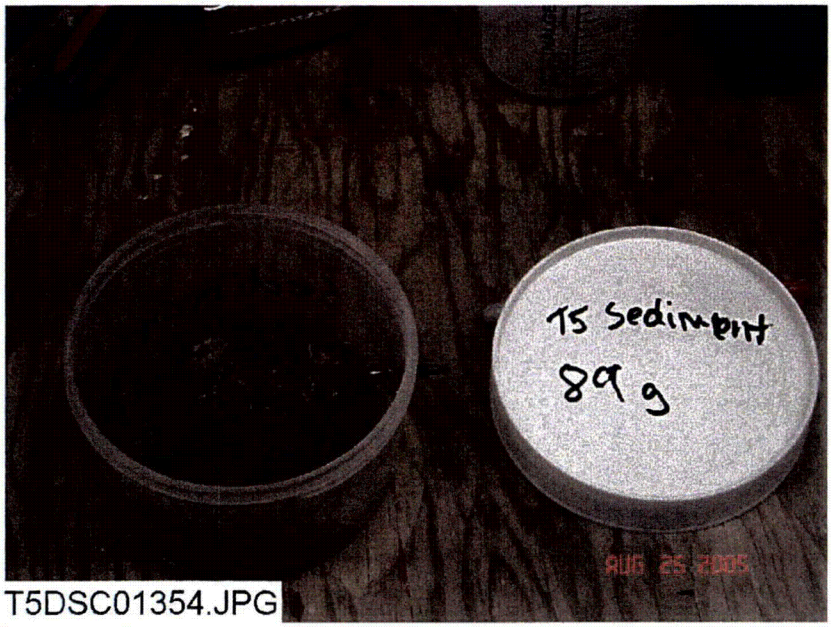

Figure 4-95. Sediment sample removed from the tank after Test #5.

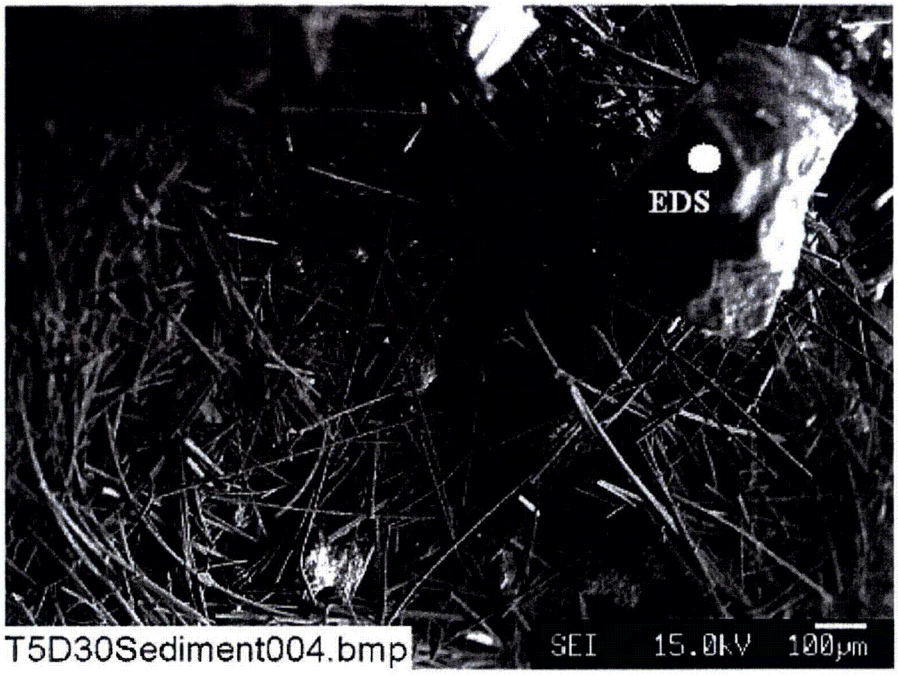

Figure 4-96. SEM image, magnified 70 times, of the Test #5, Day 30, sediment at the bottom of the tank.

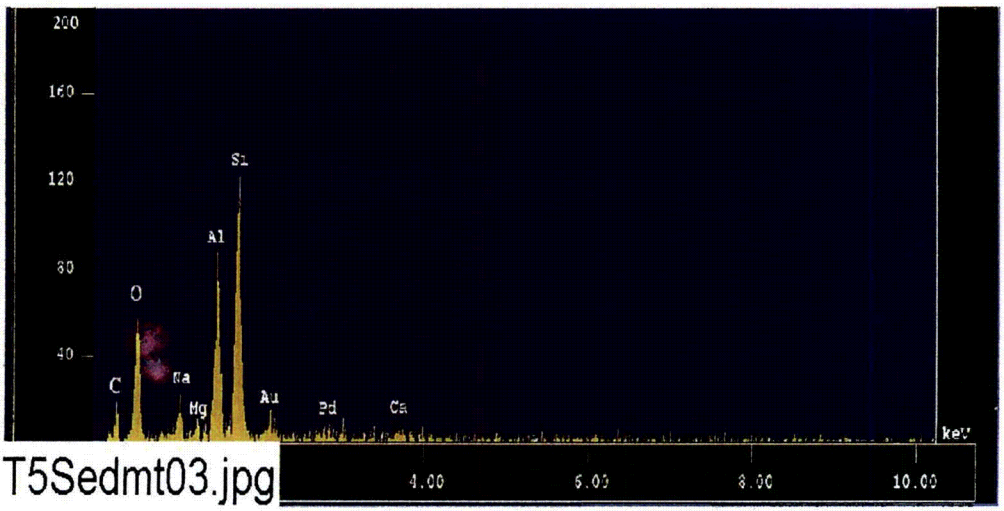

Figure 4-97. EDS counting spectrum for the big particulate deposit shown in Figure 4-96.

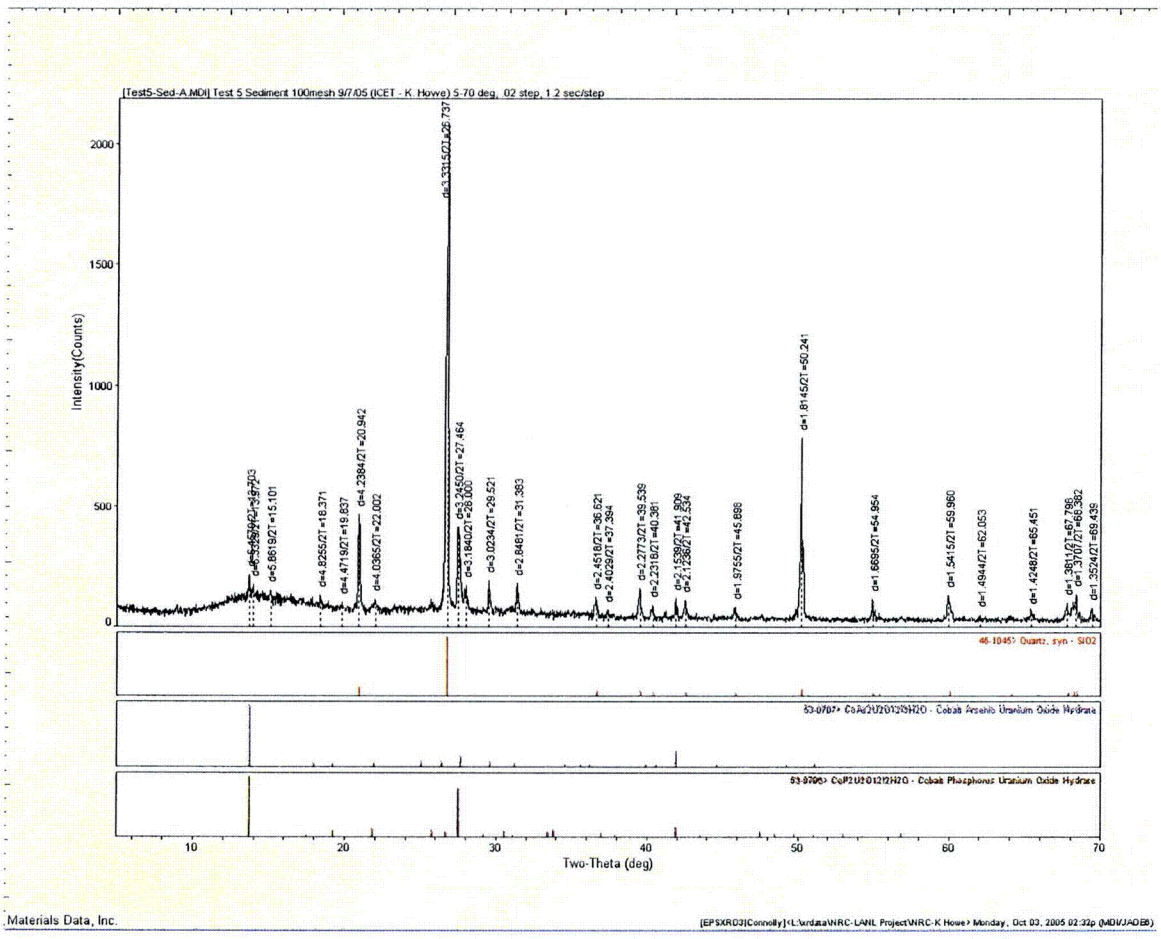

Figure 4-98. XRD results for the possible matching crystalline substances in Test #5, Day 30, sediment.

4.4. Coupons

In this section, photographs and microscopic evaluations of the approximately 12-in.-square metal coupon samples are presented. In Section 4.4.1, pre- and post-test photographs of each coupon type are shown. In Section 4.4.2, SEM/EDS results are presented, and the types of corrosion products found on the post-test coupons are discussed. In Section 4.4.3, evidence and discussion concerning the lack of corrosion on the aluminum coupons in Test #4 is given.

4.4.1. Pre- and Post-Test Coupon Photographs

Submerged Coupons

Figures 4-99 through 4-101 are pictures of submerged aluminum coupons from each test. Figure 4-102 shows an unused aluminum coupon. With the exception of Test #4, the test solution had a large effect on the aluminum coupons. Coupons in Tests #1 and #5 developed a brown coating on the surface, whereas coupons in Tests #2 and #3 accumulated white particle deposits across their surface. In addition, a copper layer was evident on the Tests #2 and #3 coupons. The layer can be attributed to electrochemical ion transfer. Tests #1 and #5 coupons had a more uniform distribution of deposit across their surface, whereas coupons in Tests #2 and #3 had more of a "blotchy" arrangement on their surfaces. The Test #4 coupon was relatively unchanged.

Figure 4-99. ICET Test#1 Al-91 post-test (left); ICET Test#2 Al-96 post-test (right).

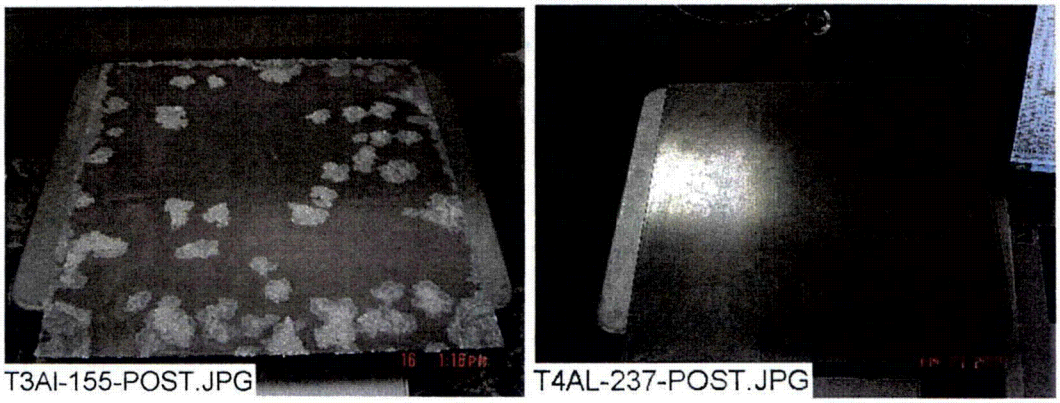

Figure 4-100. ICET Test#3 Al-155 submerged, post-test (left); ICET Test#4 Al-237 submerged, post-test, (right).

Figure 4-101. ICET Test #5 Al-93 submerged, post-test.

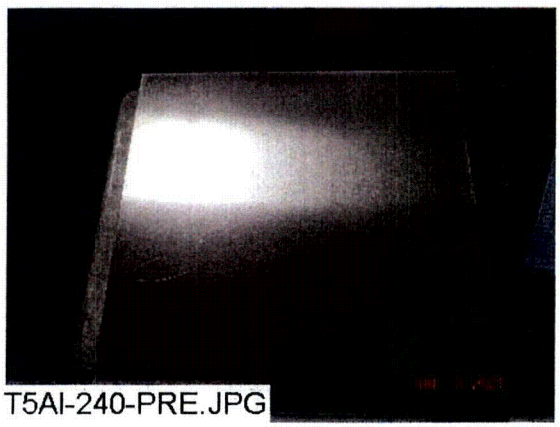

Figure 4-102. Unused Al coupon.

Figures 4-103 to 4-105 are pictures of submerged galvanized steel coupons from each test. Figure 4-106 shows an unused galvanized steel coupon. The galvanized steel coupons from Tests #1 and #5 appeared to have the same type of white deposit, although the deposition patterns are different. The deposits on these coupons were attached securely to the surface, although there was not a great amount of deposit. The Tests #2 and #3 coupons both accumulated a large amount of white particles on their surfaces. These particles could be rubbed off the coupon with relative ease. The Test #4 coupon appeared relatively unchanged from its pretest appearance.

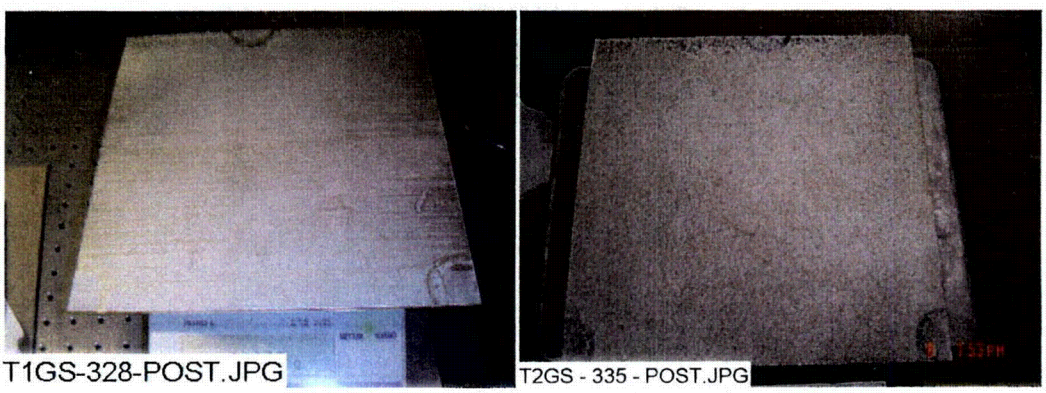

Figure 4-103. ICET Test #1 GS-328 submerged, post-test (left); ICET Test #2 GS-335 submerged, post-test (right).

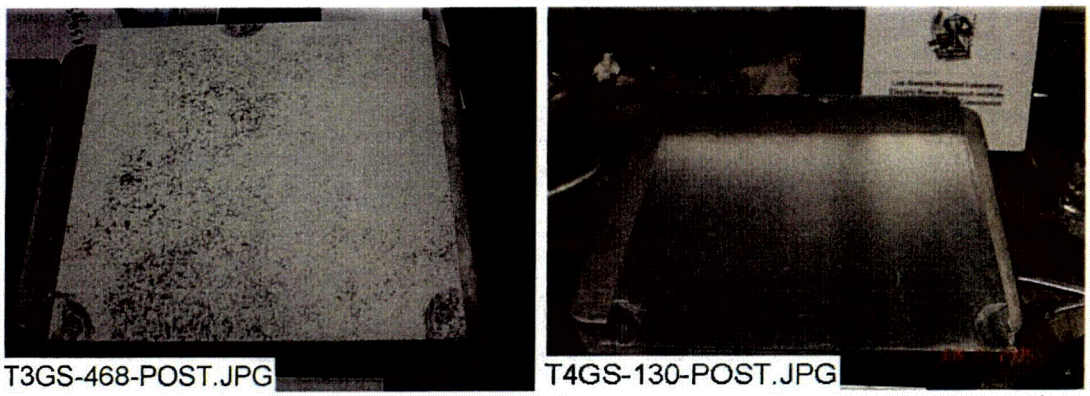

Figure 4-104. ICET Test #3 GS-468 submerged, post-test (left); ICET Test #4 GS-130 submerged, post-test (right).

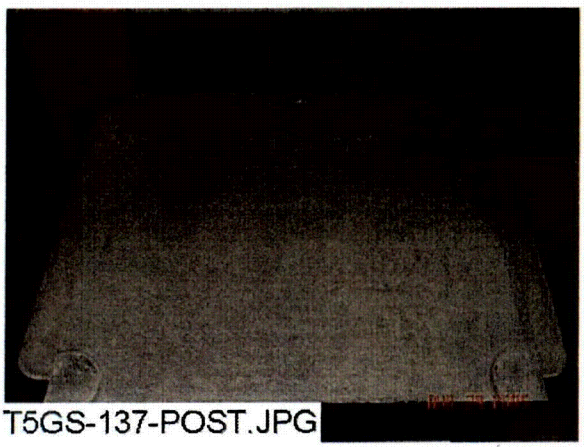

Figure 4-105. ICET Test #5 GS-332 submerged, post-test.

Figure 4-106. Unused GS coupon.

Figures 4-107 through 4-109 are pictures of submerged IOZ-coated steel coupons from each test. Figure 4-110 shows an unused IOZ-coated steel coupon. The Tests #1 and #5 coupons developed a brownish hue, with the color of Test #1 being more pronounced. The Test #2 coupon shows a relatively large amount of white deposit originating in the areas where the coupon came in contact with the rack. The Test #3 coupon had a small amount of white deposit in the areas where the coupon was in contact with the rack, as well as a small amount of white precipitate distributed across the surface of the coupon. The Test #4 coupon developed a small amount of white precipitate on the top edge of the coupon; however, it was not significantly changed from its pretest appearance.

Figure 4-107. ICET Test #1 IOZ-77 submerged, post-test (left); ICET Test #2 IOZ-79 submerged, post-test (right).

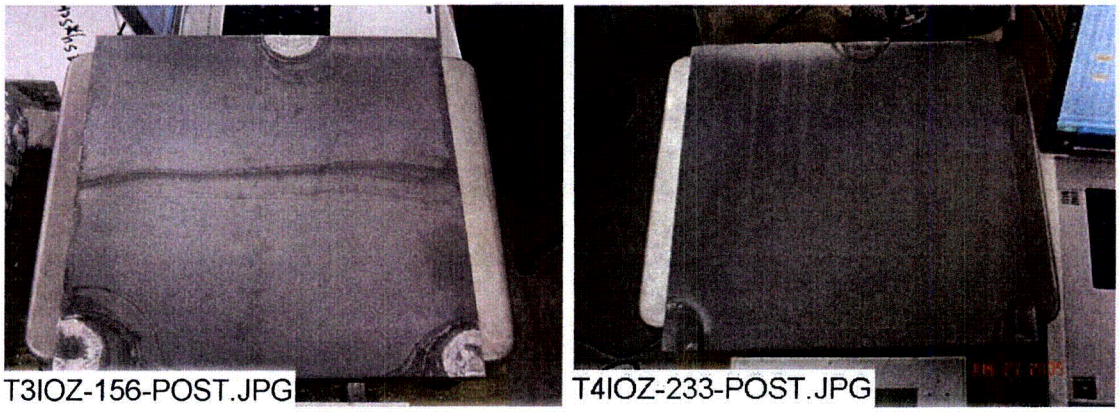

Figure 4-108. ICET Test #3 IOZ-156 submerged, post-test (left); ICET Test #4 IOZ-233 submerged, post-test (right).

Figure 4-109. ICET Test #5 IOZ-310 submerged, post-test.

Figure 4-110. Unused IOZ-coated coupon.

Figures 4-111 through 4-113 are pictures of submerged copper coupons from each test. Figure 4-114 shows an unused copper coupon. The coupons from Tests #1, #2, #4, and #5 have similar types of particle deposition. They all accumulated small amounts of white particles that were arranged in horizontal streaks across the coupon surface. The Test #3 copper coupon accumulated a large amount of white particles distributed across the coupon's entire surface. This deposition could be rubbed off relatively easily.

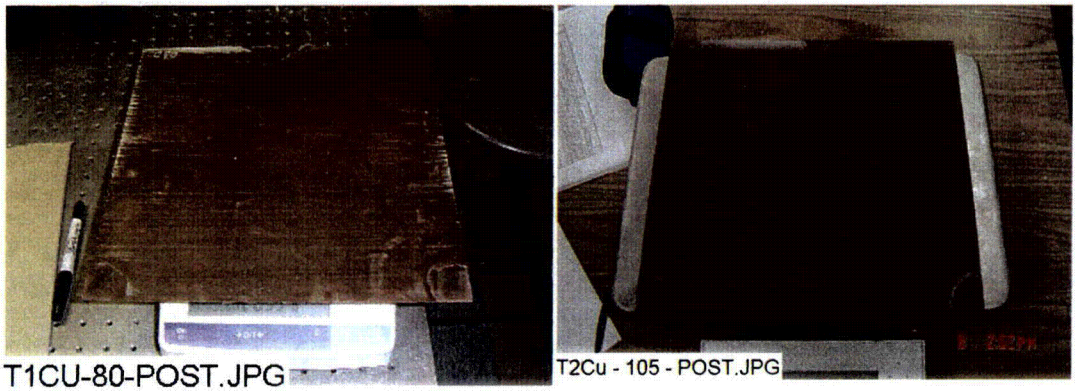

Figure 4-111. ICET Test #1 CU-80 submerged, post-test (left); ICET Test #2 CU-105 submerged, post-test (right).

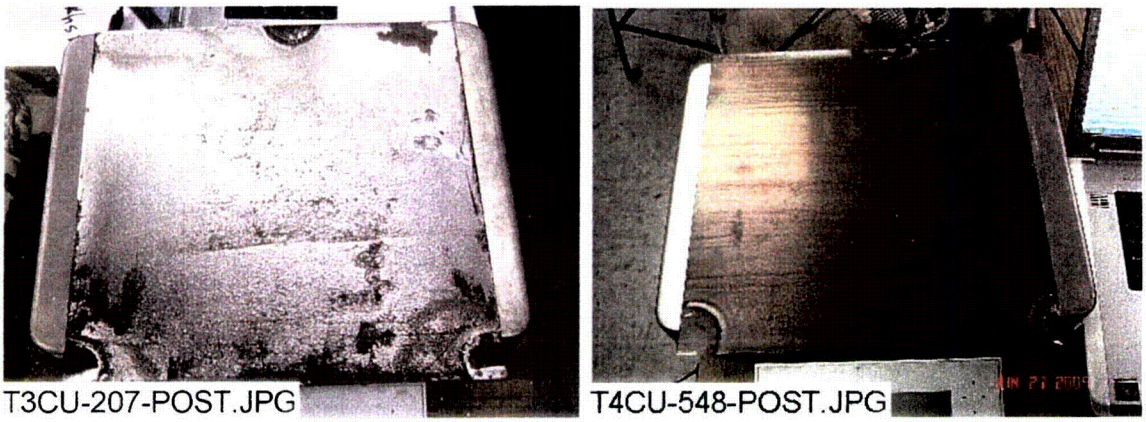

Figure 4-112. ICET Test #3 CU-207 submerged, post-test (left); ICET Test #4 CU-100 submerged, post-test (right).

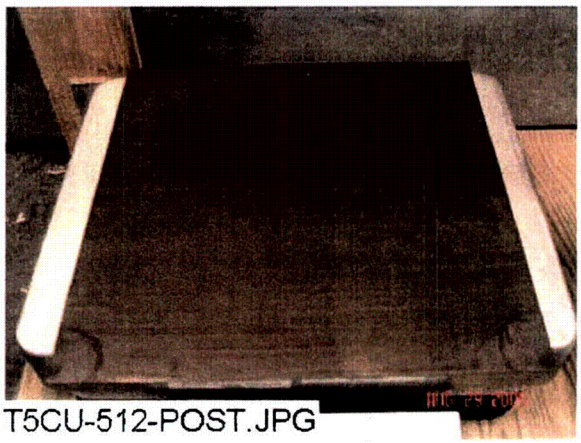

Figure 4-113. ICET Test #5 CU-100 submerged, post-test.

Figure 4-114. Unused CU coupon.

Figures 4-115 through 4-117 are pictures of submerged carbon steel (uncoated steel, US) coupons from each test. Figure 4-118 shows an unused carbon steel coupon. Tests #1 and #5 carbon steel coupons both accumulated a small amount of white particles on their surfaces. This

accumulation caused the surfaces to develop a dull, sandy finish. The Test #2 coupon developed a large amount of yellowish corrosion product on its surface, and its surface was roughened. The Test #3 coupon accumulated some white particles, distributed evenly over the surface of the coupon. Some yellowish corrosion also developed on the bottom edge of the coupon. The Test #4 coupon was largely unchanged from its pre-test condition.

Figure 4-115. ICET Test #1US-8 submerged, pre-test (left); ICET Test #2 US-7 submerged, post-test (right).

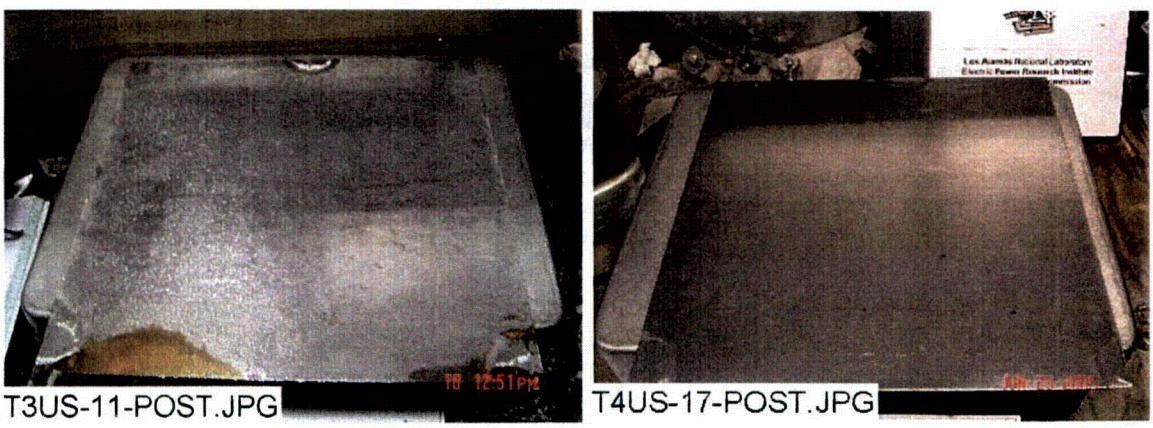

Figure 4-116. ICET Test #3 US-11 submerged, post-test (left); ICET Test #4 US-17 submerged, post-test (right).

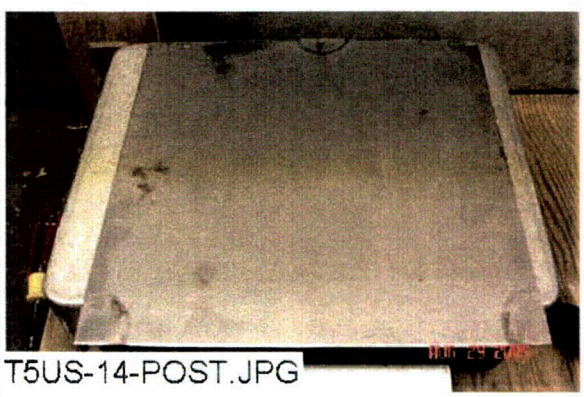

Figure 4-117. ICET Test #5 US-14 submerged, post-test.

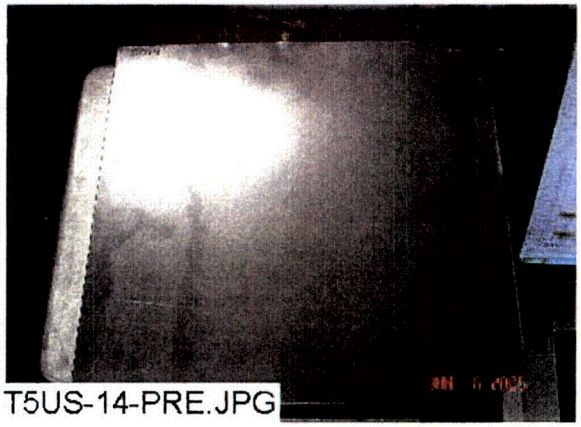

Figure 4-118. Unused US coupon.

Figures 4-119 through 4-121 are pictures of submerged concrete coupons from each test. Figure 4-122 shows an unused concrete coupon. Concrete coupons from Tests #1, #4, and #5 all developed a brownish color, with the coupons from Tests #1 and #5 having a deeper color change. The Test #2 coupon was relatively unchanged. The Test #3 coupon accumulated a large amount of white particles that were distributed evenly over the surface of the coupon.

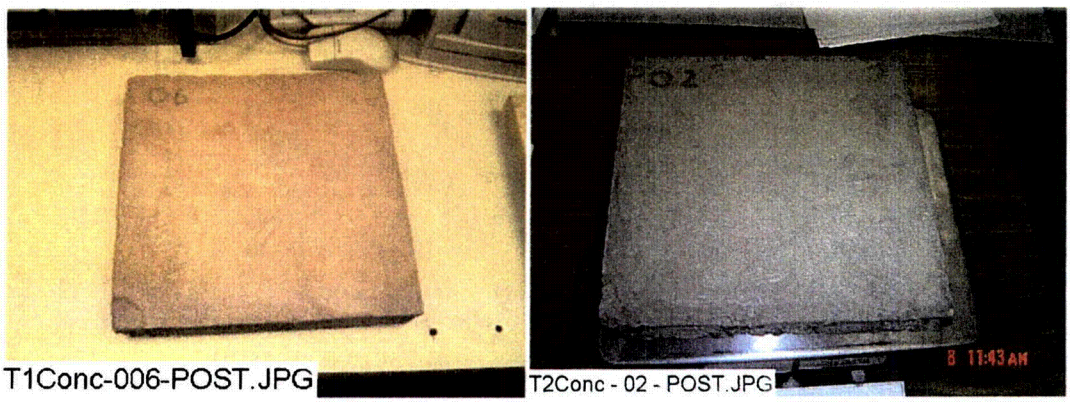

Figure 4-119. ICET Test #1 Conc-6 submerged, post-test (left); ICET Test #2 Conc-2 submerged, post-test (right).

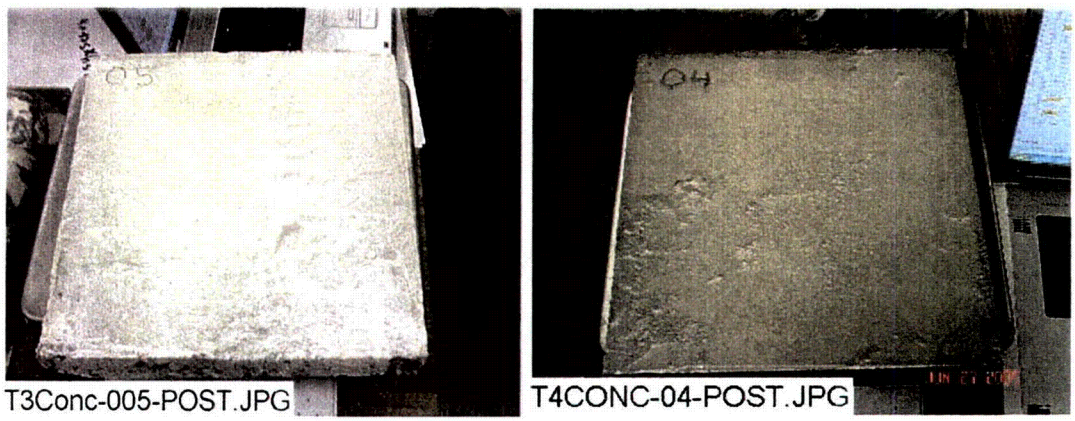

Figure 4-120. ICET Test #3 Conc-5 submerged, post-test (left); ICET Test #4 Conc-4 submerged, post-test (right).

Figure 4-121. ICET Test #5 Conc-003 submerged, post-test.

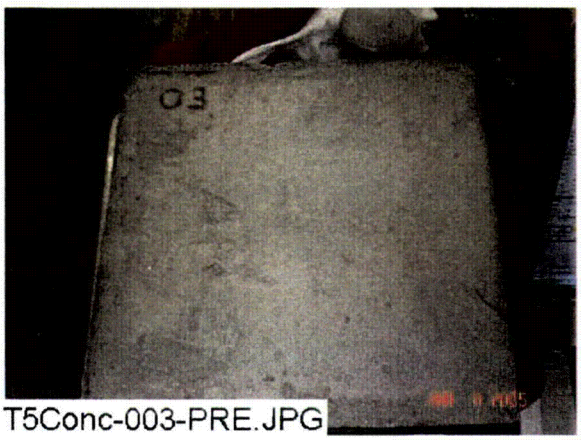

Figure 4-122. Unused concrete coupon.

Overall, the Test #4 environment resulted in less significant changes to the submerged coupon appearance.

Table 4-9 displays the mean weight gain/loss summary in grams for all of the submerged coupons.

Table 4-9. Mean Weight Gain/Loss Data for Submerged Coupons (g)

	Test Number				
Coupon Type	**1**	**2**	**3**	**4**	**5**
CU	0.1	<0.1	0.3	0.2	–0.2
IOZ	3.1	3.8	1.8	2.3	1.6
GS	0.0	28.6	15.0	0.3	0.1
AL	–98.6	–0.9	0.6	0.0	–11.2
US	–23.3	1.4	–1.1	0.2	0.0
Concrete	233.0	240.7	180.5	239.6	225.9

The submerged concrete samples' mean weight gain ranged from 180 to 241 g. Much of that weight gain is attributed to retained water in the samples. It is interesting to note that the weight

gains for Tests #1, #2, #4, and #5 were similar, while the Test #3 weight gain was 45–60 g less. It is possible that water retention was impeded by the Test #3 surface coating (Figure 4-120). The mean weight gain/loss of the submerged carbon steel (uncoated steel, US) coupons did not exceed 1.5 g, with the exception of the Test #1 coupon, which lost approximately 23 g. The aluminum coupons in Tests #1 and #5 lost significant weight, about 25% and 3% of their pretest weights, respectively. There were no significant weight changes in the aluminum coupons in the other tests. The submerged galvanized steel coupons in Tests #2 and #3 experienced mean weight gains of approximately 3% and 1.5% of their pre-test values, respectively. Tests #1, #4, and #5 coupons exhibited insignificant weight changes. The mean weight gain of the submerged inorganic-zinc-coated steel coupons ranged from 1.6 to 3.8 g. The submerged copper coupons experienced mean weight differentials that did not exceed 0.5 g.

Unsubmerged Coupons

Figures 4-123 through 4-125 are post-test pictures of unsubmerged aluminum coupons from each test. Each post-test photograph depicts coupons that were loaded in Rack 2 (see Figure 2-2), which was in the southern position of the middle tier of the tank. Using the same rack location facilitates direct comparison of aluminum coupons from each test. Each post-test aluminum coupon exhibits a similar vertical, streak pattern of white deposits. The deposit concentration was also similar for all of the displayed coupons. Each coupon is predominantly dull gray, with a tint of reddish-brown visible on the coupons from Tests #1, #4, and #5.

Figure 4-123. Test #1 Al-42 unsubmerged (left); Test #2 Al-101 unsubmerged (right).

Figure 4-124. Test #3 Al-159 unsubmerged (left); Test #4 Al-3 unsubmerged (right).

Figure 4-125. Test #5 Al-247 unsubmerged.

Figures 4-126 through 4-128 are post-test pictures of unsubmerged galvanized steel coupons from each test. Each post-test photograph depicts coupons that were loaded in Rack 3, which was in the center position of the middle tier of the tank (Figure 2-2). The concentration and pattern of deposition on the Tests #1 and #2 coupons are similar. The deposition patterns exhibited by these coupons are a combination of faint white steaks and small white clusters located in random locations. There are much fewer deposits on the Tests #3, #4, and #5 coupons. Each coupon is predominantly gray to silver, which is consistent with its original color (Figure 4-106).

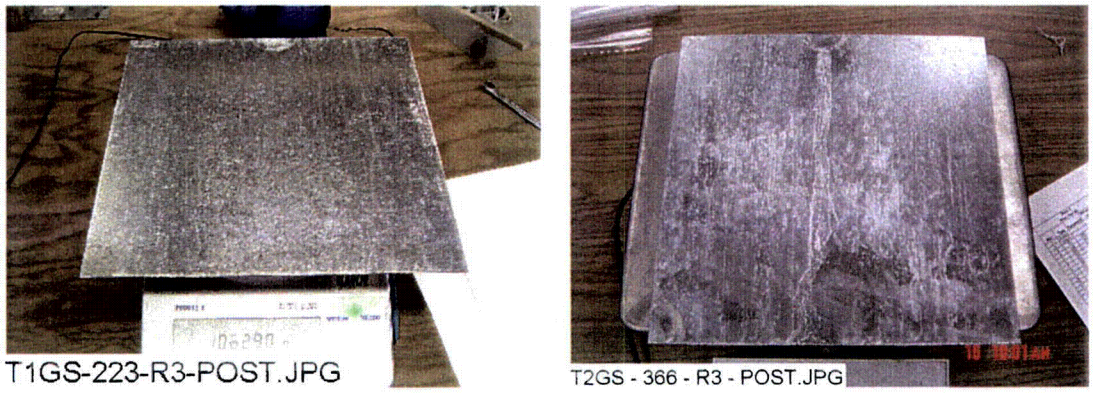

Figure 4-126. Test #1 GS-223 unsubmerged (left); Test #2 GS-366 unsubmerged (right).

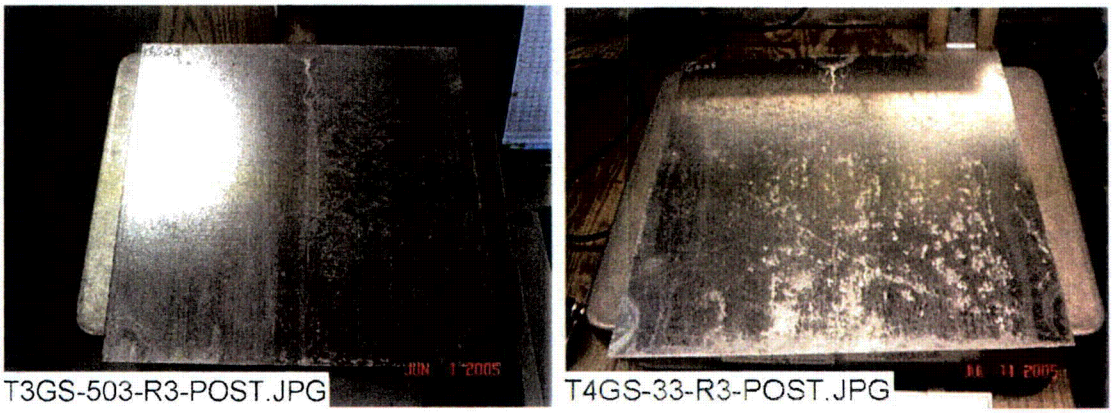

Figure 4-127. Test #3 GS-503 unsubmerged (left); Test #4 GS-33 unsubmerged (right).

Figure 4-128. Test #5 GS-167 unsubmerged.

Figures 4-129 through 4-131 are post-test pictures of unsubmerged copper coupons from each test. Each post-test photograph depicts coupons that were loaded in rack #7, which was in the northern position of the top tier of the tank (Figure 2-2). The pattern of deposition for each coupon is similar and consists of faint white, vertical streaks. The depositions on the Tests #1 and #5 coupons are the least concentrated. The deposition concentration on the remaining coupons is similar. Each coupon is predominantly reddish-brown, which is consistent with their original color (Figure 4-114).

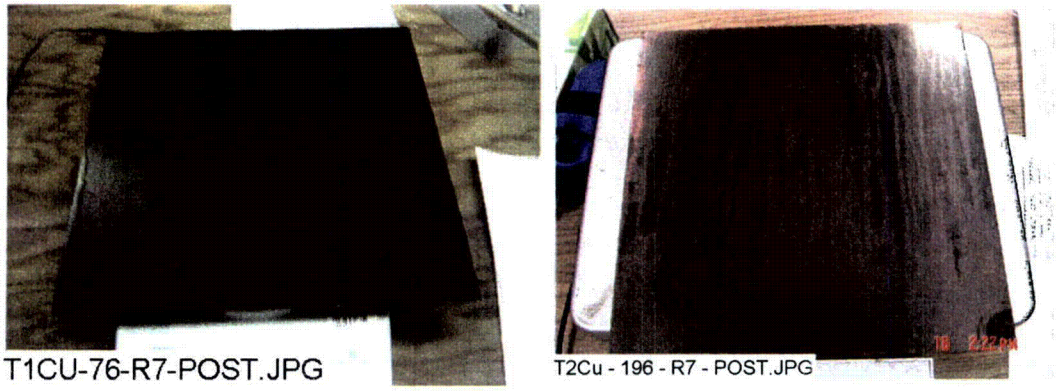

Figure 4-129. Test #1 CU-76 unsubmerged (left); Test #2 CU-196 unsubmerged (right).

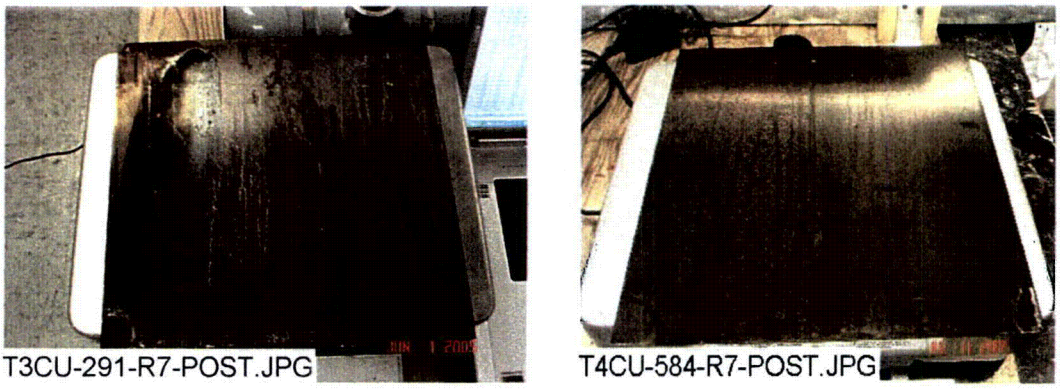

Figure 4-130. Test #3 CU-291 unsubmerged (left); Test #4 CU-584 unsubmerged (right).

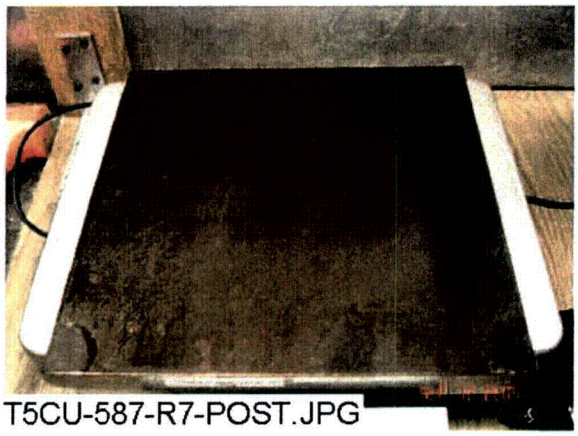

Figure 4-131. Test #5 CU-587 unsubmerged.

Figures 4-132 through 4-134 are post-test pictures of unsubmerged inorganic zinc-coated steel coupons from each test. Each post-test photograph depicts coupons that were loaded in Rack 5, which was in the southern position of the top tier of the tank. The pattern of deposition for Tests #1, #2, #4, and #5 coupons consists of lightly-concentrated, white clusters. The Test #3 coupon depositions consist of vertical streaks that are mainly congregated near the right-hand-side coupon edge. Each coupon is predominantly dull gray, which is consistent with its original appearance (Figure 4-110).

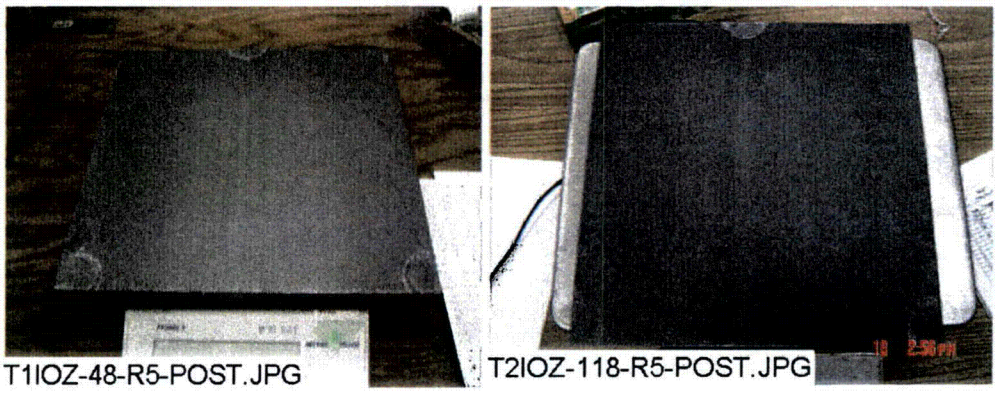

Figure 4-132. Test #1 IOZ-48 unsubmerged (left); Test #2 IOZ-26 unsubmerged (right).

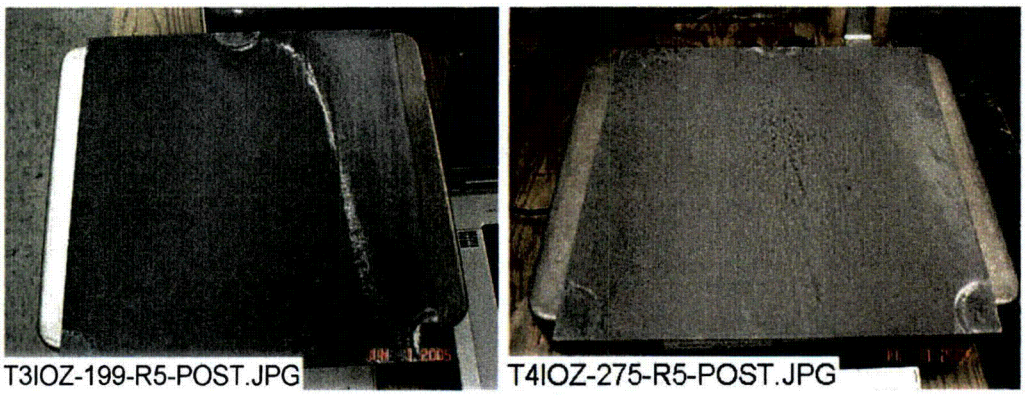

Figure 4-133. Test #3 IOZ-199 unsubmerged (left); Test #4 IOZ-275 unsubmerged (right).

Figure 4-134. Test #5 IOZ-356 unsubmerged.

Figures 4-135 through 4-137 are post-test pictures of unsubmerged uncoated carbon steel coupons from each test. Each post-test photograph depicts coupons that were loaded in Rack 6, which was in the center of the top tier of the tank (Figure 2-2). The deposits for each coupon consist of reddish-brown rust. However, the concentration of rust varies between tests. The concentration of the Tests #2 and #3 coupons is significant and covers nearly the entire surface of each coupon. The coupons from Tests #1, #4, and #5 exhibit sparsely concentrated, rust-like splotches. Each coupon is predominantly dull silver, close to its original color (Figure 4-118).

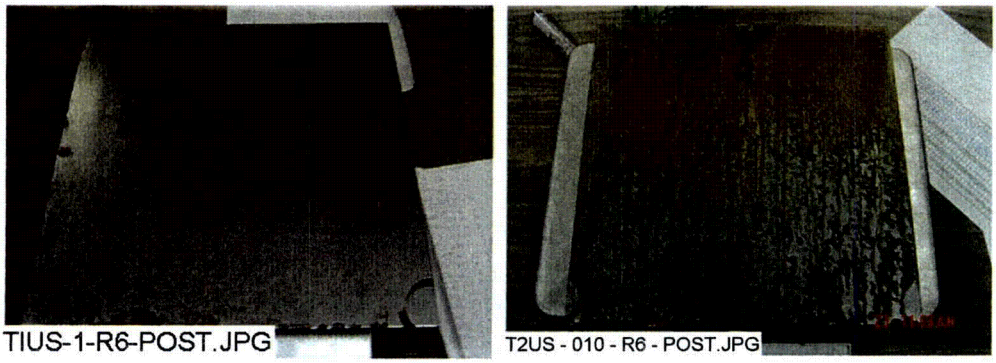

Figure 4-135. Test #1 US-1 unsubmerged (left); Test #2 US-10 unsubmerged (right).

Figure 4-136. Test #3 US-13 unsubmerged (left); Test #4 US-16 unsubmerged (right).

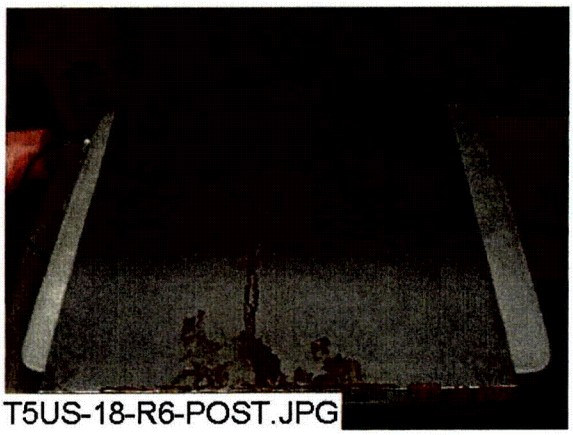

Figure 4-137. ICET Test #5 US-18 unsubmerged.

Table 4-10 displays the mean gain/loss summary in grams for all of the unsubmerged coupons.

Table 4-10. Mean Gain/Loss Data for Unsubmerged Coupons (g)

	Test Number				
Coupon Type	**1**	**2**	**3**	**4**	**5**
CU	–0.2	<0.1	0.2	0.3	0.2
IOZ	1.2	1.7	2.0	1.1	1.2
GS	0.0	0.4	0.2	0.2	0.2
AL	0.7	0.4	0.4	0.6	0.4
US	0.0	1.3	1.0	–0.4	0.2

The mean weight differentials for unsubmerged coupons are more consistent among the tests, and there are no weight gains or losses as significant as with some of the submerged coupons. The copper samples experienced mean weight changes ranging from <0.1 to 0.3 g. The range of mean weight gain for the inorganic-zinc-coated steel coupons was 1.1 to 2.0 g. The galvanized steel coupons' mean weight gain ranged from 0.0 to 0.4 g. The aluminum coupons' mean weight gain ranged from 0.4 to 0.7 g. The range of mean weight gain/loss for the carbon steel coupons was 0 to 1.3 g.

4.4.2. SEM/EDS

The surface and the morphology of metal coupons were altered by corrosion because of exposure to the test solutions, condensate, or sprays during the ICET tests. The extent of corrosion on different coupons depended on the metals and solution chemistry of each individual test, such as pH and type of insulation material (fiberglass or cal-sil). Table 4-11 lists the redox potential (Ref. 9) of the metals on the coupon surfaces. The more negative the redox potential the more likely it is that the metal will oxidize and corrode. From Table 4-11, aluminum is the metal most likely to corrode, followed by zinc, iron, and copper. It should be noted that passivation layers (such as aluminum silicate) may impede the corrosion process independent of the redox potential (see Section 4.4.3). This type of passivation may be more significant in the tests with cal-sil, which can release a significant amount of calcium and silica to solution. The data of coupon

weight gain/loss after the tests do not necessarily correlate with the amount of corrosion because weight loss caused by corrosion can be offset by weight gain caused by the deposition of corrosion products on the coupon surface. In addition to redox potential and passivation layers, solution chemistry also affects the corrosion. For example, the solubility of aluminum species is higher at pH 9 than at pH 7; therefore, the corrosion is more severe at pH 9.

Table 4-11. Standard Redox Potential of the Metals Used in the ICET Tests

Metals	Reactions	Redox Potential (E^0/V)
Aluminum	$Al^{3+} + 3e^- \leftrightarrow Al$	−1.662
Copper	$Cu^{2+} + 2e^- \leftrightarrow Cu$	0.3419
Iron	$Fe^{3+} + 3e^- \leftrightarrow Fe$	−0.037
Zinc	$Zn^{2+} + 2e^- \leftrightarrow Zn$	−0.7618

Submerged Metal Coupons

During the ICET tests, trace metal cations may be released from the submerged metal coupon surfaces because of corrosion. Subsequently, the released metal cations may form complexes with the anions from the solution, such as OH^-, SiO_3^{2-}, and CO_3^{2-}. In addition, the complexed anions may attract other cations from the solution, such as Ca^{2+}, Mg^{2+}, Al^{3+}, Cu^{2+}, Zn^{2+}, and H^+. As a result, corrosion products (deposits) may form and continuously grow on the metal coupon surfaces. The adherence between the metal coupons and the deposits is through chemical bonds, which are much stronger than van der Waals forces. Because of the vertical orientation of the metal coupons in the tank (with a small horizontal cross-sectional area), the deposits on the metal coupon surface are likely of chemical origin rather than being the result of particles settling on the surface. Corrosion also may cause pitting of the coupon surfaces. As a result, a rougher coupon surface was often observed as compared with the unused coupons.

Based on SEM/EDS results, the dominant corrosion products on the submerged aluminum coupons appear to be aluminum hydroxide, with other substances containing silicon, calcium, oxygen, and carbon also present. On the submerged copper coupons, the possible corrosion products include CuO, $Cu_2(CO_3)(OH)_2$, and substances containing calcium, silicon, aluminum, and oxygen. On the submerged galvanized steel coupons, the possible corrosion products are oxides, hydroxides, silicates, and carbonate compounds of zinc, calcium, and aluminum. On the submerged steel coupon, the possible corrosion products include oxide, hydroxide, silicate, and carbonate compounds of iron and calcium and compounds composed of iron, silicon, calcium, and aluminum. Because of the differences of specific chemicals used in each test, some specific deposits were found on submerged metal coupons. For example, because TSP was used in Test #2, phosphate-related deposits were found on the submerged copper, galvanized steel, and uncoated steel coupons. (Phosphate was mainly precipitated out by calcium as gel-like material in Test #3). The introduction of cal-sil in Tests #3 and #4 caused silicate passivation on submerged aluminum coupon surfaces (see Section 4.4.3).

Unsubmerged Metal Coupons

The unsubmerged coupons were affected by the test solution only during the 4-hour spray phase on the first day of the test and, following that, were affected by condensation throughout the test.

Compared to the submerged coupons, the unsubmerged coupons had limited contact with the test solution; thus, the effect of solution chemistry on corrosion was limited. This effect may decrease the degree of corrosion on the unsubmerged coupons. However, the unsubmerged coupons have more contact with moist air and oxygen than the submerged coupons. As a result, oxygen had a greater chance to oxidize the coupons. The relative degree of corrosion on the unsubmerged coupons depended on these two competitive processes. If the physical and chemical changes that the unsubmerged coupons experienced during the ICET tests were less significant than the changes on the submerged coupons, the solution chemistry was the limiting step for corrosion on unsubmerged coupons. Otherwise, the oxidation process by oxygen from air was important for corrosion of the unsubmerged coupons. For unsubmerged coupons, it should be noted that the initial corrosion caused by the test solution during the 4-hour spray period may affect their consequent corrosion in moist air, because the test solution may damage the passivation oxide layer on the surface of the coupons, such as aluminum (Ref. 10) and zinc (Ref. 11).

Based on SEM/EDS results, the dominant corrosion products on the unsubmerged aluminum coupons appear to be aluminum hydroxide and/or aluminum oxide, and other corrosion products containing silicon, calcium, oxygen, and carbon also exist. On the unsubmerged copper coupons, the corrosion products are likely to be CuO. The corrosion products were composed of carbon, oxygen, calcium, silicon, and chlorine on the unsubmerged galvanized steel coupon surface. On the unsubmerged steel coupons, the likely corrosion products are Fe_2O_3, $Fe(OH)_3$, and $Fe_2(CO_3)_3$.

Submerged Aluminum Coupons

Figures 4-138 through 4-140 are the SEM images of unused and submerged aluminum coupons from Tests #1 through #5, respectively. As discussed previously, the coupon surface becomes very rough after the tests. Because of the negative redox potential of aluminum and high pH value (~9.5) in Test #1, the most severe corrosion of aluminum occurred in Test #1. The aluminum concentration reached ~380 mg/L in the Test #1 solution. The Test #5 aluminum coupons also experienced significant corrosion, although less than in Test #1. Test #5 was the only other test (besides Test #1) to have a significant aluminum concentration, which rose to about 50 mg/L in the test solution.

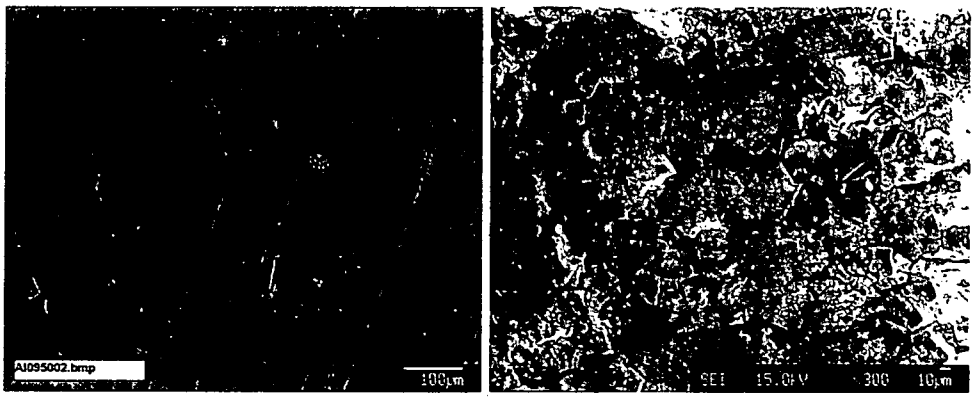

Figure 4-138. Unused aluminum coupon (left); Test #1 submerged aluminum coupon (right).

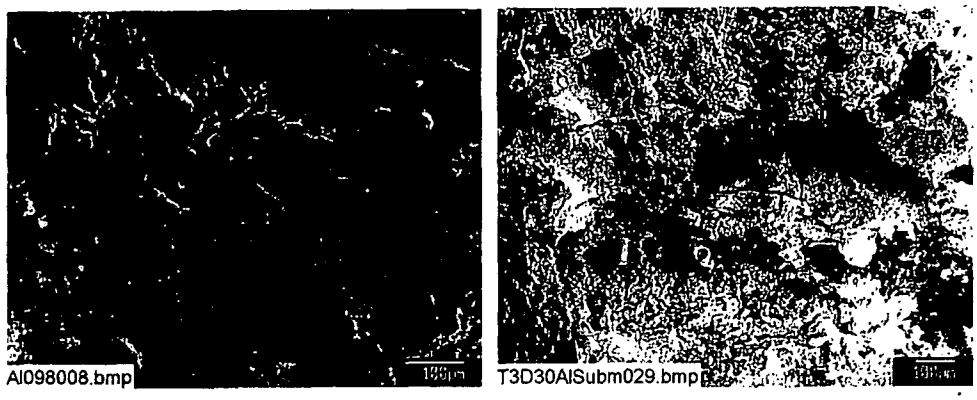

Figure 4-139. Test #2 submerged aluminum coupon (left); Test #3 submerged aluminum coupon (right).

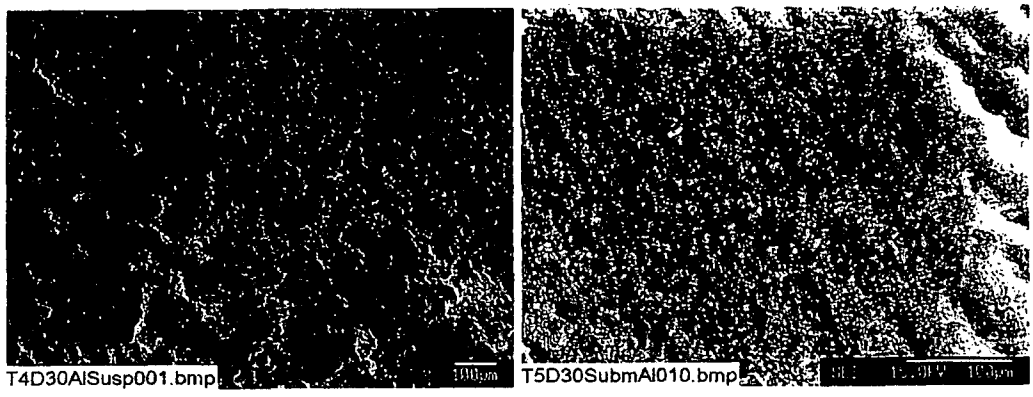

Figure 4-140. Test #4 submerged aluminum coupon (left); Test #5 submerged aluminum coupon (right).

Unsubmerged Aluminum Coupons

As shown in Figures 4-141 through 4-143, corrosion still occurred on the unsubmerged aluminum coupons because the coupons were affected by the test solution during the 4-hour spray period on the first day of the tests and by the moist air throughout the tests. However, the degree of corrosion apparently is less severe than on the submerged coupons because of limited contact with the liquid and, thus, there is limited mass transfer of the corrosion products and ionic species.

Figure 4-141. Test #1 unsubmerged aluminum.

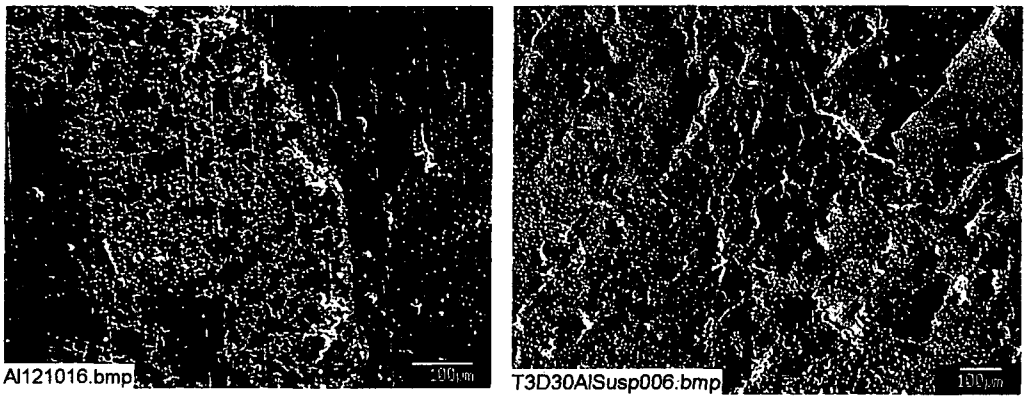

Figure 4-142. Test #2 unsubmerged aluminum (left); Test #3 unsubmerged aluminum (right).

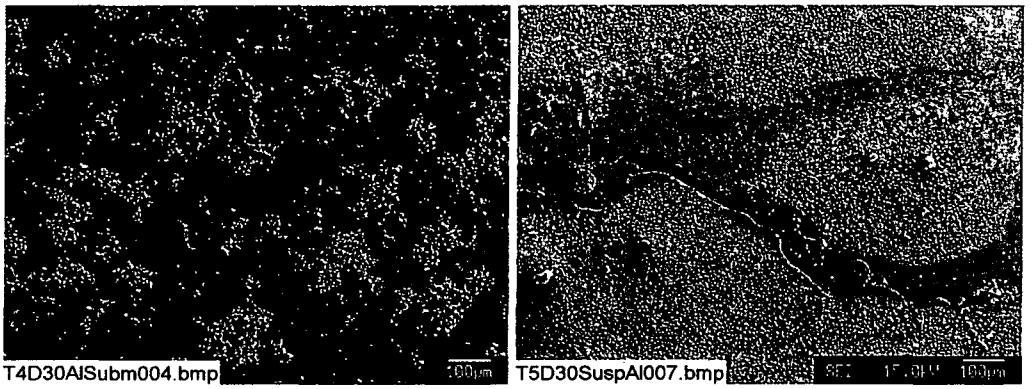

Figure 4-143. Test #4 unsubmerged aluminum (left); Test #5 unsubmerged aluminum (right).

Submerged Copper Coupons

Figures 4-144 through 4-146 show SEM images of unused and submerged copper coupons from Tests #1 through #5, respectively. As discussed previously, the coupon surface became significantly rougher after the tests. Because of the positive redox potential of copper, the corrosion of copper was less significant than the corrosion of aluminum. The copper concentration was less than 1.2 mg/L in all five of the tests, although the copper concentration may have been affected by other chemical species in the solution that complexed with copper and form precipitates.

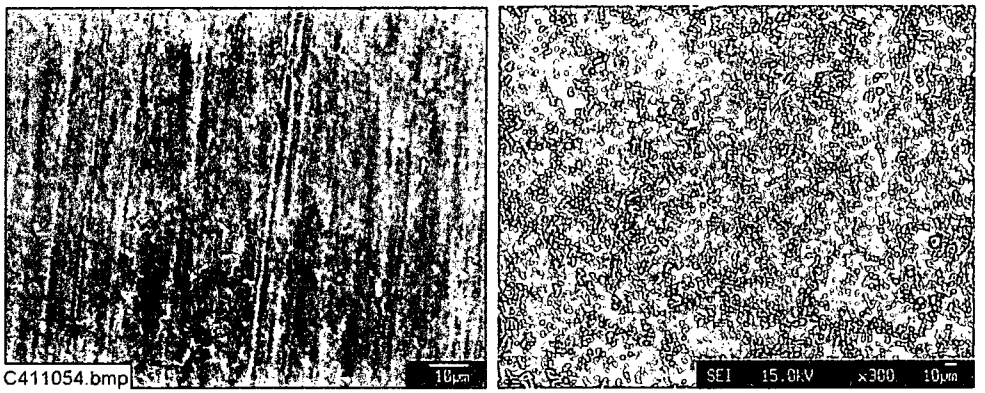

Figure 4-144. Unused copper coupon (left); Test #1 submerged copper coupon (right).

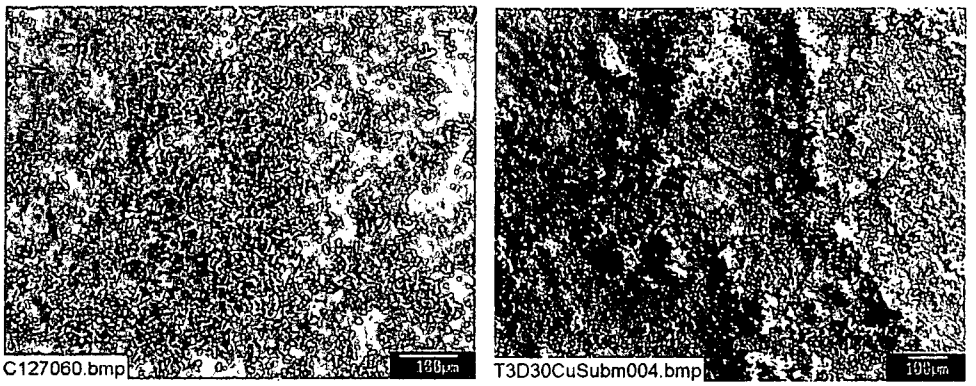

Figure 4-145. Test #2 submerged copper coupon (left); Test #3 submerged copper coupon (right).

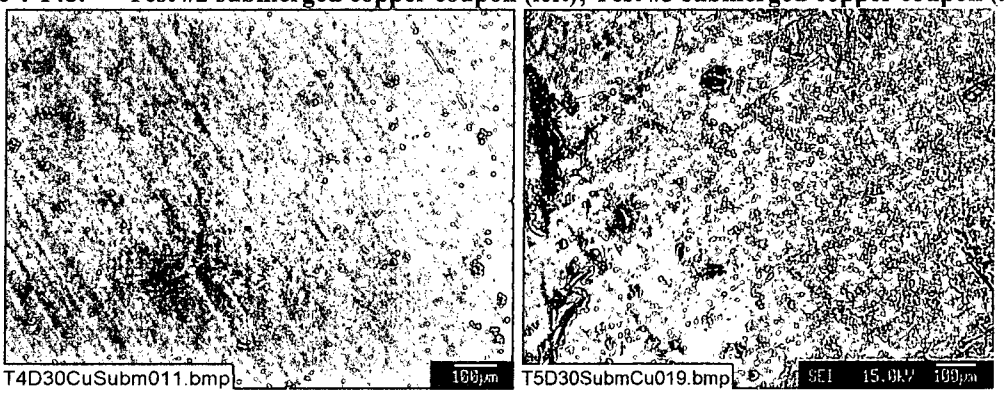

Figure 4-146. Test #4 submerged copper coupon (left); Test #5 submerged copper coupon (right).

Unsubmerged Copper Coupons

As shown in Figures 4-147 through 4-149, limited corrosion occurred on the unsubmerged copper coupons. The coupons were affected by the test solution only during the 4-hour spray period on the first day of the tests and by the moist air throughout the tests. As discussed previously, the degree of corrosion was significantly less than on the submerged copper coupons because of the limited mass-transfer process.

Figure 4-147. Test #1 unsubmerged copper.

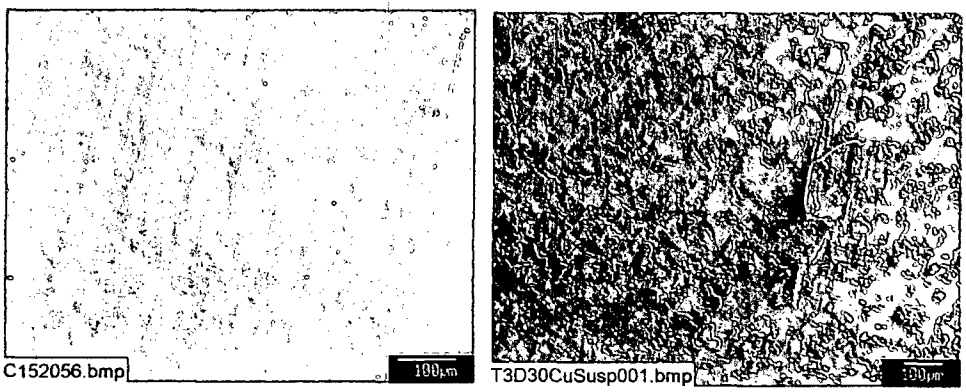

Figure 4-148. Test #2 unsubmerged copper (left); Test #3 unsubmerged copper (right).

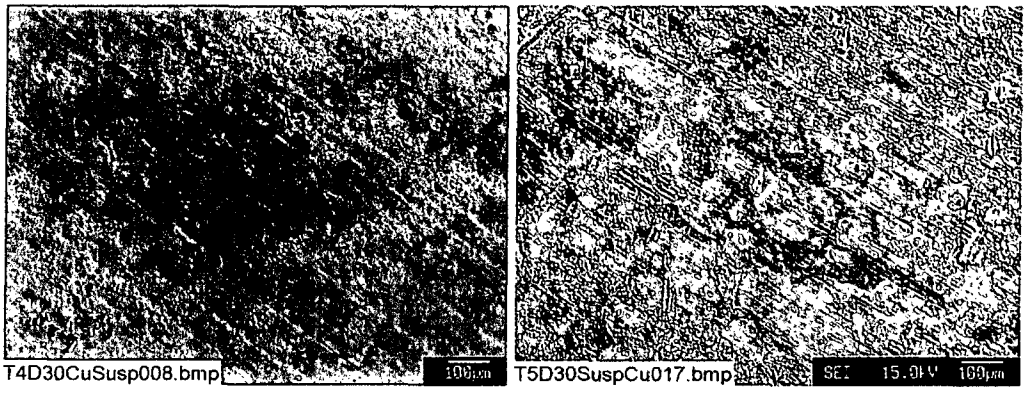

Figure 4-149. Test #4 unsubmerged copper (left); Test #5 unsubmerged copper (right).

Submerged Galvanized Steel Coupons

Figures 4-150 through 4-152 show SEM images of unused and submerged GS coupons from Tests #1 through #5, respectively. For the GS coupons, the steel surface is coated with zinc. Zinc has the second lowest redox potential, as shown in Table 4-9. The purpose of zinc galvanization is to coat iron with a material that is more likely to corrode; therefore, the corrosion of iron is prevented by the corrosion of the zinc. As a result, the corrosion of the zinc surface layer causes the coupon surface to become significantly rougher after the tests. It should be noted that the zinc

concentration was <10 mg/L in all five of the tests, which was higher than copper but generally lower than aluminum, in accordance with the redox potential. It should be noted that the zinc concentration in solution may have been affected by other chemical species that complexed with zinc and formed precipitates.

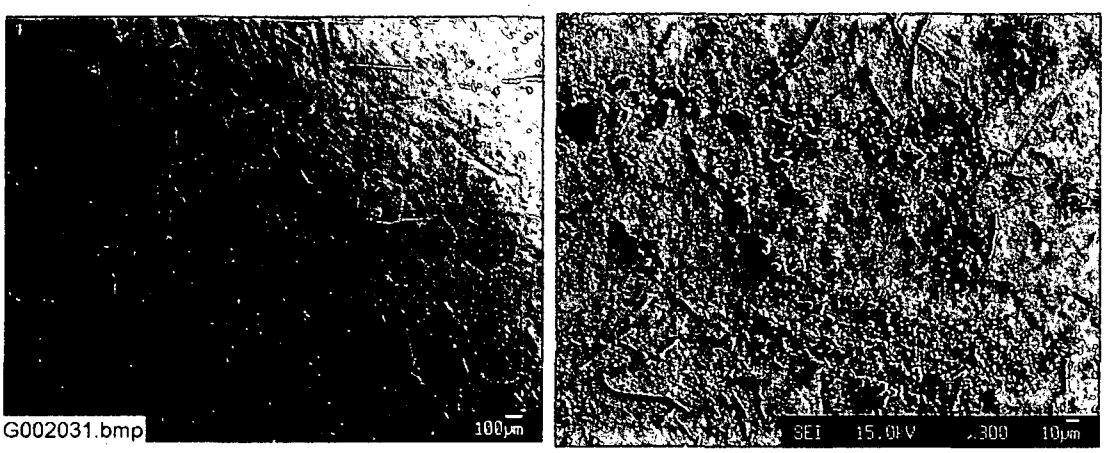

Figure 4-150. Unused galvanized steel coupon (left); Test #1 submerged galvanized steel (right).

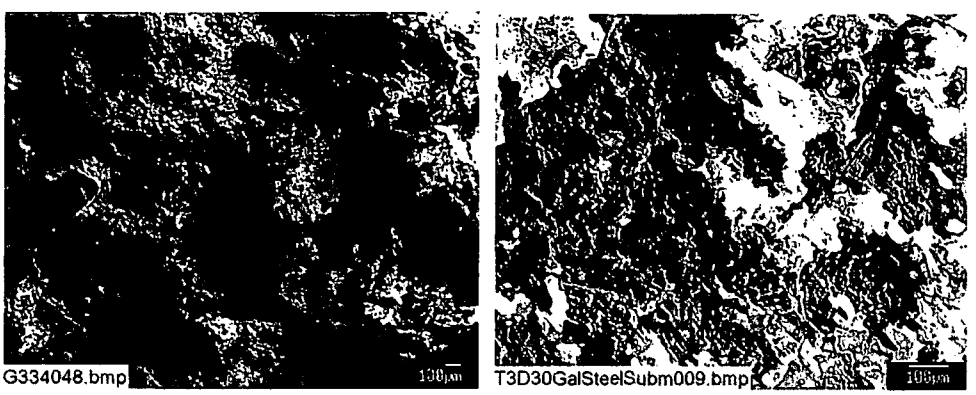

Figure 4-151. Test #2 submerged galvanized steel (left); Test #3 submerged galvanized steel (right).

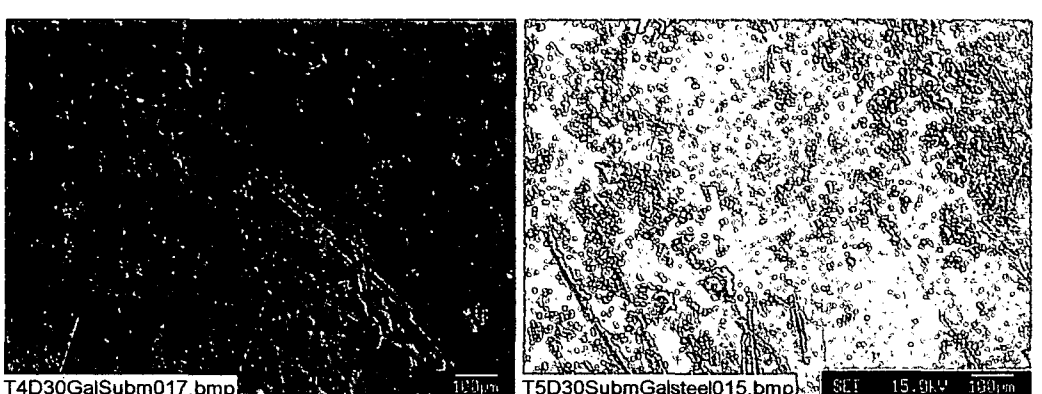

Figure 4-152. Test #4 submerged galvanized steel (left); Test #5 submerged galvanized steel (right).

Unsubmerged Galvanized Steel Coupons

As shown in Figures 4-153 to 4-155, corrosion occurred on the unsubmerged GS coupons. However, in contrast to the aluminum and copper coupons, the amount of corrosion on the unsubmerged GS coupons was not always less than on the submerged coupons. The possible reason is that oxygen from air oxidized the unsubmerged GS surfaces to a large degree.

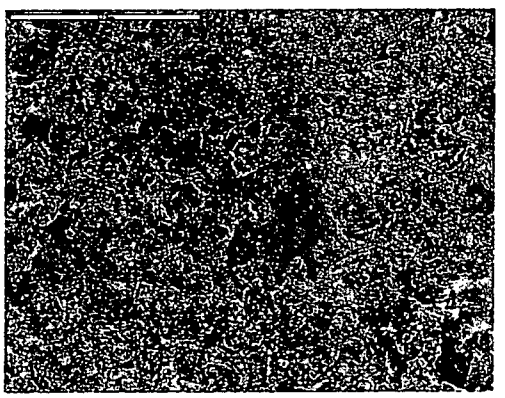

Figure 4-153. Test #1 unsubmerged galvanized steel.

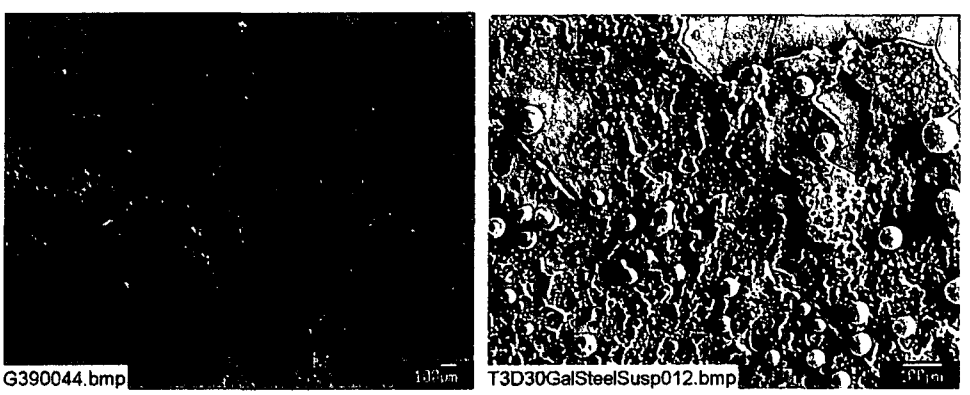

Figure 4-154. Test #2 unsubmerged galvanized steel (left); Test #3 unsubmerged galvanized steel (right).

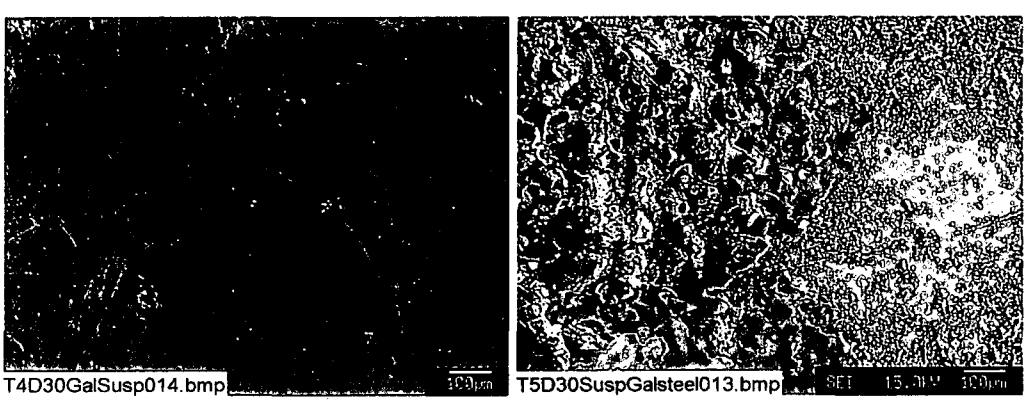

Figure 4-155. Test #4 unsubmerged galvanized steel (left); Test #5 unsubmerged galvanized steel (right).

Submerged Carbon Steel Coupons

Figures 4-156 to 4-158 are SEM images of unused and submerged carbon steel coupons from Tests #1 through #5, respectively. Iron has the second highest redox potential of the metals shown in Table 4-9. Therefore, iron is more readily oxidized than copper. As a result, corrosion was more significant with iron than with copper, based on the SEM images, i.e., the coupon surface became rough after the tests. However, the iron concentration in solution was mostly less than the detection limit in the ICET tests. The reason for the low iron concentration is that the product of iron corrosion, ferric hydroxide (rust), is extremely insoluble over the pH range of these tests and rust will form at the surface of the coupon instead of releasing soluble ferric ions into solution.

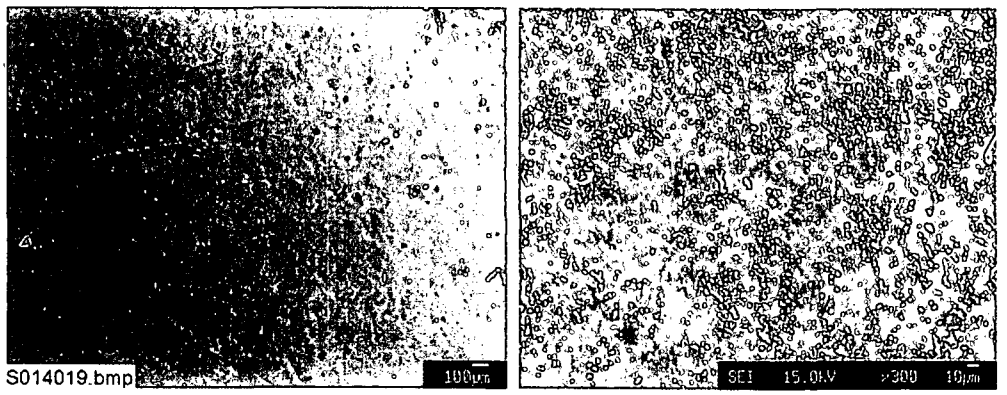

Figure 4-156. Unused carbon steel coupon (left); Test #1 submerged carbon steel (right).

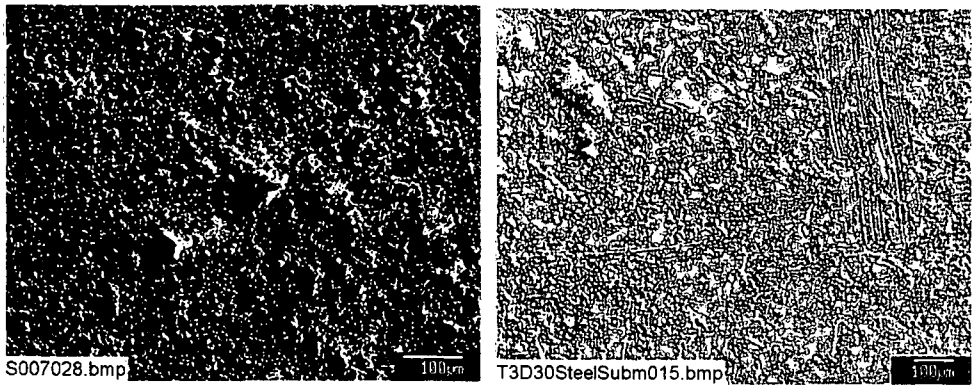

Figure 4-157. Test #2 submerged carbon steel (left); Test #3 submerged carbon steel (right).

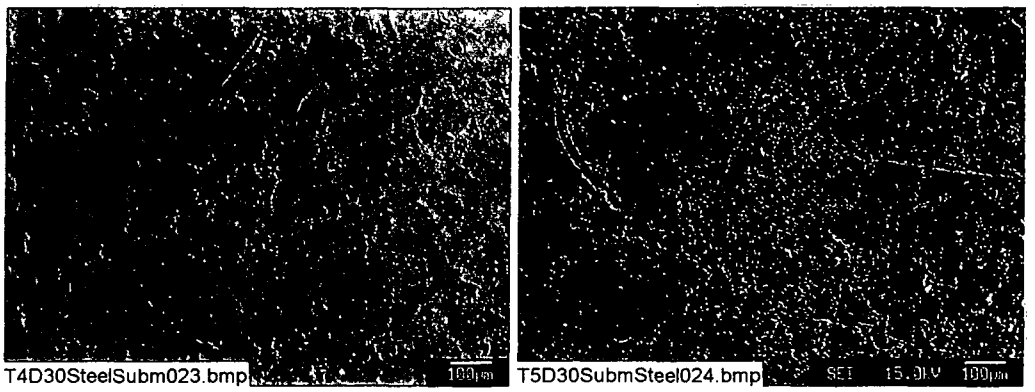

Figure 4-158. Test #4 submerged carbon steel (left); Test #5 submerged carbon steel (right).

Unsubmerged Carbon Steel Coupons

As shown in Figures 4-159 to 4-161, corrosion also occurred on the unsubmerged carbon steel coupons. As with the galvanized steel coupons, the degree of corrosion was not always greater for the submerged carbon steel coupons, especially for Tests #3 and #5. In those tests, the carbon steel corrosion rates in the moist oxygenated spray zone environment appeared to be greater than the submerged coupons.

Figure 4-159. Test #1 unsubmerged carbon steel.

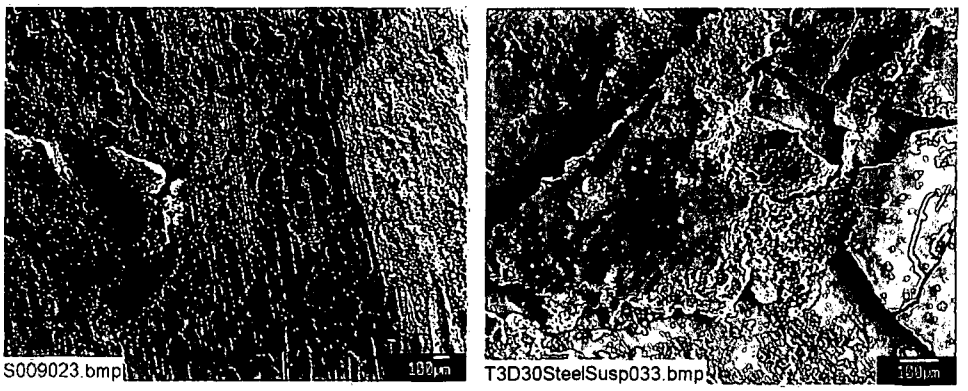

Figure 4-160. Test #2 unsubmerged carbon steel (left); Test #3 unsubmerged carbon steel (right).

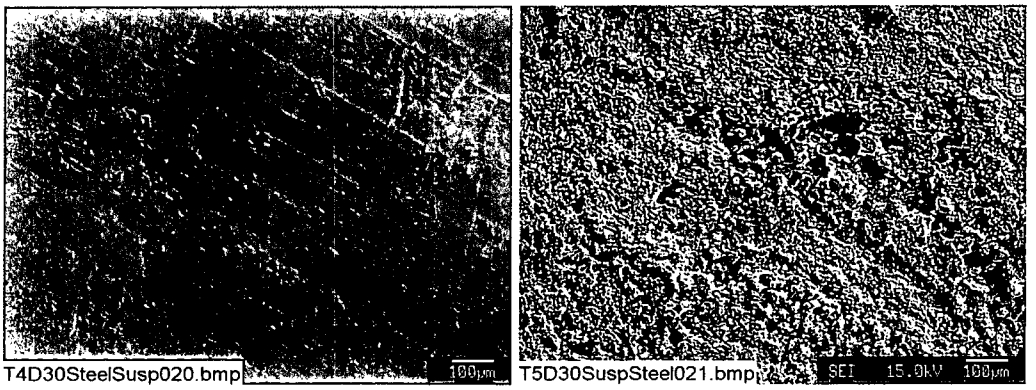

Figure 4-161. Test #4 unsubmerged carbon steel (left); Test #5 unsubmerged carbon steel (right).

4.4.3. Passivation of Test #4 Submerged Al Coupons

An interesting observation in the ICET tests is that the Test #4 submerged aluminum coupons had significantly less corrosion than the aluminum coupons in Test #1. The aluminum coupons (with an average weight of 392.0 g) had an average weight loss of 98.6 g over 30 days in Test #1 compared to an average weight loss of <0.1 g over 30 days in Test #4. The initial solution chemistry of these two tests was nearly identical, so the initial expectation was that the corrosion rates would be similar in both tests. The primary difference between the two tests was the insulation material; the Test #1 insulation was 100% fiberglass, and the Test #4 insulation was 20% fiberglass and 80% cal-sil. Since cal-sil was the only component that was in Test #4 and not in Test #1, it is possible that the cal-sil contributed to the critical difference in solution chemistry that prevented corrosion of the aluminum coupons in Test #4. Additional insights on the differences in aluminum corrosion in these tests can be found in Ref. 12.

Experimental results indicated differences in some aqueous concentrations over the duration of Tests #1 and #4. As shown in Figure 4-162, the aluminum concentration in Test #1 started at ~50 mg/L, increased until Day 16, and leveled off at ~350 mg/L, after Day 18. In contrast, the aluminum concentration in Test #4 was measured near the detection limit on the first 2 days and stayed below the detection limit for the remainder of the test. The increase in aluminum concentration over the first half of Test #1 suggests that corrosion proceeded over a number of days but stopped because the surface of the coupon was passivated and additional corrosion was impeded. Thus, it is likely that the differences in corrosion were because of differences in passivation of the coupon surfaces. Bench-scale experimentation and modeling verified that the solubility limit of aluminum at this pH and temperature was above the observed steady state concentration. Therefore, the leveling-off of aluminum concentration in Test #1 was not because of solubility considerations.

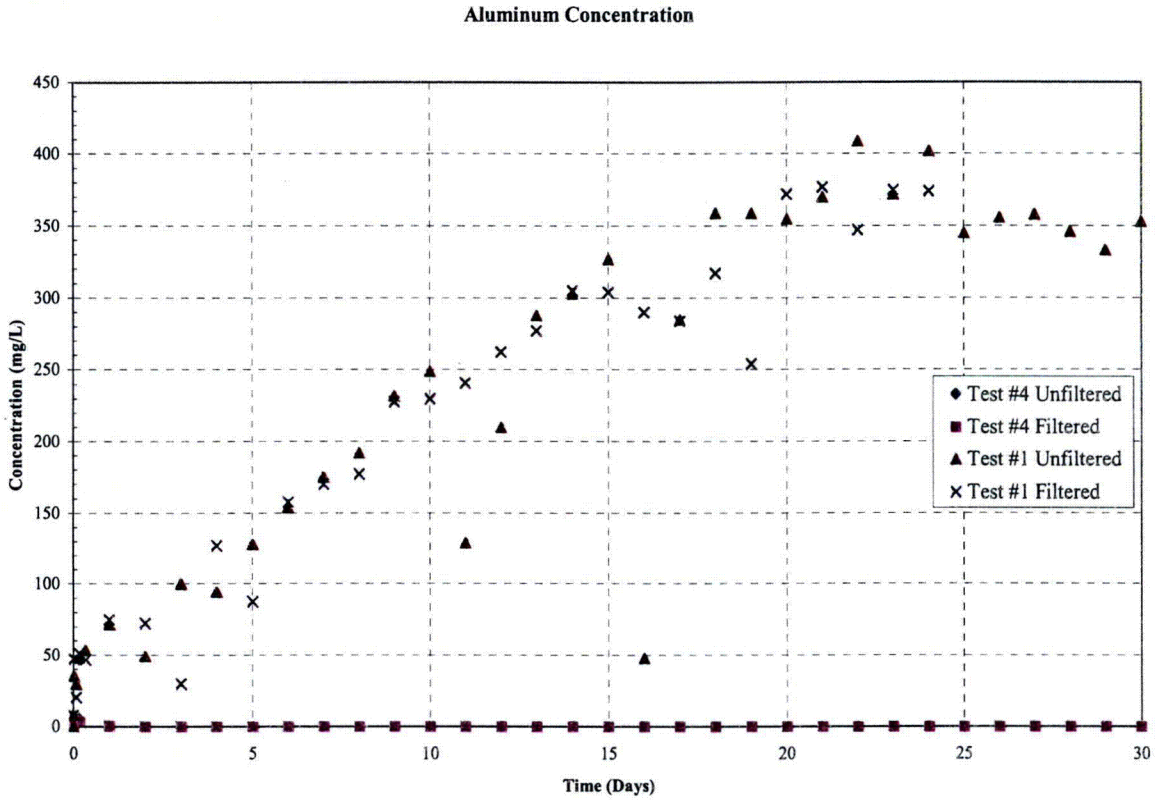

Figure 4-162. Aluminum concentration in ICET Test #1 and Test #4 daily water samples.

Figure 4-163 indicates that the silica concentration in the Test #4 solution was about one order of magnitude higher than in Test #1. The higher silica concentration was likely because of dissolution of cal-sil and the release of silicate to the solution in Test #4. A result may have been a reaction that formed an insoluble aluminum silicate coating on the coupons. To investigate this possibility, SEM and EDS analyses were performed on the Test #1 and #4 aluminum coupons. SEM images of an aluminum coupon after 30 days of submersion in Test #4 are shown in Figures 4-164 and 4-165, and EDS analyses associated with this coupon are shown in Figures 4-166 and 4-167. The SEM images show the formation of a crystalline material on the surface of the aluminum coupons, and the EDS in Figure 4-166 indicates that the major components on this crystalline structure were aluminum, oxygen, silicon, sodium, and calcium, with small amounts of carbon and magnesium. In contrast, the EDS of regions that appear to be the original coupon surface shows that the material was composed primarily of aluminum and oxygen, with small amounts of silicon and sodium. The difference in elemental composition of these two locations is compared in Table 4-12. The amount of oxygen in the area that appears to be the original surface may be an aluminum oxide or aluminum hydroxide surface layer. Aluminum oxide is very effective at passivating aluminum in air but may be less effective at passivating aluminum in aqueous solutions similar to those found in the ICET tests.

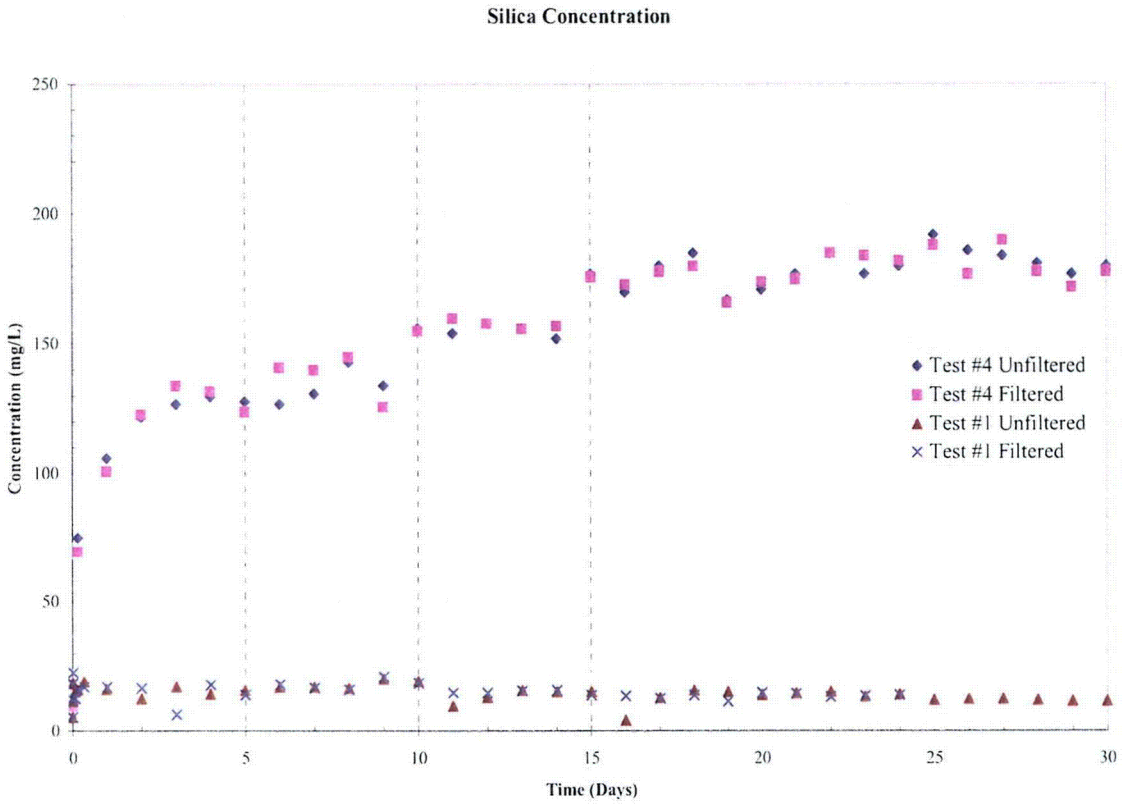

Figure 4-163. Silica concentration in ICET Test #1 and Test #4 daily water samples.

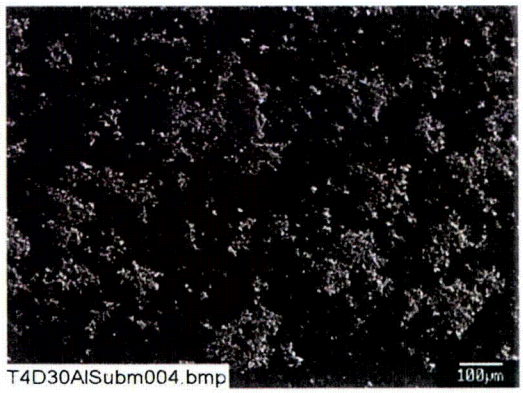

Figure 4-164. SEM image, magnified 100 times, of a Test #4, Day 30, submerged aluminum coupon sample. (T4D30AlSubm004.bmp)

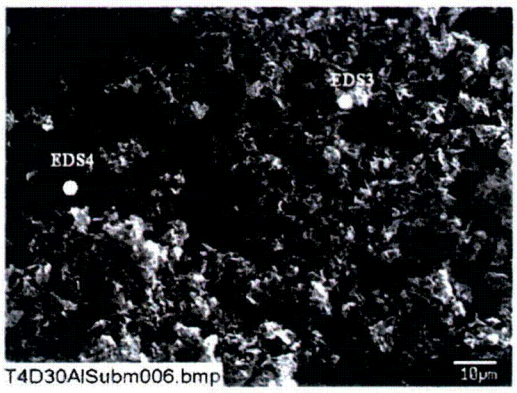

Figure 4-165. Annotated SEM image, magnified 1000 times, of a Test #4, Day 30, submerged aluminum coupon sample. (T4D30AlSubm006.bmp)

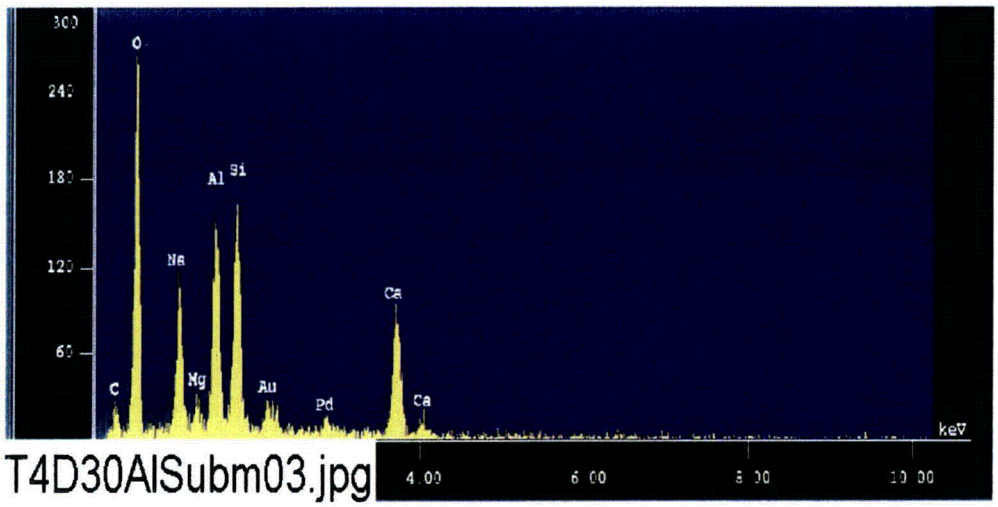

Figure 4-166. EDS counting spectrum for the deposits (EDS3) on the coupon surface shown in Figure 4-165. (T4D30AlSubm03.jpg)

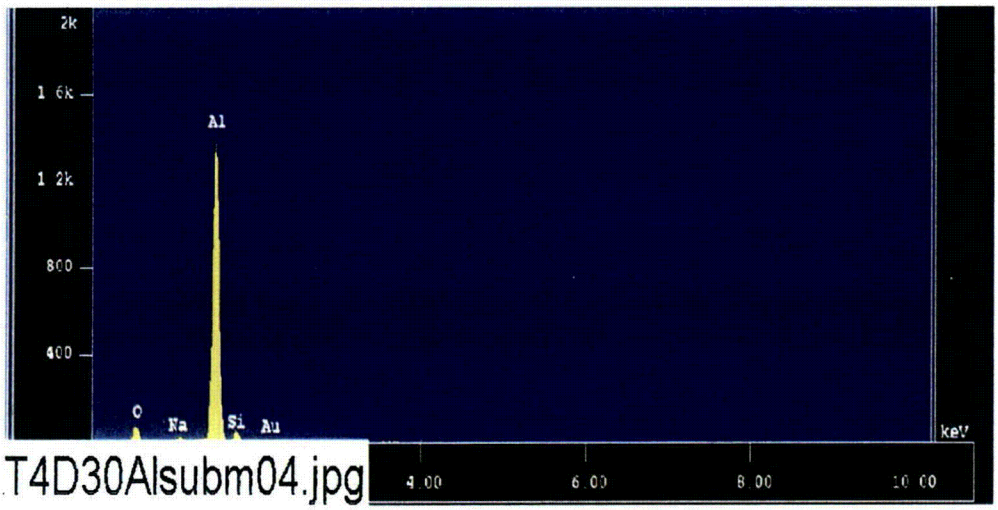

Figure 4-167. EDS counting spectrum for the flat coupon surface (EDS4), as shown in Figure 4-165. (T4D30AlSubm04.jpg)

Table 4-12. Elemental Compositions (by Mass %) of the Deposits and the Aluminum Coupon Surface, as Shown in Figure 4-163

Type	Al	Si	O	Ca	Na	Mg	C
Deposits (EDS3)	9.8	8.5	57.5	10.5	10.1	1.5	2.0
Submerged Aluminum Coupon Surface (EDS4)	74.6	3.5	20.7	N/D[a]	1.2	N/D	N/D

[a]N/D: Not detected

SEM images of an aluminum coupon after 30 days of submersion in Test #1 are shown in Figures 4-168 and 4-169. In contrast to Test #4, the SEM images show that the submerged aluminum coupon from Test #1 was rough and had many cracks, whereas the Test #4 aluminum coupon was smooth and integrated. EDS analyses associated with this coupon from Test #1 are shown in Figures 4-170 and 4-171. The elemental composition associated with this EDS analysis is presented in Table 4-13. From this analysis it is seen that silicon also was present on the aluminum coupon surface. Thus, it is possible that an insoluble aluminum silicate was responsible for passivating the aluminum coupons according to the following scenario. In Test #1, the aqueous silica concentration was low, and passivation did not occur until a high aluminum concentration was reached. In Test #4, passivation was achieved with a low aluminum concentration because the silica concentration was higher. A higher silica concentration in Test #4 solution was effective in forming a dense passivation layer on the submerged aluminum coupon surface. As a result, the corrosion was much less in Test #4. It should be noted that calcium might also have contributed to the passivation on the aluminum coupons. However, EDS results do not show the presence of calcium on the Test #4 aluminum coupon surface, except for loose deposits. Therefore, it is less likely that calcium was important for passivation in Test #4.

Figure 4-168. SEM image, magnified 300 times, of a Test #1, Day 30, submerged aluminum coupon sample. (Test1submAl015.bmp)

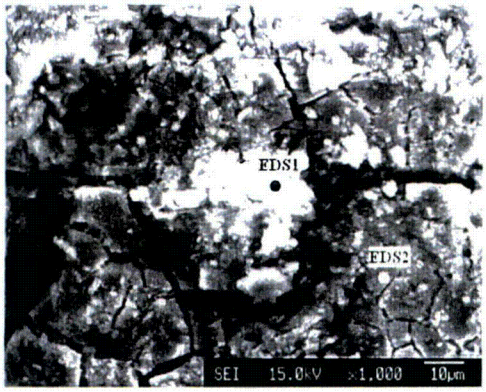

Figure 4-169. SEM image, magnified 1000 times, of a Test #1, Day 30, submerged aluminum coupon sample. (Test1submAl016.bmp)

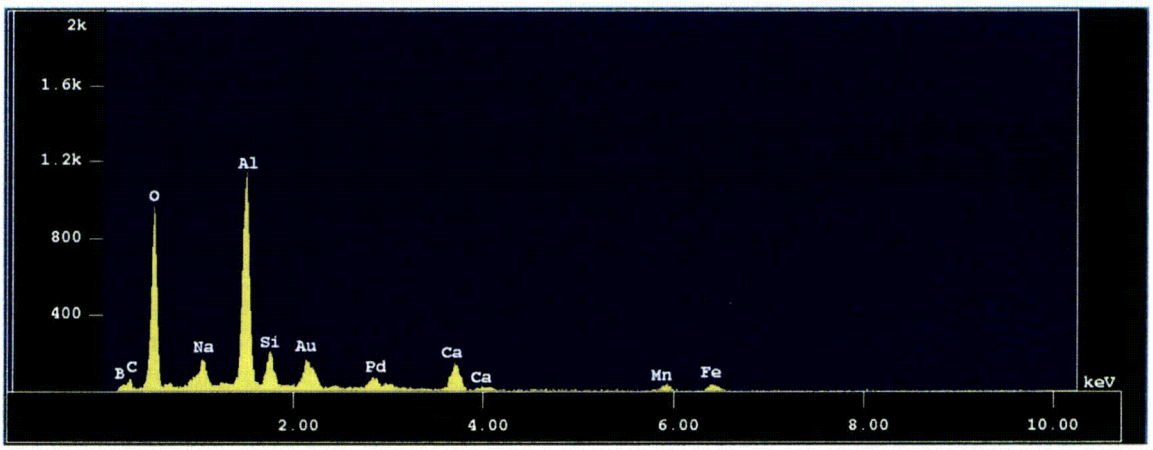

Figure 4-170. EDS counting spectrum for the light spot (EDS1) on the coupon surface shown in Figure 4-169. (T1AlEDS10.tif)

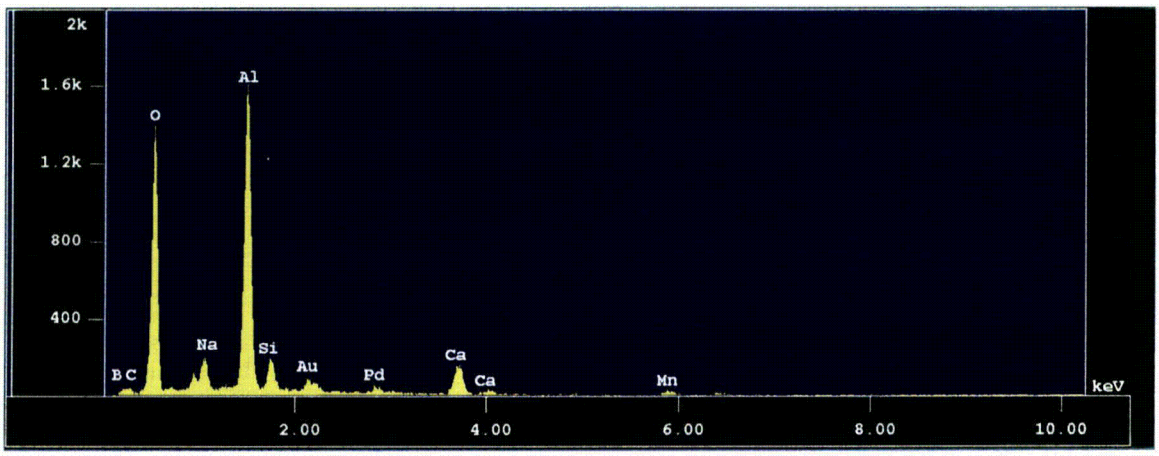

Figure 4-171. EDS counting spectrum for the grey coupon surface (EDS2) shown in Figure 4-169. (T1AlEDS11.tif)

Table 4-13. Elemental Compositions (by Mass %) of the Light and Grey Coating on the Aluminum Coupon Surface, as Shown in Figure 4-167

Type	Al	Si	O	Ca	Na	Mn	C	B	Fe
Light Coating (EDS1)	15.4	2.7	54.3	4.4	2.3	3.9	0	13.2	3.9
Grey Coating (EDS2)	18.4	2.2	60.8	4.6	2.4	2.7	0	8.9	N/D[a]

[a]N/D: Not detected

4.5. Deposition Products

Another phenomenon of interest in the ICET tests is the presence of deposition products because of corrosion, chemical precipitation, and/or physical sedimentation. These deposition products were fine powders that were extracted from horizontal and/or vertical pieces of the submerged CPVC coupon rack. Beginning with Test #2, deposition products were collected after each of the ICET tests was completed. The deposition products were collected by directly adhering the sample onto double-sided carbon tape suitable for SEM/EDS examination. After the samples were dried in air, a gold/palladium coating was applied to enhance the surface conductivity of the samples and to prevent possible charging problems during the SEM examination.

In general, the deposition products were composed of a variety of substances including insulation debris material (i.e., fiberglass and cal-sil), chemical precipitates, corrosion products, and other substances. In Tests #2 and #5, 100% of the insulation material was fiberglass; consequently, fiberglass debris was observed in the deposition products of these tests. In contrast, 80% of the fiberglass was replaced with cal-sil in Tests #3 and #4; as a result, cal-sil particles were likely present in the deposition products in these tests. In addition, because TSP was used in Tests #2 and #3, phosphorus was found in the elemental composition of the deposition products in those tests. This fact suggests that phosphate likely reacted with metal cations in the test solution and formed precipitates as deposition products. In addition, in Test #2, some white residues on a horizontal piece of the submerged CPVC rack were found to be rich in zinc. The result suggests that the residues likely originated from galvanized steel corrosion products.

Test #2 Deposition Products

Figures 4-172 and 4-173 show the SEM images of the deposition products collected from a vertical section of the submerged CPVC rack. In Figure 4-172, the cylindrical debris appears to be fiberglass, which mixed with other corrosion/precipitation products and debris. EDS results from Figure 4-174 indicate that the deposition products shown in Figure 4-173 were composed mainly of oxygen, phosphorus, magnesium, and carbon, with small amounts of aluminum, silicon, calcium, and sodium. Because TSP was used in Test #2, a precipitate of phosphate salts such as magnesium phosphate may have deposited on the submerged CPVC rack, in addition to other carbonate and metallic salts precipitates.

Figure 4-172. SEM image at 650× magnification of a Test #2, Day 30, sample of fine powder on a vertical piece of the submerged PVC rack. (T2D30_Cor_Prod003_Fine Powder)

Figure 4-173. SEM image at 1000× magnification of a Test #2, Day 30, sample of fine powder on a vertical piece of the submerged PVC rack. (T2D30_Cor_Prod002_Fine Powder)

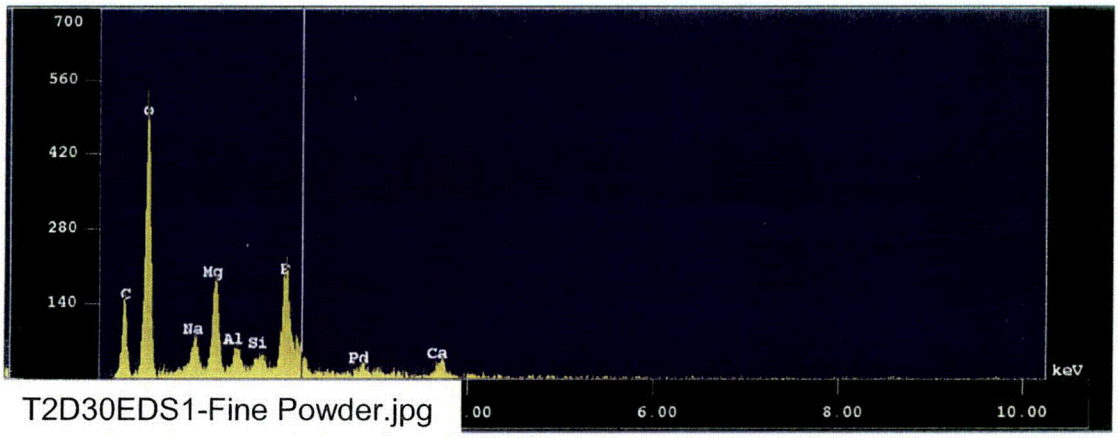

Figure 4-174. EDS counting spectrum for the entire SEM image shown in Figure 4-173. (T2D30EDS1-Fine Powder)

In addition, some white particulate residues were collected from a horizontal piece of the submerged CPVC rack and examined. The SEM image and EDS spectrum are shown in Figures 4-175 and 4-176, respectively. Semi-quantitative EDS results indicate that the mass composition of the white residue was primarily zinc, carbon, and oxygen, with smaller amounts of other

elements, as shown in Table 4-14. Because of a high zinc content in the substance, it is likely that the white residue originated from the corrosion products of galvanized steel, which peeled off the coupon and subsequently settled on the horizontal piece of the submerged CPVC rack.

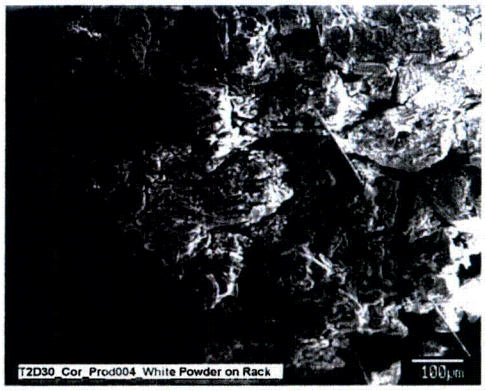

Figure 4-175. SEM image (130×) of a Test #2, Day 30, sample of white residue on a horizontal piece of the submerged CPVC rack. (T2D30_Cor_Prod004_White Powder on Rack)

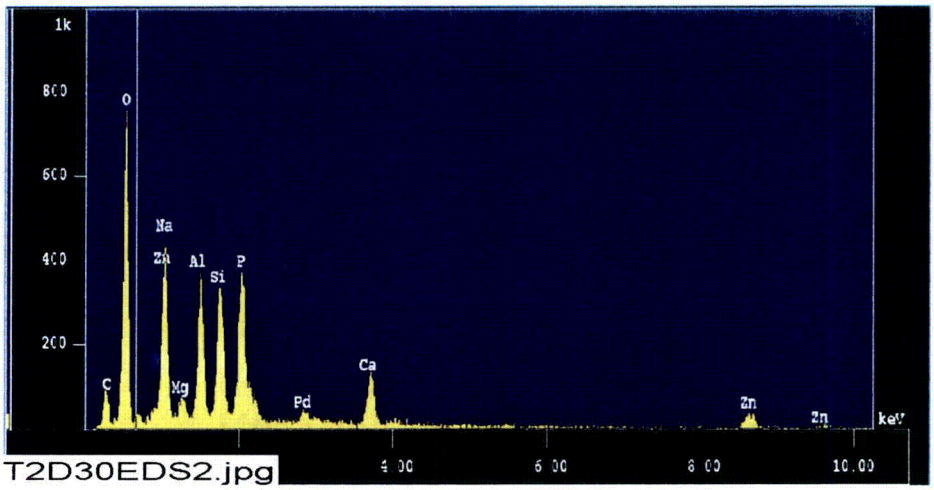

Figure 4-176. EDS counting spectrum for the white residue shown in Figure 4-175. (T2D30EDS2)

Table 4-14. Elemental Composition of Deposition Products Collected from Horizontal Surfaces on CPVC Coupon Racks after Tests Were Complete

Element	Test #2	Test #3	Test #4	Test #5
C	27	N/D[a]	1	35
O	39	48	52	50
Na	2	1	8	2
Mg	1	N/D[a]	N/D[a]	1
Al	4	N/D[a]	4	5
Si	4	3	15	6
P	6	13	N/D[a]	N/D[a]
Ca	3	34	19	2
Zn	14	N/D[a]	N/D[a]	N/D[a]
Likely dominant product	Zinc oxides, zinc carbonates	Calcium phosphate	Cal-sil	Carbonates

[a]N/D: Not detected.

Test #3 Deposition Products

After completion of Test #3, the fine powders on a horizontal piece of the submerged CPVC rack were collected for SEM/EDS analysis, and results are shown in Figures 4-177 and 4-178. Figure 4-177 indicates that the deposition products were composed mainly of particulate substances. The semi-quantitative EDS elemental analysis results show that the deposition products were composed mainly of calcium, phosphorus, and oxygen, with small amounts of sodium and silicon, as shown in Table 4-12. Because 80% of the fiberglass was replaced by cal-sil and TSP was used in Test #3, the deposition products are likely composed of precipitates such as calcium phosphate and cal-sil debris.

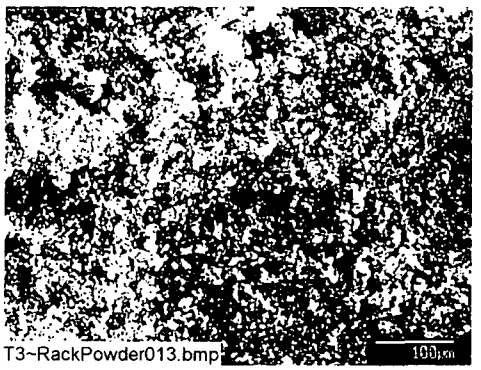

Figure 4-177. SEM image, magnified 200 times, of a Test #3, Day 30, powder on the submerged rack. (T3~RackPowder013)

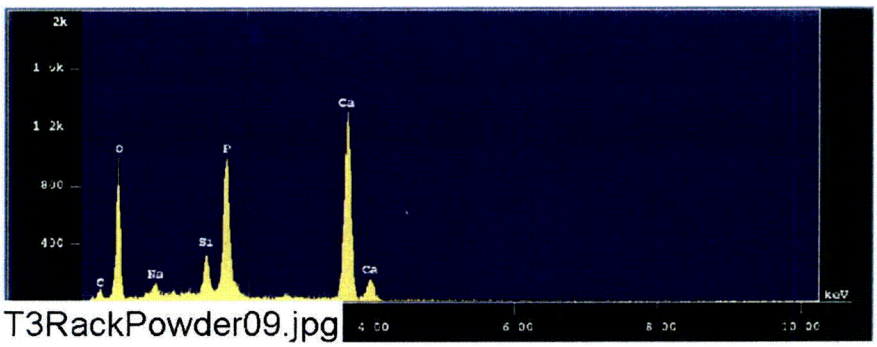

Figure 4-178. EDS counting spectrum for the powder on the submerged rack shown in Figure 4-177. (T3RackPowder09)

Test #4 Deposition Products

Fine powders on a horizontal piece of the submerged CPVC rack were collected when Test #4 ended. Figure 4-179 indicates that the deposition products were composed mainly of particulate substances. The EDS results are shown in Figure 4-180. Further semi-quantitative elemental analyses results indicated that the deposition products were composed mainly of calcium, silicon, oxygen, and small amounts of sodium, aluminum, and carbon, as shown in Table 4-14. Because 80% of the fiberglass was replaced by cal-sil and no TSP was used in Test #4, the deposition products likely are composed of cal-sil debris and other chemical precipitates.

Figure 4-179. SEM image, magnified 1000 times, of a Test #4, Day 30, fine powder on the submerged rack. (T4D30RackPowder030.bmp)

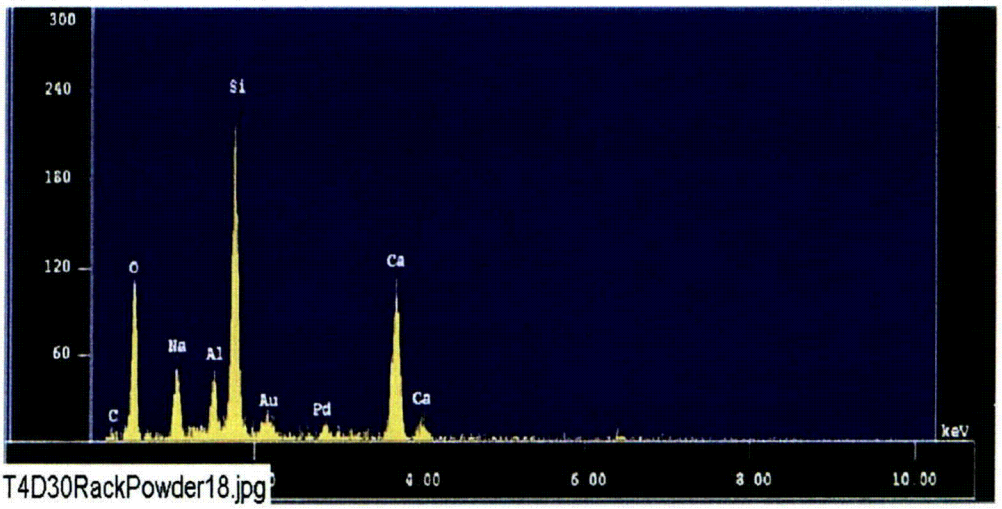

Figure 4-180. EDS counting spectrum for the particles (whole image) shown in Figure 4-179. (T4D30RackPowder18.jpg)

Test #5 Deposition Products

The deposition products collected upon completion of Test #5 were fine yellow powders that had deposited on a horizontal piece of the submerged CPVC rack. The SEM images of the deposition products are shown in Figures 4-181 and 4-182. From the figures, the deposition products were composed mainly of fiberglass debris and other substances. (Note that cal-sil was used only in Tests #3 and #4). The yellow color of the deposition products is consistent with the color of the fiberglass used in the test. Figure 4-183 shows the EDS spectrum of a particle as labeled in Figure 4-182, which was composed of carbon and oxygen, with smaller amounts of aluminum, silicon, sodium, calcium, and magnesium, as summarized in Table 4-14. As a result, the substance was likely a carbonate precipitate.

Figure 4-181. SEM image, magnified 100 times, of the Test #5 Day 30, fine yellow powder on the submerged rack. (T5D30YellowDeposits001.bmp)

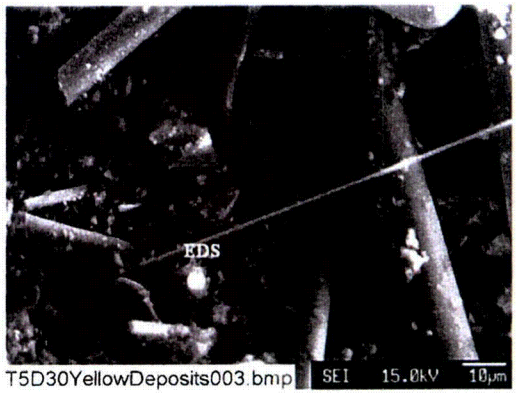

Figure 4-182. Annotated SEM image, magnified 1000 times, for the Test #5, Day 30, fine yellow powder on the submerged rack. (T5D30YellowDeposits003.bmp)

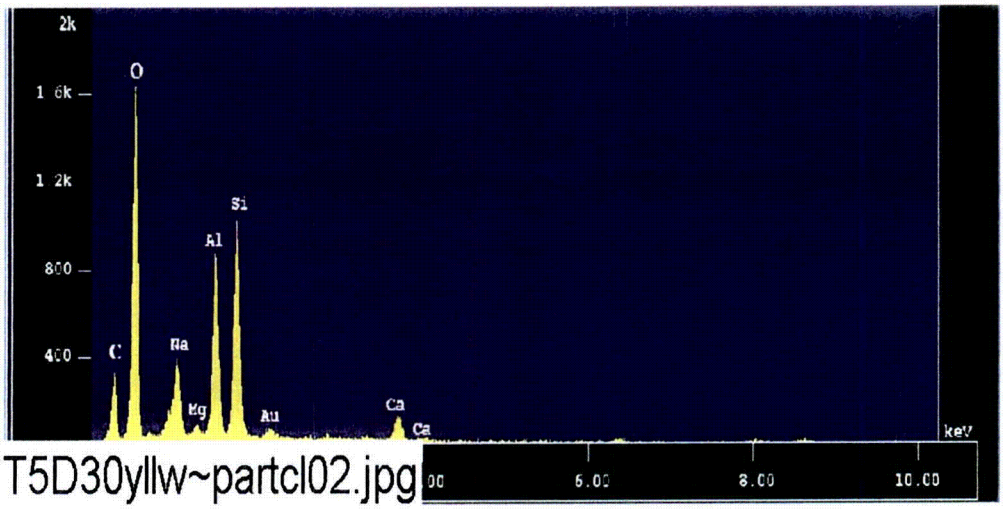

Figure 4-183. EDS counting spectrum for the particulate deposit shown in Figure 4-182. (T5D30yllw~partcl02.jpg)

4.6. Gel Analysis

There were two unique observations from ICET Test #3. First, a significant amount of white gel-like precipitates were observed in the test solution for several hours on the first day of the test during and after the injection of TSP. Looking through the tank's submerged view window, the test solution appeared to be nearly saturated with these precipitates that were moving robustly in a circular pattern. Second, when the test was completed, deposits of pinkish-white gel-like material were found on the top of the sediment and on other objects on the tank bottom. This material covered the majority of objects on the tank bottom including the birdcage, but it was not a continuous covering. Figures 4-184 and 4-185 are photographs of the gel-like material.

Figure 4-184. Stainless steel mesh covered with gel-like material.

Figure 4-185. Gel-like material recovered from the bottom of the tank.

SEM images of the gel-like material are shown in Figures 4-186 and 4-187. EDS results (Figure 4-188 and Table 4-15) indicated that 92% of the gel-like material was composed of calcium, oxygen, and phosphorus. Comparable ESEM and EDS images are shown in Figures 4-189 and 4-190. Consistently, XRF results (Table 4-16) indicated that the gel-like precipitates contained significant amounts of calcium and phosphorus. Therefore, it is likely that the gel-like material was $Ca_3(PO_4)_2$. In addition, EDS and XRF results indicated that the gel-like material had a small amount of carbon, possibly resulting from carbonate (CO_3^{2-}) and/or organic carbon from the test solution.

Based on water quality modeling using Visual Minteq 2.30 and on XRD results (Figure 4-191), the white gel-like material contained crystalline substances of $Ca_5(PO_4)_3OH$ (hydroxylapatite), $Ca_9HPO_4(PO_4)_5OH$ (calcium hydrogen phosphate hydroxide), and $Ca_3(PO_4)_2 \cdot xH_2O$ (calcium phosphate hydrate). It should be noted that XRD can detect only crystalline substances. Consequently, any amorphous substances would not be reflected in the XRD results.

Significant amounts of the gel-like material were deposited on top of the birdcage. SEM/EDS analyses were performed to compare the gel-like material on top of the birdcage with the particulate deposits on the exterior of fiberglass samples taken from inside the birdcage. Those analyses showed that their compositions were not exactly the same. The gel-like material contained higher amounts of phosphorus and lower amounts of silicon than did the particulate deposits on the fiberglass. As with any SEM sample, the gel-like material was dried before the analyses. Because its consistency was similar to that of a thick slurry, the drying process was unlikely to affect the major solid composition of the sample.

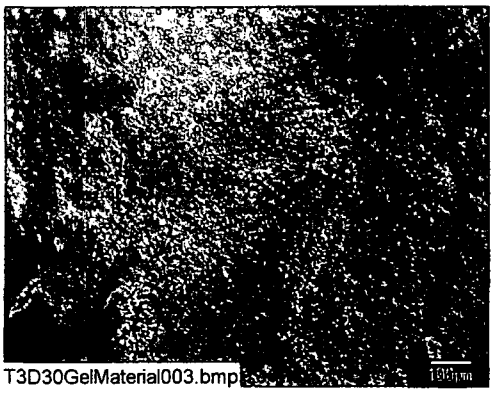

Figure 4-186. SEM image of a Test #3, Day 30, white gel-like material from the top of the birdcage, magnified 100 times. (T3D30GelMaterial003, 5/9/05)

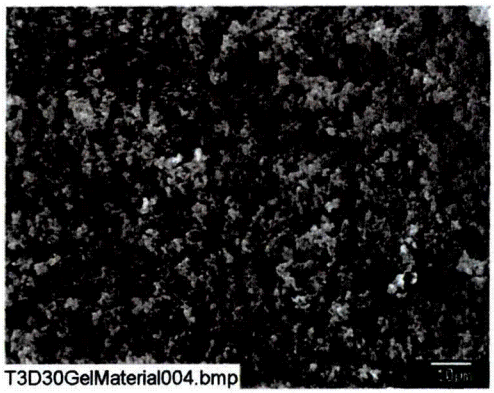

Figure 4-187. SEM image of a Test #3, Day 30, white gel-like material from the top of the birdcage, magnified 1000 times. (T3D30GelMaterial004, 5/9/05)

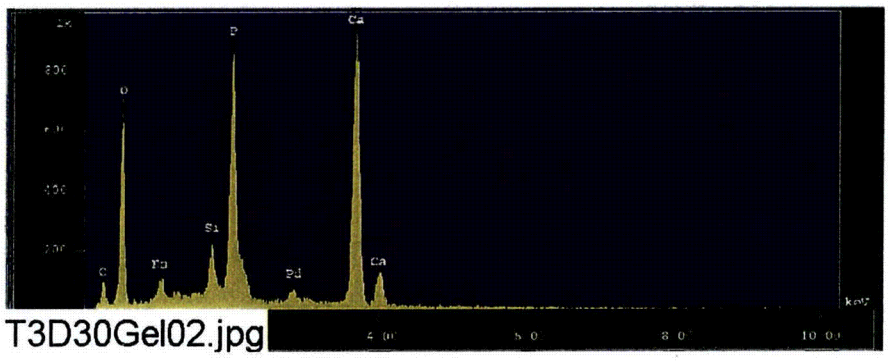

Figure 4-188. EDS counting spectrum for the white, gel-like material (whole image) shown in Figure 4-187. (T3D30Gel02, 5/9/05)

Table 4-15. The Chemical Compositions for Figure 4-188

May 9 2005

Group : NRC
Sample : T3D30 ID# : 2
Comment : GelMaterial
Condition : Full Scale : 20KeV(10eV/ch,2Kch)
Live Time : 60.000 sec Aperture # : 1
Acc. Volt : 15.0 KV Probe Current : 1.606E-09 A
Stage Point : X=79.625 Y=59.260 Z=11.424
Acq. Date : Mon May 9 11:42:11 2005

Element	Mode	ROI(KeV)	K-ratio(%)	+/-	Net/Background
C K	Normal	0.09- 0.46	0.6057	0.0005	338 / 119
O K	Normal	0.25- 0.77	12.2043	0.0032	4587 / 68
Na K	Normal	0.81- 1.27	0.5675	0.0010	613 / 50
Si K	Normal	1.50- 2.05	0.9391	0.0005	1366 / 271
P K	Normal	1.75- 2.38	8.4975	0.0055	7628 / 107
Ca K	Normal	3.39- 4.30	17.1295	0.0038	12109 / 26

Chi_square = 42.7915

Element	Mass%	Atomic%	ZAF	Z	A	F
C	4.355	7.8616	3.7318	1.0194	3.6611	0.9999
O	45.521	61.6928	1.9361	0.9721	1.9917	1.0000
Na	1.639	1.5456	1.4989	1.0256	1.4614	1.0000
Si	2.072	1.5994	1.1451	0.9756	1.1812	0.9937
P	13.776	9.6435	0.8415	1.1708	0.7203	0.9978
Ca	32.638	17.6571	0.9890	0.9947	0.9943	1.0000

Total 100.000 100.0000
Normalization factor = 1.9265
Total 100.000 100.0000
Normalization factor = 2.1120

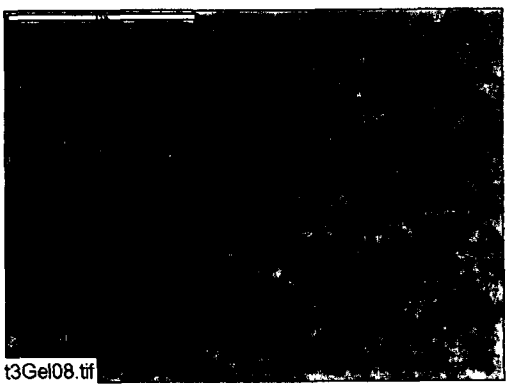

Figure 4-189. ESEM image of a Test #3, Day 30, white gel-like material from the top of the birdcage, magnified 1000 times. (t3Gel08, 5/6/05)

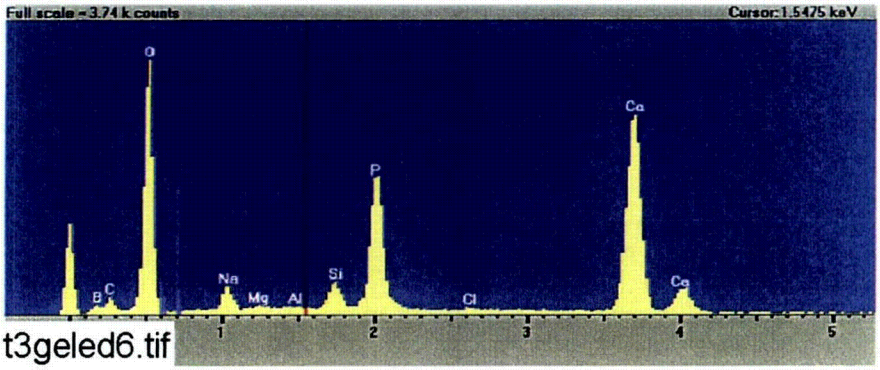

Figure 4-190. EDS counting spectrum for the white, gel-like material shown in Figure 4-189. (t3geled6, 5/6/05)

Table 4-16. Dry Mass Composition (%) of a Test #3 Day 30, White Gel-Like Sample by XRF Analysis

Compound	%
SiO_2	5.26
TiO_2	0.02
Al_2O_3	0.63
Fe_2O_3	0.07
FeO	0.00
MnO	0.00
MgO	0.25
CaO	35.01
Na_2O	2.39
K_2O	0.06
P_2O_5	27.09
$H_2O(-)$	4.75
$H_2O(+)CO_2$	19.24
Total	94.77

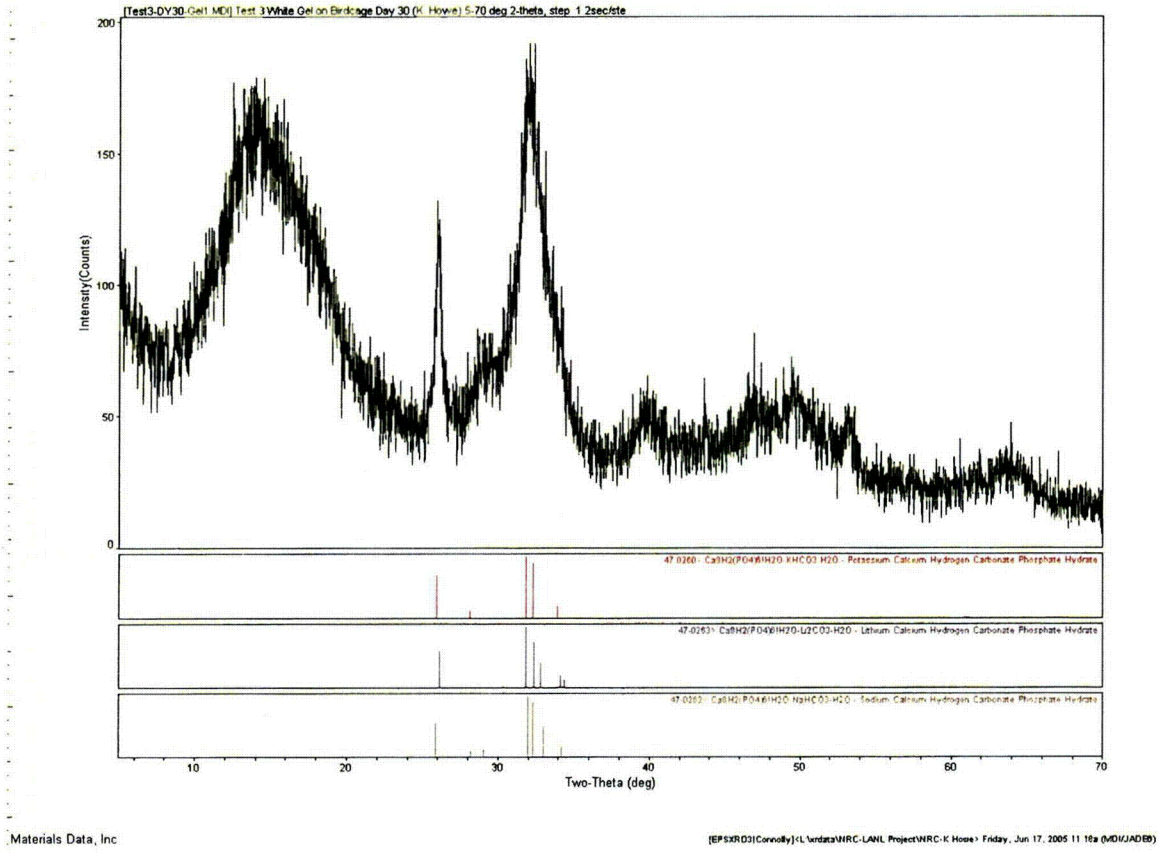

Figure 4-191. XRD results for a Test #3, Day 30, white gel-like sample.

5. CONCLUSIONS

The primary objectives for the ICET test series were (1) to determine, characterize, and quantify chemical-reaction products that may develop in the containment sump under a representative post-LOCA environment and (2) to determine and quantify any gelatinous material that might be produced during the post-LOCA recirculation phase. Five tests were performed under different conditions, and they produced a variety of results.

In Test #1, the submerged aluminum coupons experienced a prominent reduction in mass over the 30 days of testing, which was attributable to the system pH of 9.4–9.5. Aluminum was detected in the test solution shortly after the test began and rose to a maximum pseudo-steady-state concentration of ~350 mg/L after 20 days. This increase in soluble aluminum is characteristic of continuous corrosion and subsequent passivation of the coupons, possibly caused by aluminum silicates, which occurred late in the test.

Although the presence of a gelatinous substance was not visually detected at the test temperature (60°C) during the entire test, chemical product precipitation occurred upon reduction of the solution temperature. The precipitate appeared to form more rapidly and in larger amounts over the test duration. ICP analysis of the precipitate revealed that it was composed largely of aluminum, sodium, and boron. TEM analysis helped determine that the precipitate was amorphous in nature. It was also noted that the precipitate did not fully re-dissolve when the solution was reheated.

Other observations were consistent with the presence of precipitates in the Test #1 solution. At 23°C, the turbidity was greater than at 60°C, and it increased over the duration of the test. Kinematic viscosity at 23°C was also greater than at 60°C, and it increased as the test progressed. The test solution was Newtonian at test temperature. However, at 25°C it demonstrated shear thinning, a characteristic of a non-Newtonian fluid.

Test #2 system interactions did not produce significant amounts of chemical precipitates or gelatinous material in the test solution. The system pH of 7 provided an environment of low corrosion of the metal coupons, which limited the effect of a complicated chemical environment. The observed chemical deposits, upon analysis of the fiberglass within the system, were attributed to the chemical byproducts formed in the test or from the drying process for sample analysis.

Analysis of the Test #3 system revealed large amounts of chemical precipitation and significant amounts of a gel-like material. Chemical precipitation occurred in solution at the test temperature during the first 4 hours of testing but was not observed afterwards, even on cooling, throughout the remainder of the test. During the test, the pH increased from 7.3 to 8, which decreased the buffering capability of the system and allowed for corrosion.

After the test solution was drained from the tank, a gel-like material was found as the top layer of the large sediment bed at the bottom of the tank, as well as on insulation samples placed within the tank. EDS results from the gel-like layer showed that 92% of the deposit was composed of calcium, oxygen, and phosphorus. It is likely that this layer was composed largely of $Ca_3(PO_4)_2$. Based on XRD results, the gel-like precipitates contained crystalline substances. Analysis of the

insulation samples showed large amounts of deposits on the exterior of the samples, which increased as the test progressed. The interior of the fiberglass was relatively pristine. Phosphorus was present on the outside surface of some of the submerged cal-sil chunks, while no significant phosphorus was found in the interior part of the cal-sil chunks. Analysis of the sediment suggested that it consisted largely of the cal-sil that was added at the beginning of the test, as well as fiberglass insulation and corrosion products.

During Test #4, large amounts of chemical deposit were detected on the fiberglass insulation samples as in Test #3. No measurable amount of chemical precipitates or gelatinous structures was detected in the test solution. A system pH of 9.8 was expected to promote the corrosion of the aluminum coupons; yet very little corrosion occurred. The lack of corrosion is hypothesized to result from passivation by an insoluble aluminum silicate coating on the coupons. This hypothesis is supported by EDS analysis of the coupons and solution chemistry.

The Test #5 environment did produce small amounts of chemical precipitates when the test solution cooled, but not at the test temperature. The precipitates took several days to form, and their quantity did not increase appreciably over the test duration. The presence of a gelatinous substance was not detected during the test. Aluminum was detected in the test solution shortly after the test began and rose to a maximum concentration of ~50 mg/L by the middle of the test. The presence of aluminum in solution was attributable to the system pH of 8.2 to 8.5, which promoted aluminum corrosion. When the solution cooled, small amounts of precipitate were observed. The precipitates were composed largely of aluminum, boron, calcium, and sodium. Few, if any, deposits were detected on the fiberglass samples obtained from the tank.

Behavior of the Test #5 test solution at 23°C was similar to the behavior of the Test #1 solution at the same temperature. Turbidity and kinematic viscosity at 23°C were greater than at 60°C, although they did not increase significantly throughout the test. The solution also exhibited shear thinning at 25°C, indicative of a non-Newtonian fluid.

The ICET series used three different buffering agents. When comparing these agents, sodium hydroxide and sodium tetraborate produced a solution pH that facilitated corrosion of the submerged aluminum coupons. Corrosion of the aluminum coupons could lead to the formation of chemical precipitates, which could transform to gelatinous products upon temperature reduction. The presence of cal-sil in the Test #4, high-pH system appeared to inhibit corrosion of the coupons, thus limiting the chemical constituents' formation of precipitates during decreases in temperature. Trisodium phosphate provided a neutral pH of 7, which had a decreased effect on the promotion of corrosion. When cal-sil was mixed into the Test #3 trisodium phosphate system, large amounts of chemical precipitation quickly occurred, and the formation of a gel-like material was observed.

The particle size distribution of the test solution was monitored throughout each of the five ICET tests. In Test #1, the particle size was smaller than 1 μm. In the other tests, the particle size distribution remained within the range of 1 to 100 μm. The distribution within that range varied from test to test.

6. REFERENCES

1. "Test Plan: Characterization of Chemical and Corrosion Effects Potentially Occurring inside a PWR Containment Following a LOCA, Rev. 13," July 20, 2005.

2. J. Dallman, J. Garcia, M. Klasky, B. Letellier, and K. Howe, "Integrated Chemical Effects Test Project: Test #1 Data Report," NUREG/CR-6914, Volume 2, U.S. Nuclear Regulatory Commission, Washington, D.C., 2006.

3. J. Dallman, B. Letellier, J. Garcia, M. Klasky, W. Roesch, J. Madrid, K. Howe, and D. Chen, "Integrated Chemical Effects Test Project: Test #2 Data Report," NUREG/CR-6914, Volume 3, U.S. Nuclear Regulatory Commission, Washington, D.C., 2006.

4. J. Dallman, B. Letellier, J. Garcia, J. Madrid, W. Roesch, D. Chen, K. Howe, L. Archuleta, and F. Sciacca, "Integrated Chemical Effects Test Project: Test #3 Data Report," NUREG/CR-6914, Volume 4, U.S. Nuclear Regulatory Commission, Washington, D.C., 2006.

5. J. Dallman, B. Letellier, J. Garcia, J. Madrid, W. Roesch, D. Chen, K. Howe, L. Archuleta, and F. Sciacca, "Integrated Chemical Effects Test Project: Test #4 Data Report," NUREG/CR-6914, Volume 5, U.S. Nuclear Regulatory Commission, Washington, D.C., 2006.

6. J. Dallman, B. Letellier, J. Garcia, J. Madrid, W. Roesch, D. Chen, K. Howe, L. Archuleta, and F. Sciacca, "Integrated Chemical Effects Test Project: Test #5 Data Report," NUREG/CR-6914, Volume 6, U.S. Nuclear Regulatory Commission, Washington, D.C., 2006.

7. K. Kasza, J. H. Park, B. Fisher, J. Oras, K. Natesan, and W. J. Shack, "Chemical Effects Head-Loss Research in Support of Generic Safety Issue 191," NUREG/CR-6913, U.S. Nuclear Regulatory Commission, Washington, D.C., 2006.

8. This reference is intentionally omitted.

9. *CRC Handbook of Chemistry and Physics*, 83rd edition, D. R. Lide, Ed. (CRC Press) 2002.

10. Corrosion of Aluminum and Aluminum Alloy, J. R. Davis, Ed. (ASM International: Materials Park, Ohio) p. 27, 1999.

11. K. R. Trethewey, and J. Chamberlain, *Corrosion for Students of Science and Engineering* (Longman Scientific & Technical: Hong Kong) 1988.

12. M. Klasky, J. Zhang, M. Ding, B. Letellier, D. Chen, and K. Howe, "Aluminum Chemistry in Prototypical Post-LOCA PWR Containment Environment," NUREG/CR-6915, U.S. Nuclear Regulatory Commission, Washington, D.C., 2006.

Appendix A

ICET Background Information

List of Figures

List of Tables

Appendix A. ICET Background Information

A.1. Project Test Plan Requirements

The ICET project represents a joint effort by the U.S. NRC and the nuclear utility industry, undertaken through the Memorandum of Understanding on Cooperative Nuclear Safety between the NRC and Electric Power Research Institute, Addendum on Integral Chemical Effects Testing for PWR ECCS Recirculation. As part of its contribution to the project, industry wrote "Test Plan: Characterization of Chemical and Corrosion Effects Potentially Occurring Inside a PWR Containment Following a LOCA." That test plan underwent several revisions during the ICET testing; Revision 12a was in place when ICET Test #1 began, and Revision 13 (Ref. A.1) was in place when Test #5 was conducted.

As stated in the test plan, the report addressed four topical areas: definition of test parameters, definition of the test loop, test performance, and characterization of test samples. The test plan served as the high-level guidance document for the ICET project. Selected information from the test plan is presented here.

The ICET project was begun with the objective of conducting five tests. Table A-1 shows the main parameters for each test. Each test ran for 30 days.

The materials included in the tests were zinc, aluminum, copper, carbon steel, concrete, and insulation materials such as fiberglass and cal-sil. The amounts of each material are given in the form of ratios (material surface area to water volume) in Table A-2, with three exceptions: concrete dust, which is presented as a ratio of mass to water volume, and fiberglass and cal-sil, which are presented as a ratio of insulation volume to water volume. Also shown in the table are the percentages of material that was submerged and unsubmerged in the test chamber.

Table A-1. Test Series Parameters

Run	Temp (°C)	TSP	NaOH	Sodium Tetraborate	pH	Boron (mg/L)	Notes
1	60	N/A	Yes	N/A	10	2800	100% fiberglass insulation test. High pH, NaOH concentration as required by pH
2	60	Yes	N/A	N/A	7	2800	100% fiberglass insulation test. Low pH, TSP concentration as required by pH.
3	60	Yes	N/A	N/A	7	2800	80% cal sil/20% fiberglass insulation test. Low pH, TSP concentration, as required by pH
4	60	N/A	Yes	N/A	10	2800	80% cal-sil/20% fiberglass insulation test. High pH, NaOH concentration, as required by pH.
5	60	N/A	N/A	Yes	8 to 8.5	2400	100% fiberglass insulation test. Intermediate pH, sodium tetraborate (borax) buffer.

Table A-2. Material Quantity/Sump Water Volume Ratios for ICET

Material	Value of Ratio for the Test (Ratio Units)	Percentage of Submerged Material (%)	Percentage of Unsubmerged Material (%)
Zinc in GS	8.0 (ft^2/ft^3)	5	95
Inorganic zinc primer coating (non–top coated)	4.6 (ft^2/ft^3)	4	96
IOZ primer coating (Top Coated)	0.0 (ft^2/ft^3)	–	–
Aluminum	3.5 (ft^2/ft^3)	5	95
Copper (including Cu-Ni alloys)	6.0 (ft^2/ft^3)	25	75
Carbon steel	0.15 (ft^2/ft^3)	34	66
Concrete (surface)	0.045 (ft^2/ft^3)	34	66
Concrete (particulate)	0.0014 (lbm/ft^3)	100	0
Insulation material (fiberglass or cal-sil)	0.137 (ft^3/ft^3)	75	25

The physical and chemical parameters that (1) are critical for defining the tank environment and (2) have a significant effect on sump-flow blockage potential and gel formation are summarized in Tables A-3 and A-4.

Table A-3. Physical Parameters for the ICET Tests

Water volume in the tank	949 L	250 gal.
Circulation flow	0–200 L/min	0–50 gpm
Spray flow	0–20 L/min	0–5 gpm
Sump temperature	60°C	140°F

Table A-4. Chemical Parameters for the ICET Tests

H_3BO_3 concentration	2800 mg/L as boron[a]
$Na_3PO_4 \cdot 12H_2O$ concentration	As required to reach pH 7 in the simulated sump fluid
NaOH concentration	As required to reach pH 10 in the simulated sump fluid
Sodium tetraborate (borax)	As required to reach boron concentration of 2400 mg/L
HCl concentration	100 mg/L*
LiOH concentration	0.7 mg/L as Li*

[a]Concentrations applicable for Tests #1 to #4. Concentrations for Test #5 are 2400 mg/L boron, 43 mg/L HCl, and 0.3 mg/L Li.

Appendix B contains information on ICET materials, including chemicals. Supplemental information is included here for concrete dust, latent debris, demineralized water, hydrochloric acid, sodium hydroxide, and lithium hydroxide.

Concrete dust was prepared by grinding material chipped from a corner of a surplus concrete coupon. Latent debris consisted of three size distributions and two different materials. Sand made up the two larger size distributions, which were 0.075–0.59 mm and 0.59–2 mm. These accounted for 35% and 28% of the total latent debris, respectively. Clay was used for the smallest size distribution, which was <0.075 mm.

Demineralized water was produced by reverse osmosis on-site using a commercially available Osmonics E-4 RO system, using tap water as the feed water, with no chemical additives. The conductivity produced by the system was typically <10 uS/cm (the test plan called for <50 uS/cm).

Hydrochloric acid was added as a liquid. It was ACS grade. The FW was 36.46 and assay (HCl) 36.5% to 38.0%. (Note: Actual concentrations of individual bottles were determined from lot numbers and used in calculations.) The source was EMD Corporation.

Sodium hydroxide was added as solid pellets. It was ACS grade. The FW was 40.00 and assay (NaOH) > 97%. The source was EMD Corporation.

Lithium hydroxide was added as anhydrous powder. The FW was 23.95 and the assay (LiOH) >96%. The source was Fisher Scientific Corporation.

Additional guidance in the test plan was translated into the ICET apparatus design, analytical methods and measurements of the test solution and samples, and project instructions within the QA program that determined test operations. Key aspects of these different areas are provided in Sections A.2 through A.4.

A.2. Test Apparatus Design

The functional design of the ICET test apparatus followed requirements in the test plan. Functional aspects of the test apparatus are as follows:

1. The central component of the system is a test tank. The test apparatus was designed to prevent solids from settling in the test piping.

2. The test tank can maintain both a liquid and a vapor environment, as would be expected in post-LOCA containment.

3. The test loop controls the liquid temperature at 60°C (±3°C).

4. The system circulates water at flow rates that simulate spray flow rates per unit area of containment cross section.

5. The test tank provides for submerged test coupons to be subjected to water flow that is representative of containment pool fluid velocities expected at plants.

6. Piping and related isolation valves are provided such that a section of piping can be isolated without interrupting the test.

7. The pump discharge line is split in two, one branch directing the spray header into the tank's vapor space and the other returning to the liquid side of the tank. Each branch is provided with an isolation valve, and the spray line includes a flow meter.

8. The recirculation piping includes a flow meter.

9. The pump circulation flow rate is controlled at the pump discharge to be within ±5% of the flow required to simulate fluid velocities in the tank. Flow is controlled manually.

10. The tank accommodates a rack of immersed sample coupons, including the potential reaction constituents identified in the test plan.

11. The tank also accommodates six racks of sample coupons that are exposed to a spray of liquid that simulates the chemistry of a containment spray system. Provision is made for these racks to be visually inspected.

12. The coupon racks provide sufficient space between the test coupons to preclude galvanic interactions among the coupons. The different metallic test coupons are also electrically isolated from each other and from the test stand to prevent galvanic effects resulting from metal-to-metal contact between specimens or between the test tank and the specimens.

13. The fluid volumes and sample surface areas are based on scaling considerations that relate the test conditions to actual plant conditions.

14. All components of the test loop are made of corrosion-resistant material (for example, SS for metallic components).

The as-built test loop consists of a test tank, a recirculation pump, 2 flow meters, 10 isolation valves, and pipes that connect the major components, as shown schematically in Figure A-1. P, T, and pH represent pressure, temperature, and pH probes, respectively. Figures A-2 and A-3 are photographs of the test loop and the data-acquisition system, respectively.

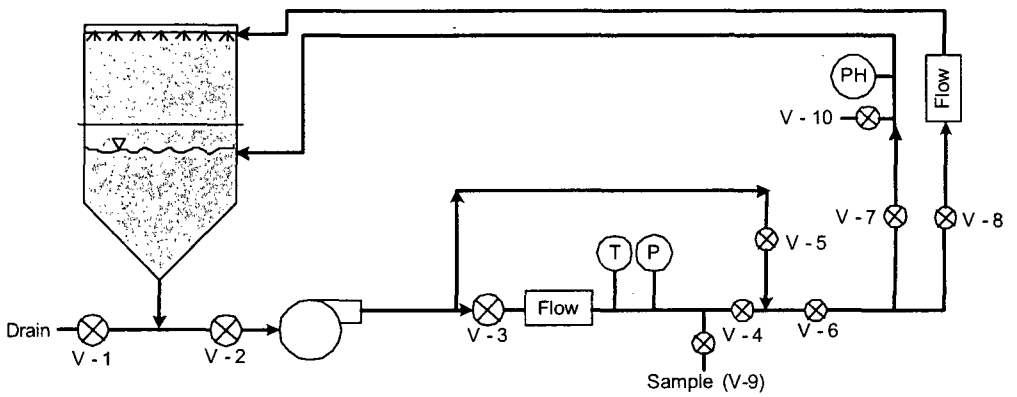

Figure A-1. Test loop process flow diagram.

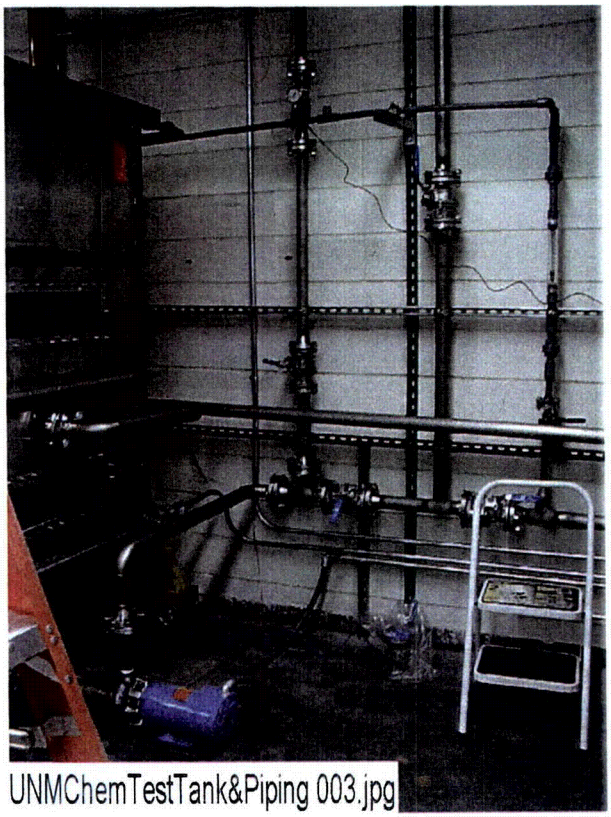

Figure A-2. Photograph of the test loop.

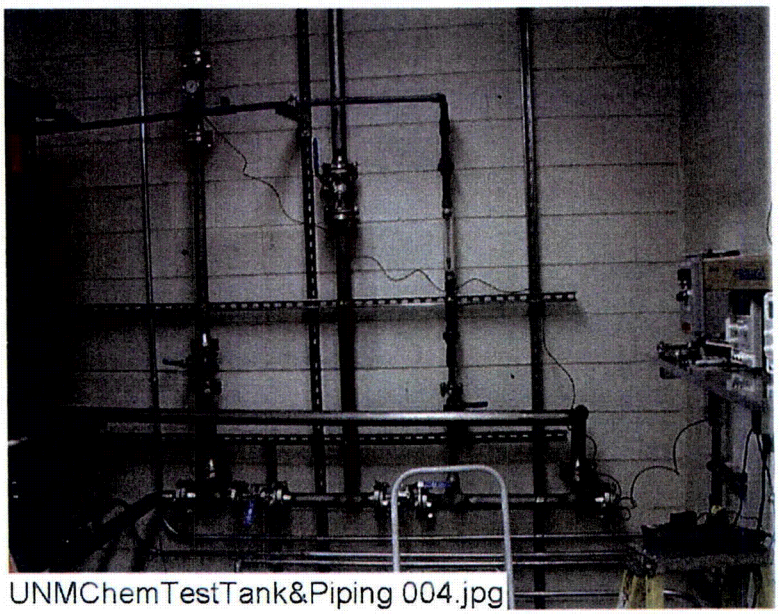

Figure A-3. Photograph of the data-acquisition system.

Materials

The tank, piping, and components were made of materials that are chemically resistant to a mixture of RO-treated water, sodium hydroxide, TSP, lithium hydroxide, hydrochloric acid, and boric acid in a pH range of 7.0 to 12.0 and a temperature of 140°F. Only one pH control chemical, either NaOH (resulting in a pH of ~10) or TSP (resulting in a pH of ~7), was used in a given test. The tank is constructed of type 304 SS, with polycarbonate view windows and Goretex® gaskets. The bottom portion of the tank is constructed of 1/8-in.-thick sheet steel, reinforced with 1/4-in.-thick by 2-in.-wide angle iron. The upper portion of the tank is constructed of 1/16-in.-thick sheet steel with 1/4-in.-thick by 2-in.-wide angle iron supports. The lid is 1/16-in.-thick sheet steel with 1/4-in.-thick by 2-in.-wide angle iron. One polycarbonate window with Goretex® gaskets is located in the bottom tank section, the top tank section, and the tank lid, for a total of three observation ports.

SS was used for the circulation piping to eliminate the possibility of chemicals leaching from the material into the solution. SS was also chosen for the recirculation pump, tank internals, and instruments to ensure that no leaching occurred. To facilitate the construction and assembly of the flow path from the recirculation piping to the spray nozzles, a different material, CPVC piping, was chosen.

Although leaching from the SS was not an issue, some of the other materials could not be guaranteed against leaching based only on their material descriptions. Thus, separate leaching tests were conducted with bench-scale experiments. CPVC pipe and the solvent used to connect fittings were soaked in a solution of the test chemicals for five days at 70°C. The solution was then tested; results indicated that the level of chloride (the element that might be expected to leach) was not detectable. A secondary concern was whether the CPVC would absorb chemicals, notably boron or sodium. The samples were tested, and results indicated only trace amounts of boron and sodium.

Similarly, the Goretex® gasket material was tested for possible leaching in the test solution chemistry. Chloride and silica are the two elements that could possibly leach from the gasket material. It was found that the scaled amount that did leach was 2 orders of magnitude less than what was expected from the test additives and fiberglass insulation.

Thus, it was concluded that the test apparatus materials would not contribute chemically to the test solution in concentrations that would impact the test results.

Tank Sizing

The tank holds 250 gal. of chemical solution, with 2–3 in. between the top of the water level and the top half of the tank. The bottom half of the tank can accommodate 250 gal. of solution, a single 60-coupon rack, and mesh cassettes containing 4 ft^3 of fiberglass insulation. The upper portion of the tank can accommodate 6 coupon racks, each containing up to 60 coupons. The tank is nominally 4 ft × 4 ft × 6.6 ft high, as shown in Figure A-4.

Figures A-4 through A-8 are photographs of the ICET tank, the cover lid, and the internal components, which include the top and bottom angle irons for supporting the racks, the distribution headers, the heaters, the thermocouples, and the spray nozzles.

Figure A-4. External view of the ICET tank.

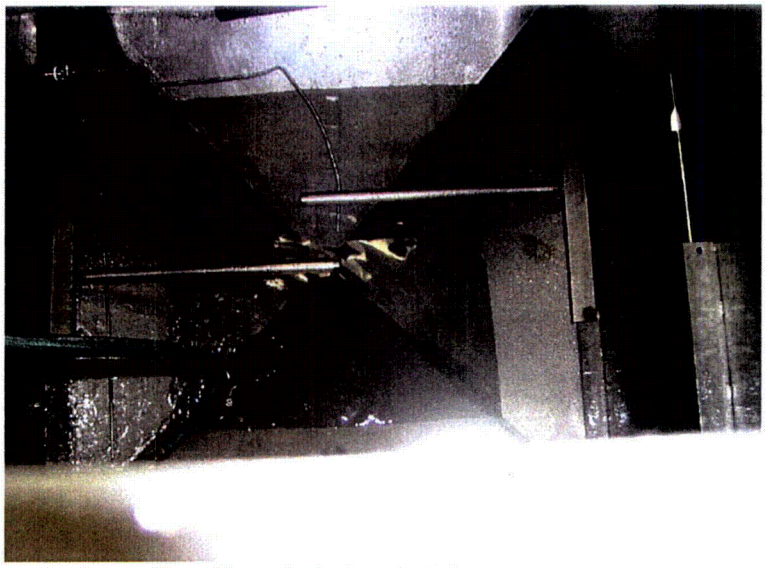

Figure A-5. The distribution header, heaters, and thermocouples inside the lower tapered reservoir of the ICET tank.

Figure A-6. **The top and bottom angle irons for supporting coupon racks in the upper section of the ICET tank.**

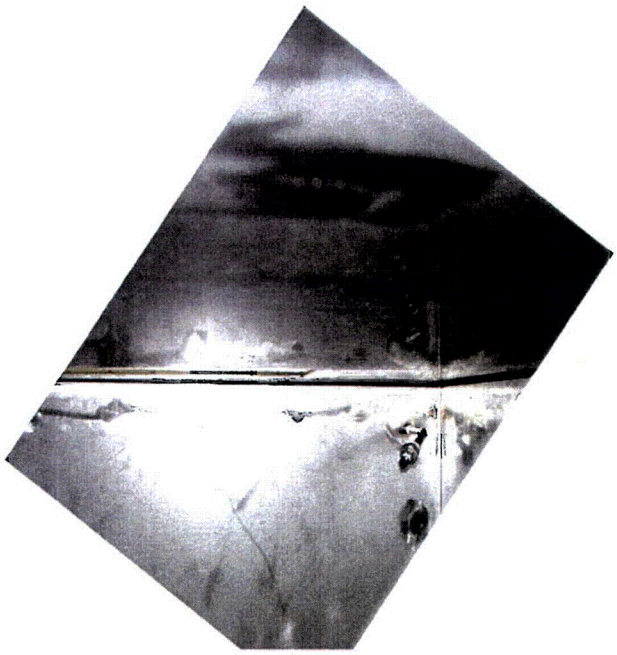

Figure A-7. **One of four spray nozzles located in each upper corner of the ICET tank. This photo was taken through the upper access hatch while the lid was in place.**

Figure A-8. The cover lid of the ICET tank showing the top observation window (lower) and top access hatch with handle (upper).

Figure A-9 and A-10 are as-built-dimensions drawings of the tank and piping system from both the front and side views, respectively. Given that the tank system is oriented approximately along the standard geographic compass directions, the front view depicts the east face of the tank, and the side view depicts the north face of the tank.

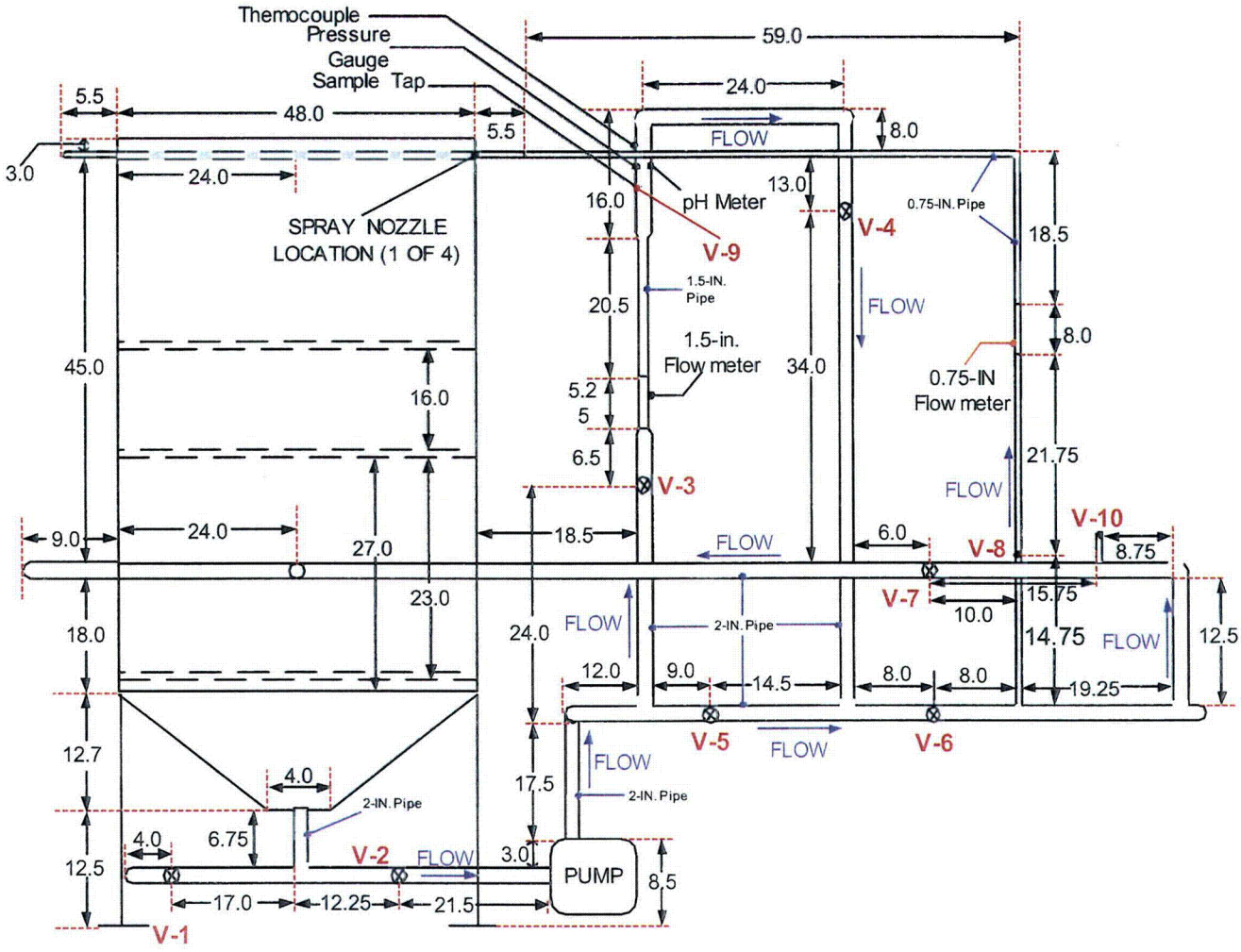

Figure A-9. **Front-view, as-built dimensions of the tank and piping system. Dimensions are in inches; shaded regions represent CPVC piping.**

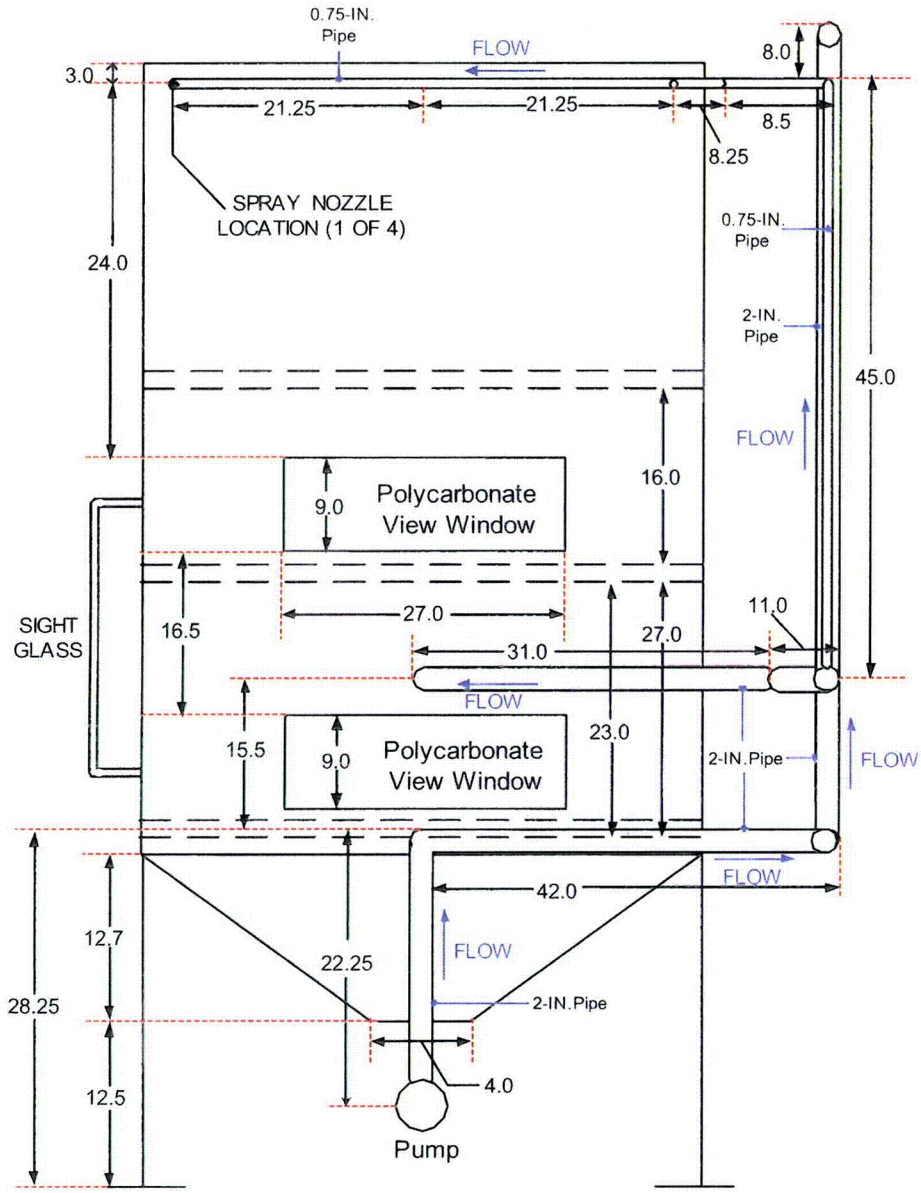

Figure A-10. Side-view, as-built dimensions of the tank and piping system. Dimensions are in inches; shaded regions represent CPVC piping.

Coupon Racks

The coupon racks are constructed of 1.5-in.-diam CPVC plastic piping. Figure A-11 shows a typical loaded rack. The racks prevent metal-to-metal contact between adjacent coupons and between the coupons and the rest of the tank assembly. This feature limits galvanic corrosion potential. Leaching tests were performed on the CPVC material and welding solvent to ensure that no detectable contributions to the chemical system would occur. Two complete sets of racks were built to facilitate staging of coupons for subsequent tests. The coupons can add up to 180 lb of weight to each CPVC-rack assembly. At elevated temperatures, the racks require support from 2-in.-wide SS angle irons strapped to the bottoms of the racks. These supports bridge the gap between the two sides of the tank and rest on the internal 2-in.-wide

SS angle irons. A 16-in. gap exists on each of the internal support angle irons to accommodate the lowering and emplacement of the nominal 14-in.-wide racks. The gap is then bridged with a length of angle iron that is pinned in place before the next tiers of racks are placed on top.

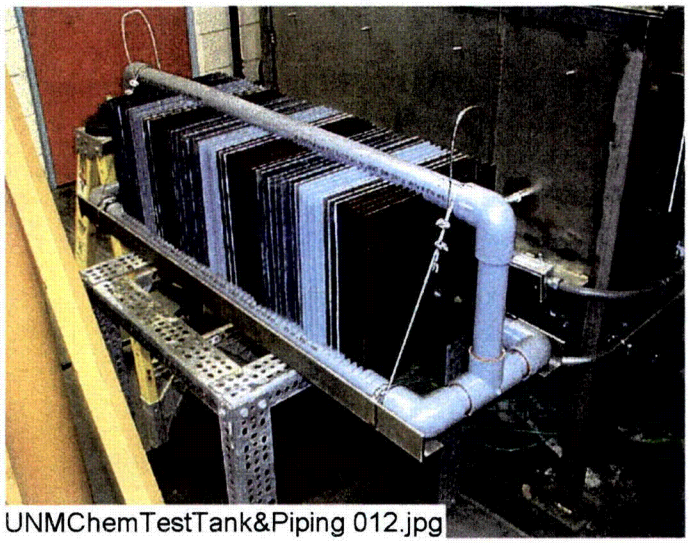

Figure A-11. Photograph of a loaded coupon rack.

Each ICET experiment exposed metallic and concrete coupons to anticipated post-LOCA environments. Each coupon is ~12 in. square. The metallic coupons are ~1/16 in. thick, except for the inorganic zinc-coated steel coupons, which are ~3/32 in. thick. The concrete coupons (one per test) are ~1-1/2 in. thick. Each test subjected seven racks of coupons to the specified environment, with one being submerged in the test tank and the remaining six being held in the tank's gas/vapor space. The number of each coupon type is shown in Table A-5.

Table A-5. Quantity of Each Coupon Type in Each Test

Material	No. of Coupons
Coated steel (CS)	77
Aluminum (Al)	59
Galvanized steel (GS)	134
Copper (Cu)	100
Uncoated steel (US)	3
Concrete	1

Note: Inorganic zinc (IOZ) coated steel and CS are the same coupon type.

The arrangement of the coupon racks in the test tank is schematically illustrated in Figure A-12. The figure shows a side view of the ICET tank, with the ends of the seven CPVC racks illustrated. The normal water level is indicated by the blue line in the figure. Rack 1 is the only submerged rack, and it sits on angle iron. It is centered in the tank so that flow from the two headers reaches it equally. Racks 2–4 are positioned above the water line, supported by angle iron in the tank. Racks 5–7 are positioned at a higher level, also supported

by angle iron. Racks 2–7 are exposed to spray. In the figure, north is to the right, and south is to the left. Directions are used only to identify such things as rack locations and sediment locations.

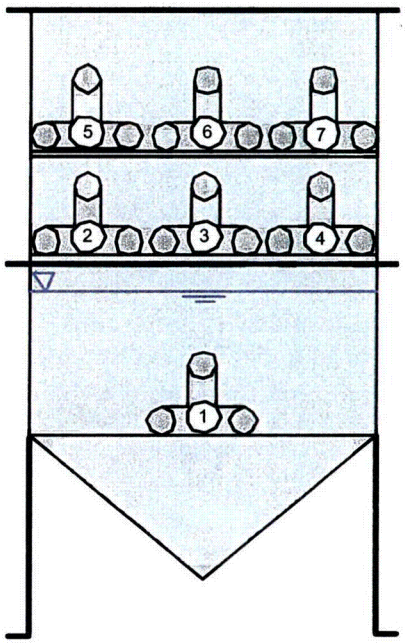

Figure A-12. Coupon rack configuration in the ICET tank. The blue line represents the surface of the test solution.

Figure A-13 shows the configuration of a typical unsubmerged coupon rack loaded with metal coupons and sitting in the ICET tank. The loading pattern of the racks was nearly identical, varying by only one or two coupons. Shown in the figure from left to right, the coupons are arranged as follows: four Cu, four Al, four inorganic zinc (IOZ), seven GS, four Cu, three Al, four IOZ, seven GS, four Cu, three Al, four IOZ, and seven GS.

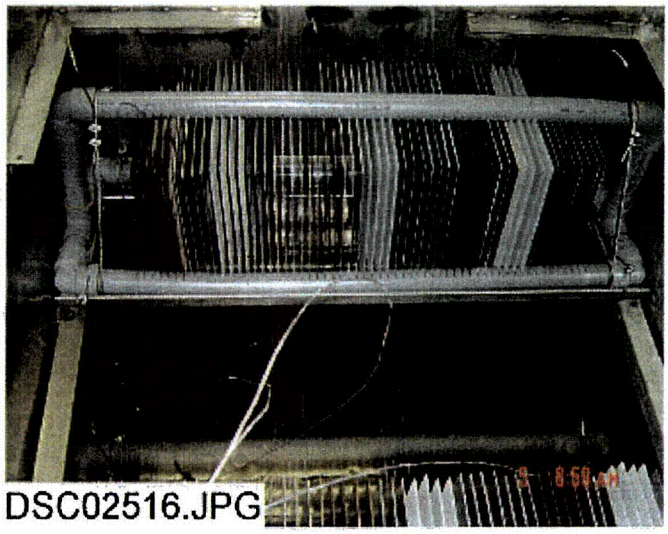

Figure A-13. A typical loaded coupon rack sitting in the ICET tank.

Tank Insulation

The tank is insulated with fiberglass boards. The surface area of the tank and top is ~130 ft^2. Approximately 50 linear feet of 2-in.-diam pipe remain uninsulated. The temperature of the fluid is nominally 140°F, and the outside surrounding air is ~70°F. The resulting heat loss from the tank and piping is ~1.2 kW.

Tank Heaters

The tank heaters are titanium jacketed to prevent corrosion and interaction of solution chemistry during the test series. Each heater is rated to supply 3.5 kW, thus providing excess (greater than the 1.2 kW required) redundant heating capacity and the ability to operate the tank assembly at higher temperatures if desired in the future. This additional capacity permits the convenience of having uninsulated piping runs. Under the existing electrical wiring configuration, only one heating element can be operated at a time. The locations of the two heaters inside the ICET tank are shown in Figure A-5.

Recirculation Pump.

The pump-wetted parts are SS, and the seals are compatible with boric acid and sodium hydroxide solutions. The pump is sized to provide a flow rate of up to 100 gpm. The pump has a variable speed controller so that the desired flow can be achieved, regardless of the system head loss. Loop shakedown resulted in a nominal flow rate of ~25 gpm during test operation. 25 gpm was chosen to yield fluid velocities over the submerged coupons from 0–3 cm/s. Figure A-14 is a photograph of the pump selected for the ICET system.

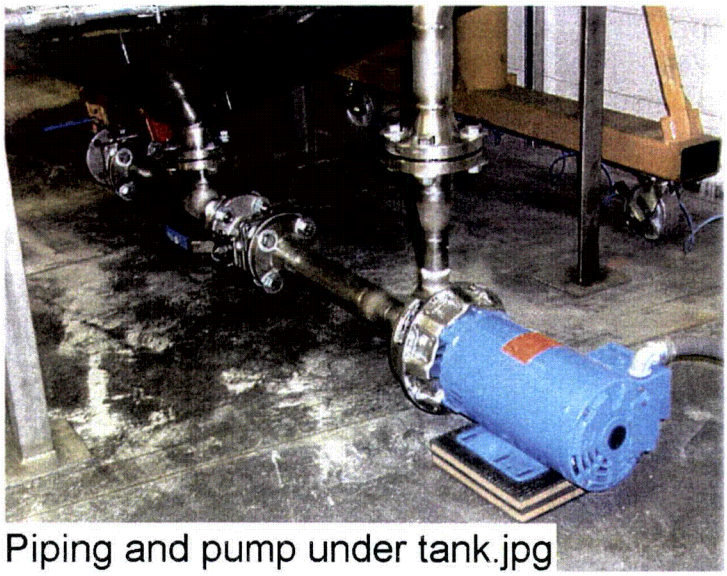

Figure A-14. Circulation pump for the ICET system.

Each of the two injection flow headers, placed below the water line along the top of the submerged coupon rack, consists of a 1-in.-diam pipe with a symmetric pattern of holes to distribute the solution discharge. The desired flow velocity across the submerged coupons was accounted for, along with the desired loop flow rate and pump characteristics. The

number and size of holes in the flow headers were calculated, and the holes were drilled symmetrically in each header. The primary goal of header design was to achieve a uniform flow pattern across the submerged coupons, with velocities in the 0–3 cm/s range. This velocity range is typical of that found in a post-LOCA containment pool. During loop shakedown activities, plastic streamers were placed at various spots in the tank to provide a visualization of the flow pattern. Then, the hole sizes were adjusted to achieve the desired pattern. Finally, food dye was introduced to determine the actual velocities. Tank velocities within the desired range were obtained.

The as-built configuration provided excess pressure head and flow capacity, even permitting for a doubling of the flow rate, if desired.

A.3 Analytical Methods and Measurements

Data collected during the ICET tests includes the on-line measurements of temperature, pH, and loop flow rate. During the water grab sample analysis, bench-top measurements were obtained for temperature, pH, turbidity, total suspended solids (TSS), and kinematic viscosity. Water, fiberglass, and metal samples are taken to other laboratory locations for additional analyses. These analyses include strain-rate viscosity, scanning electron microscopy (SEM), energy-dispersive spectroscopy (EDS), transmission electron microscopy (TEM), inductively coupled plasma (ICP) mass spectrometry, x-ray fluorescence (XRF), and x-ray diffraction (XRD). These analytical methods are described below.

Scanning Electron Microscopy (SEM)

The primary use of SEM is to study the surface topography of solid samples. The resolution of this technique is ~2 orders of magnitude better than optical microscopes and 1 order of magnitude less than TEM. SEM was used to examine the precipitate from the Day-15 and Day-30 high-volume water samples.

Principle of Operation. An electron beam passing through an evacuated column is focused by electromagnetic lenses onto the specimen surface. The beam is then scanned over the specimen in synchrony with the beam of the cathode-ray display screen. The incident beam electrons (from the electron gun) do not simply reflect off the sample surface. As the beam travels through the sample, it can do three things: First, it can pass through the sample without colliding with any of the sample atoms (matter is mostly space). Second, it can collide with electrons from the sample atoms, creating secondary electrons. Third, it can collide with the nucleus of the sample atom, creating a backscattered electron.

The incident beam is composed of highly energized electrons. If one of these electrons collides with a sample atom electron, an electron will be knocked out of its shell.

Figure A-15 illustrates this action. The released electron is called a secondary electron and is weak in energy. If these secondary electrons are close enough to the sample surface, they can be collected to form an SEM image.

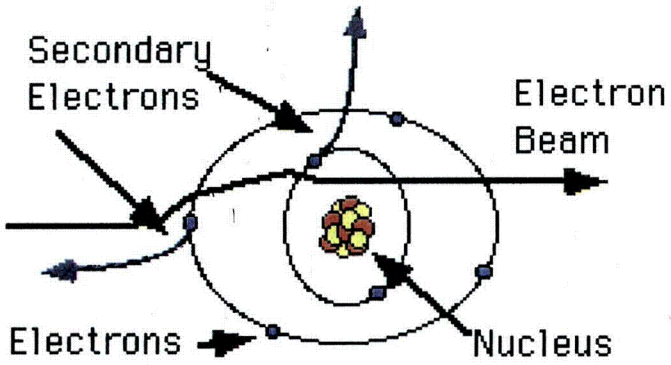

Figure A-15. Production of secondary electrons from an electron beam.

The incident beam electron loses little energy in this collision. In fact, a single electron from the beam will produce a shower of thousands of secondary electrons until it does not have the energy to knock these electrons from their shells. Inelastically scattered secondary electron emission from the sample is used to modulate the brightness of the cathode-ray display screen, thereby forming the image.

If the incident beam collides with a nucleus of a sample atom, it bounces back out of the sample as a backscattered electron (Figure A-16). These electrons have high energies, and because a sample with a higher density will create more of them, they are used to form backscattered electron images, which generally can discern the difference in sample densities. In this case, the image contrast is determined largely by compositional differences in the sample surface rather than by topographic features. Additional information on SEM may be found in Ref. A.2.

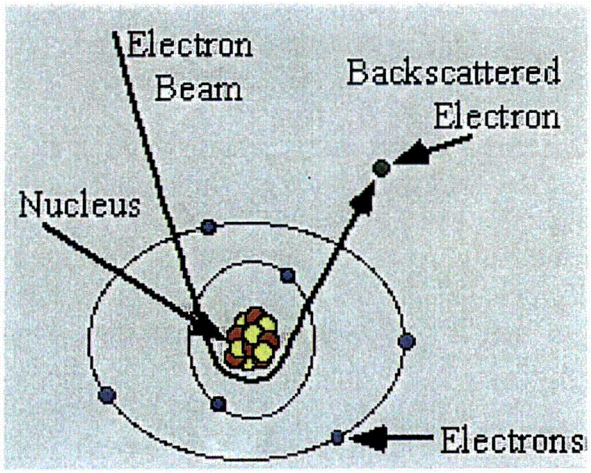

Figure A-16. Production of backscattered electrons from an electron beam.

Limitations. The principal limitation of SEM is the resolution. Typical resolution is limited to between 1.5 and 3 nm, which is ~1 order of magnitude less than TEM resolution. In addition, only the surface of the specimen can be viewed. Finally, the SEM operates under high vacuum and therefore is unsuitable for examining materials with a liquid component unless the materials dried first.

Energy-Dispersive Spectroscopy (EDS)

EDS can provide information on the elemental composition of a specimen. Combining the EDS system with SEM allows the microstructure-level identification of compositional gradients at grain boundaries, second phases, impurities, inclusions, and small amounts of material. EDS was used to examine the various structures formed on the fibers, which were similar for the Day-15 and Day-30 test samples. This examination allowed for a quantitative estimate of the elemental composition of the precipitate and the material deposited between the fibers.

Principle of Operation. As an incident electron beam interacts with the specimen, it loses energy. Characteristic x-rays are in turn emitted by the atomic species in the material. These characteristic x-rays are then converted into an electrical pulse with specific characteristics of amplitude and width. A multichannel analyzer measures the pulse and increments as a corresponding "energy slot" in a monitor display. The location of the slot is proportional to the energy of the x-ray photon entering the detector. The display is a histogram of the x-ray energy received by the detector, with individual "peaks," the heights of which are proportional to the amount of a particular element in the specimen being analyzed. Additional information on EDS may be found in Ref. A.2.

Limitations. The design of the equipment complicates the technique of detecting elements lighter than carbon. In general, a poorer sensitivity for light elements (low atomic weight) also exists in a heavy matrix. Resolution of the x-ray energy levels limits the positive identification of certain elements due to overlapping energy slots. Quantitative analysis is usually limited to flat, polished specimens. Unusual geometries, such as fracture surfaces, individual particles, and films on substrates can be analyzed, but with considerably greater uncertainty.

Transmission Electron Microscopy (TEM)

TEM is used to study the local structure, morphology, and chemistry of materials by examining the diffracted and transmitted electron intensities, as well as the characteristic x-rays and energies lost by the incident beam. TEMs are often coupled with EDS to give information about the local chemistry of the material. The high resolution of the TEM, at least 1 order of magnitude greater than SEM resolution, allows for qualitative size assessment of the underlying visible structures and aggregates. TEM was used on the precipitate from the Day-15 and Day-30 high-volume samples.

Principle of Operation. In transmission electron microscopes, a beam of high-energy electrons, typically 100–400 keV, is generated. The generated beam then is collimated by a magnetic lens and allowed to pass through the specimen under high vacuum. The resulting diffraction pattern, which consists of a transmitted beam and many diffracted beams, can be imaged on a fluorescent screen below the specimen. From the diffraction pattern, the lattice spacing information for the structure under consideration can be obtained. Alternatively, the transmitted beam or one of the diffracted beams can be used to form a magnified image of the sample. Finally, if the transmitted beam and one or more of the diffracted beams are

allowed to recombine, a high-resolution image can be obtained that contains information about the atomic structure of the material.

As the incident electron beam interacts with the specimen, it loses energy. Characteristic x-rays are in turn emitted by the atomic species in the material. These characteristic x-rays and the energy losses suffered by the incident electron can then be detected and analyzed to yield the EDS spectrum. Additional detail on TEM may be found in Ref. A.3.

Limitations. A TEM can have extremely high resolution, and research-level instruments can see individual atoms. However, a TEM has some limitations because the electron beam must travel through the sample, and lengthy sample preparation is usually required to make the sample thin enough. Because the beam is traveling though the sample, the sample bulk, not the surface, is being imaged.

Inductively Coupled Plasma - Atomic Emission Spectroscopy (ICP-AES)

ICP-AES is a rapid, sensitive way of measuring the elemental concentrations of solutions. More than 75 elements can be determined. ICP was used to determine the elemental composition of the daily water samples to assist in the overall understanding of the solution chemistry and corrosion behavior.

Principle of Operation. The first step in the procedure is conversion of the molecules in the sample to individual atoms and ions using a high-temperature, radio-frequency-induced argon plasma. The sample is introduced into the plasma as a solution. The sample is then pumped to a nebulizer, where it is converted to a fine spray and mixed with argon in a spray chamber. The purpose of the spray chamber is to ensure that only droplets in a narrow size range make it through into the plasma. Most of the sample drains away from the chamber; the rest is carried into the plasma and instantly excited by the high temperatures (5000–10,000 K). Atoms become ionized with 99% efficiency. The excited elements emit photons that are detected by one or more photomultiplier tubes. Additional information on ICP may be found in Ref. A.4.

Limitations. A notable limitation is the inability to measure hydrogen, carbon, nitrogen, and oxygen. In addition, silicon quantification is determined better by XRF because silicon will be lost to the vapor phase during ICP acid digestion procedures (as will certain trace elements, such as Hg, Se, As, and possibly Pb and Cd). The other notable disadvantage with the technique is that some minerals may not dissolve completely during the digestion procedure needed to use the ICP. Therefore, for samples containing substantial amounts of minerals (solids must be dissolved before analysis), XRF analysis is likely more appropriate for elemental determination. Interferences may also occur during ICP-AES due to overlap of the emission lines from the analyte and the interfering element and due to matrix effects. Finally, ICP is not suitable for determining chemical speciation.

X-Ray Fluorescence (XRF)

This x-ray technique is used to determine, both qualitatively and quantitatively, the elemental composition of a wide range of materials. XRF was used to examine the high-volume water sample precipitate on Days 15 and 30.

Principle of Operation. XRF is based on the photoelectric effect. When an atom is irradiated with highly energetic photons, an electron from one of the inner shells may be ejected (Figure A-17). As the vacancy is filled by an electron from an outer shell, a photon is released, the energy of which is characteristic of the atom. This radiation is called fluorescent radiation, and each element has its own set of characteristic emission lines. The intensity and the energy of these lines are measured using a spectrometer that detects wavelength-dispersive XRF or energy-dispersive XRF. Additional detail on XRF may be found in Ref. A.5.

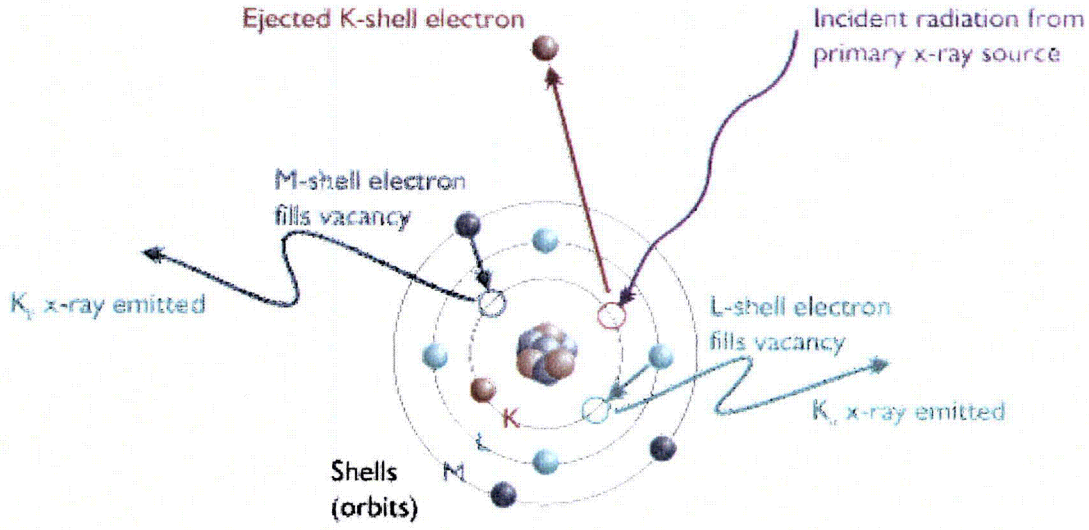

Figure A-17. Illustration of the operation principle of XRF.

Limitations. The accuracy of the results depends on how closely the standards resemble the sample. In addition, the principal limitation with this technique is the decreased sensitivity that occurs with decreasing atomic weight. Most XRF instruments cannot reliably detect elements lighter than carbon. Another limitation is that for accurate quantitative analysis, standards that are similar in composition and morphology to the unknown are required.

X-Ray Diffraction (XRD)

X-ray powder diffraction is used to obtain information about the structure, composition, and state of polycrystalline materials. The determination of the crystalline structure of the precipitate allows for the development of an understanding of the means by which the precipitate is formed. XRD analyses were performed on the post-test sludge precipitate. The target anode was copper in the x-ray tube.

Principle of Operation. If a beam of monochromatic x-rays is directed at a crystalline material, reflection or diffraction of the x-rays is observed at various angles with respect to the primary beam. The relationship between the wavelength of the x-ray beam, λ, the angle of diffraction, 2θ, and the distance between each set of atomic planes of the crystal lattice, d, is given by the Bragg equation:

$$N\lambda = 2\,d\sin\theta\ ,$$

where N represents the order of diffraction.

From this equation can be calculated the interplanar distances of the crystalline material being studied. The interplanar spacing depends solely on the dimension of the crystal's unit cell, whereas the intensities of the diffracted rays are a function of the placement of the atoms in the unit cell.

Limitations. Conventionally, the largest limitation of XRD is its restriction to crystalline materials because amorphous materials do not diffract. Milligram samples may be analyzed if the analysis time is not important. The requirement of sample quantity (typically several hundred milligrams) is to provide the enormous number of small crystallites oriented in every conceivable direction. Thus, when an x-ray beam traverses the material, a significant number of the particles can be expected to be oriented to fulfill the Bragg condition for reflection from every conceivable interplanar spacing.

Wet Chemistry Analyses

The standard methods used for wet chemistry analyses are shown in Table A-6. Additionally, the following paragraphs provide supplemental data for nonstandard methods.

Table A-6. Methods for Wet Chemistry Analysis

Parameter	Method[a]	Major Equipment
pH	SM 4500-H^+ (Electrometeric)	Orion Model 720 A
Turbidity	SM 2130 (Nephelometeric)	Hach Turbidimeter Model 18900
Total suspended solids	SM 2540D	–
Temperature	SM 2550	–
Kinematic viscosity	–	Cannon-Fenske Capillary Viscometer
Shear-rate viscosity	-	Bohlin CS-10 rheometer

[a]SM = *Standard Methods for the Examination of Water and Wastewater* (20th Edition) (APHA et al. 1998).

The pH meter was calibrated before use with a three-point calibration curve using certified pH buffers at 4, 7, and 10. The pH was recorded to the nearest 0.01 pH unit. The bench-top pH measurements correspond to the actual temperature of the sample at the time it was measured. An automatic temperature compensation pH probe was used to provide a temperature-corrected pH, using a 3-point calibration curve. It is noted that pH varies by only 0.04 units between 25°C and 60°C within the pH range of interest. So, the temperature had very little effect on the measurements that were reported. The turbidimeter was calibrated with Gelex secondary standards before testing. Turbidity was recorded to the nearest 0.01 Nephelometric Turbidity Unit (NTU).

For TSS, a standard volume of 500 mL was filtered for all samples. A 0.7-μm glass fiber filter was used. The filters were weighed in aluminum boats for the pre-sample and post-sample weights, with the post-sample filters completely dried in an oven. The difference in weights was the amount of TSS in the volume, and the TSS was recorded to the nearest 0.1 mg/L.

Kinematic viscosity was measured with a Cannon-Fenske capillary viscometer, size 50. Viscosity was measured on both filtered and unfiltered samples, each at a temperature of 60(±1.0)°C [140(±1.8)°F] and again at 23(±2.0)°C [73.4(±3.6)°F]. The viscosity of water is highly sensitive to temperature, and the allowed temperature range results in a variation of viscosity of 2% between 59°C (138.2°F) and 61°C (141.8°F) and a 9.3% variation between 21°C (69.8°F) and 25°C (77.0°F). For this reason, temperature was measured to 0.1°C accuracy with a National-Institute-of-Standards-and-Technology-traceable thermometer for all viscosity measurements, and the measured viscosity values were corrected to a common temperature to facilitate comparisons. The corrected temperatures chosen for comparison were 60.0°C (140°F) and 23.0°C (73.4°F). Equations were derived to correct viscosity by fitting an equation to viscosity data and minimizing the coefficient of determination (R^2). The formulas used to correct the viscosity were

$$\nu_{23} = \nu_M \left(1.0235\right)^{(T_M - 23)}$$

and

$$\nu_{60} = \nu_M \left(1.0146\right)^{(T_M - 60)} \quad ,$$

where

T_M = temperature at which viscosity measurements are made (°C),
ν_M = measured kinematic viscosity at temperature T_M (mm^2/s),
ν_{60} = kinematic viscosity corrected to 60.0°C (mm^2/s), and
ν_{23} = kinematic viscosity corrected to 23.0°C (mm^2/s).

In addition, duplicate measurements were made at each condition until Day 25 of the test. In nearly all cases, the replicate viscosity measurements varied by considerably less than 1%. From Day 25 of Test #1, duplicate measurements of viscosity were no longer taken because of the consistency previously noted.

Shear-rate viscosity was measured using a Bohlin CS-10 rheometer. The instrument was calibrated, and a trained operator followed the manufacturer's instructions to obtain the actual measurements. Samples were analyzed after 1 day of testing and weekly thereafter. Both filtered and unfiltered samples were analyzed for Test #1. Because there were no significant differences between filtered and unfiltered, only unfiltered samples were analyzed for Tests #2 through #5.

All measurements were conducted with a shear-stress range of 0.0095 to 0.12 Pa. Samples were first measured at 60°C and then cooled to 25°C. The samples were transported to the Bohlin CS10 Rheometer in a cooler containing a hot-water bottle to maintain a warm temperature. Any samples that were not immediately analyzed were placed into an oven set at 60°C until they could be measured. When samples were placed in the rheometer, their temperatures were controlled to the desired value. Through this procedure, the test sample was maintained continuously at the desired temperature.

The purpose of shear-rate viscosity measurements was to investigate the physical response of the test solution to a driving shear-stress. The conclusion derived was whether the solution behaved as a Newtonian or non-Newtonian fluid.

A.4 QA Program

A project QA manual was developed to satisfy the contractual requirements that applied to the ICET project. Specifically, those requirements were to provide credible results by maintaining an appropriate level of QA in the areas of test loop design, sampling, chemicals, operation, and analysis. These requirements were summarized in the contract requirement that QA was to be consistent with the intent of the appropriate sections of 10CFR50, Appendix B.

The 18 criteria of 10CFR50, Appendix B, were addressed separately in the QA manual, and the extents to which they apply to the ICET project were delineated. A resultant set of QA procedures was developed. In addition, test-specific project instructions (PIs) were written to address specific operational topics that required detailed step-by-step guidance. PIs generally applicable to all tests were written for the following topics:

- Data Acquisition System (DAS)
- Coupon Receipt, Preparation, Inspection, and Storage
- DAS Alarm Response
- Chemical Sampling and Analysis
- TEM Examination of Test Samples
- SEM Characterization of Test Samples
- Viscosity Measurements

Each project instruction that governed test operations was revised for nearly every test. Those PIs consisted of the following:

- Pre-Test Operations
- Test Operations
- Post-Test Operations

Beginning with the Test #2 data report, the test-specific PIs for pre-test, test, and post-test operations were included as report appendices.

Samples from the tests were taken to an off-site analytical laboratory for ICP-AES analyses. That laboratory operated according to its own approved QC program. To ensure the accuracy of the ICP results, several QC steps were performed with every batch of samples run on the instrument. Those QC steps were as follows:

Lab Control Spike (LCS)—The LCS consists of a known concentration of each analyte (typically 1 to 5 mg/L, depending on analyte) in deionized water. The measured concentration is compared with the spike concentration, and a percent recovery is reported. An exception is noted if the percent recovery of any analyte is outside the acceptable range. The acceptable range is based on previous QA procedures developed for the instrument.

Method Blank (MB)—The MB is a sample of deionized water. All analytes are expected to be below the detection limit. An exception is noted if the measured concentration of any analyte is above the detection limit.

Matrix Duplicate (MD)—The MD is a second analysis of one of the samples in the run. The measured concentration for each analyte is compared between the two samples, and an exception is noted if the two results do not agree to within 20%.

Matrix Spike (MS)—The MS consists of a known concentration of each analyte (typically 1 to 5 mg/L, depending on analyte) added to one of the samples in the run. The difference in the measured concentrations between the original sample and spiked sample is compared with the spike concentration, and a percent recovery of the spiked concentration is reported. An exception is noted if the percent recovery of any analyte spike is outside the acceptable range.

Matrix Spike Duplicate Accuracy (MSDA)—The MSDA is a repetition of the MS. An exception on the MSDA is identical to an exception on the MS.

Matrix Spike Duplicate Precision—The two runs of the matrix spikes (MS and MSDA) are compared with each other. An exception is noted if the two measured spike concentrations do not agree to within a relative percent difference of 20%.

Serial Dilution—One of the samples in the run is diluted with deionized water by a factor of 5. The measured concentration of the diluted sample is compared with the predicted concentration, which is calculated from the dilution rate and the measured concentration of the original (undiluted) sample. An exception is noted if the differences between the measured and calculated concentrations are not within the acceptable range.

It was necessary for the analytical laboratory to perform a 10:1 dilution of the samples to lower the concentration of borate to reduce interferences between borate and the analytes. This process had the effect of raising the detection limit for these analyses to a value 10 times higher than the instrument detection limit, but the higher detection limit had no impact on the results. The instrument detection limit was significantly below 1 mg/L for all analytes, and the higher detection limit was still well below the levels of concern for this experiment.

The water samples were totally digested before the ICP measurement and represented the solution plus any precipitate present. Samples were kept at 4°C after they were extracted until they were digested. Each laboratory batch of samples had its own specific uncertainty, depending on the results of its QC checks. They were within the accepted uncertainties of the laboratory QC program, or the analyses were rerun. A typical set of measurement uncertainties was as follows: aluminum, ±20%; calcium, –14% and +19%; sodium, ±20%; magnesium, –13% and +20%; and silica, –9% and +12%. The minimum detection limits are given in Table A-7.

Table A-7. ICP-AES Minimum Detection Limits for Elements, in mg/L

Cl	B	Ca	Pb	Li	Mg	K	Si	Zn	Na	Al	Cu	Fe	Ni
0.5	0.01	0.5	0.005	0.002	0.5	0.5	0.5	0.01	1.0	0.05	0.02	0.01	0.002

A.4. References

A.1. "Test Plan: Characterization of Chemical and Corrosion Effects Potentially Occurring inside a PWR Containment Following a LOCA, Rev. 13," July 20, 2005.

A.2. Goldstein, J., Scanning Electron Microscopy and X-ray Microanalysis, 2nd ed., Plenum Press: New York (1992).

A.3. Williams, D. B., "X-ray Spectrometry in Electron Beam Instruments; Plenum Press: New York (1995).

A.4. Montaser, A., "Inductively Coupled Plasmas in Analytical Atomic Spectrometry"; VCH Publishers, Inc.: New York (1987).

A.5. Jenkins, R., "Quantitative X-Ray Spectrometry, Marcel Dekker Inc.: New York (1981).

Appendix B

Materials Used in ICET Testing

Prepared by:
EPRI; John M. Gisclon, Consultant

Appendix B. Materials Used in ICET Testing

B.1 Introduction

This appendix provides information on the materials used in the ICET test runs, including specifications, quantity, and relationship to the Test Plan. Test materials include water, chemicals, insulation materials, metallic coupons, concrete and sediment. The materials used in each ICET run were chosen to create a post-LOCA containment sump chemical environment representative of that which might exist in a hypothetical LOCA with ECCS recirculation. Materials and chemicals used were typical of those that would be present in nuclear power plant containments. Five combinations of insulation and buffer chemicals were used for the test matrix, Table B-1, below: This table was derived from Table 5 of the Test Plan.

Table B-1. ICET Test Matrix

Run	Temp., ^{0}C	Buffering Agent	pH	Boron Conc., ppm	Notes
1	60	Sodium Hydroxide	10	2800	100% fiberglass insulation test. NaOH concentration as required by pH. NaOH to be injected into spray fluid in first 30 minutes for a spray pH $\leq$ 12.
2	60	Tri-sodium phosphate	7	2800	100% fiberglass insulation test. Tri-sodium phosphate concentration as required by pH.
3	60	Tri-sodium phosphate	7	2800	80% calcium silicate insulation/ 20% fiberglass insulation test. Tri-sodium phosphate concentration as required by pH.
4	60	Sodium Hydroxide	10	2800	80% calcium silicate insulation/ 20% fiberglass insulation test. NaOH to be injected into spray fluid in first 30 minutes for a spray pH $\leq$ 12.
5	60	Sodium Tetraborate	8 – 8.5 (est.)	2400	100% fiberglass insulation test with sodium tetraborate buffer. The sump solution is to be targeted to simulate the solution mixture of a representative ice condenser plant after melting of ice beds. The planned solution boron concentration is 2400 ppm.

To be inclusive of most plants that would use the buffers and insulation mixtures specified in the Test Plan matrix, the quantities of materials tended toward the highest amounts that could be anticipated in plants. For example, the pH range in the ICET runs is high compared with what would be anticipated for most plants, but it is not a maximum value. Similarly, the amount of some metals such as aluminum would be high as well.

B.2 Scaling and Relationship with Test Plan

Information is presented below in Table B-2 that relates the surface area, mass, or volume of containment materials to the sump fluid (water) volume. This information was derived from Table 1 of the Test Plan.

Table B-2, Material Quantity/Sump Water Volume Ratios Planned to be Tested

Material	Value of Ratio Tested (Ratio Units)
Zinc in galvanized steel	8.0 ft^2/ft^3
Inorganic zinc primer coatings (non-top coated)	4.6 ft^2/ft^3
Aluminum	3.5 ft^2/ft^3
Copper (including Cu-Ni alloys)	6.0 ft^2/ft^3
Carbon steel	0.15 ft^2/ft^3
Concrete (surface)	0.045 ft^2/ft^3
Concrete (particulate)	0.0014 lbm/ft^3
Insulation material (fiberglass or calcium silicate)	0.0137 ft^3/ft^3 Note: This ratio of insulation to sump inventory is to be used both for the 100% fiberglass and the 20% fiberglass/ 80% calcium silicate tests.

The Test Plan (Table 3) also provides information regarding the location of materials within containment, whether submerged or not submerged. This is important, as material that would be submerged during ECCS recirculation is subject to a different environment than that which is not submerged. However, the non-submerged material would also be subjected to containment spray for a period of time, and it was deemed necessary to provide this exposure during the test run. The submerged and non-submerged quantities of test materials are derived from the Test Plan and are presented in Table B-3, below.

Table B-3, Percentage of Surface Areas Above and Below Containment Flood Levels

Material	Submerged %	Non-submerged %	Comments
Zinc, galvanized	5	95	The submerged value accounts for grating and duct work that may be submerged.
Zinc coatings, un-topcoated	4	96	Addresses both un-topcoated zinc primer and primer exposed as a result of delamination of topcoat.
Aluminum	5	95	Aluminum is generally not located at elevations in containment where it may be submerged.
Copper	25	75	Majority of surface from control rod drive mechanism coolers and instrument air lines.
90/10 Cu-Ni	25	75	Majority of surface present in containment fan coolers.
Concrete	34	66	The submerged value accounts for limited damage to floor and wall surface areas that will be submerged due to primary RCS piping being elevated above containment floor.
Carbon steel	34	66	
Fiberglass	75	25	The submerged value accounts for most of the fiberglass remaining in areas where it will wash down into the sump pool.
Calcium silicate	75	25	The submerged value accounts for most of the fiberglass remaining in areas where it will wash down into the sump pool.

For the purpose of the ICET test runs, it was decided to perform the testing in a manner that preserved the relationship between sump water volume and material surface area, volume or mass between that expected in post-LOCA containment and that in the test run. This was achieved for ICET by providing a surface area, volume, or mass of material to be placed in the test loop in submerged and non-submerged areas for the ICET test loop sump water volume of 250 gallons (33.48 ft^3). This information is presented in Table B-4 of this appendix.

Table B-4, Material Requirements for ICET Test Runs

Material	Total ratio for test, surface, mass, or volume per ft^3 of sump volume	Total test area, mass or volume	Non-submerged fraction	Submerged fraction	Non-submerged area, mass, or volume	No. of 12x12 plate coupons, non-submerged	Submerged area, mass or volume	No. of 12x12 plate coupons submerged	No. of coupons, mass or volume	Coupons, mass, or volume required for each run
Zinc, Galvanized surface	8(ft^2/ft^3)	267.38	0.95	0.05	254.01	127.01	13.37	6.68	133.69	134 coupons
Non-top-coated inorganic zinc coated surface	4.6(ft^2/ft^3)	153.74	0.96	0.04	147.59	73.8	6.15	3.07	76.87	77 coupons
Aluminum surface	3.5(ft^2/ft^3)	116.98	0.95	0.05	111.13	55.56	5.85	2.92	58.49	59 coupons
Copper surface	6(ft^2/ft^3)	200.53	0.75	0.25	150.4	75.2	50.13	25.07	100.27	100 coupons
Carbon steel surface	0.15(ft^2/ft^3)	5.01	0.66	0.34	3.31	1.65	1.7	0.85	2.51	3 coupons
Concrete, Surface	0.045(ft^2/ft^3)	1.5	0.66	0.34	0.99	0.5	0.51	0.26	0.75	1 coupon*
Concrete, particulate mass	0.0014(lbm/ft^3)	0.0467	0	1	0		0.0467		0.0467	0.0467 lb
Insulation volume	0.137(ft^3/ft^3)	4.58	0.25	0.75	1.14		3.43		4.58	4.58 ft3

Table B-4 note*: Since only one concrete coupon was fabricated, it was decided to conservatively locate the entire coupon in a submerged test coupon rack.

B.3 ICET Test Materials

Table B-5 is a list of the test materials used in the ICET program and includes specifications, composition, preparation or pre-test treatment and the source of the materials.

Table B-5, ICET Test Material Information				
Material	**Specifications or Composition**	**Preparation or Pre-Test Treatment**	**Source or Supplier**	**Additional Remarks**
De-mineralized water				See Appendix A
Boric Acid	Boric Acid, nuclear grade pure boric acid granular, 99.90% w/o H_3BO_3 minimum		Donated by a nuclear power plant.	
Lithium Hydroxide				See Appendix A
Hydrochloric Acid				See Appendix A
Sodium Hydroxide				See Appendix A
Tri-Sodium Phosphate	Trisodium phosphate dodecahydrate, crystal, technical grade		Donated by a nuclear power plant.	
Sodium Tetraborate	20 Mule Team Borax; borax decahydrate, sodium tetraborate decahydrate		Donated by a nuclear power plant.	Supplied by Dial Corporation.
Fiberglass Insulation	NUKON® base wool, low-density (2.4lb/ft3) fiberglass insulation, half of the material at 3 ½ inch thickness and half of the material at 3 inch thickness.	Bake at ~600F on one side for 24 hours to simulate conditions as would be expected in insulation service in a representative plant (this heating will decompose some of the phenolic resin binder). After baking, the material shall be prepared for testing by shredding and homogenizing, e.g. run twice through a leaf shredder to produce "representative" fiberglass debris.	Performance Contracting, Inc.	

Table B-5, ICET Test Material Information				
Material	**Specifications or Composition**	**Preparation or Pre-Test Treatment**	**Source or Supplier**	**Additional Remarks**
Calcium Silicate Insulation	Pabco Super Caltemp Gold Insulation: This material contains about ½ to ¾ %/w/o rayon fiber, ½% pulp,< ½% alkali resistant fiber glass, < ½% yellow iron oxide for color and the remainder is Tobermorite calcium silicate. In initial heat up, the rayon and pulp will decompose and give off water vapor and CO_2.	Please see note (1)	Donated by a nuclear power plant	Pabco was sold to Johns Manville in 1998, and the material was renamed "Thermo-12 Gold". Tobermorite is a crystalline calcium silicate mineral that is stable up to 1250^0F.
Galvanized steel coupons	Galvanized steel sheet, hot dipped; ASTM A-653 CS Type B, (Note 2)		**The Techs** ®	
Inorganic zinc coated coupons	ASTM A1008 hot-rolled carbon steel sheet coated with inorganic zinc primer (Note 2)	Note 3	NUCOR Steel (steel sheet) Carboline (coating)	
Aluminum coupons	ASTM B-209 aluminum sheet (Note 2)		Commonwealth Metal Corporation	Note 4: composition
Copper coupons	ASTM B-152, copper sheet (Note 2, Note 5)		Not available	Chemical analysis, Cu+Ag=99.93%
Carbon steel coupons	ASTM A-1008 hot rolled carbon steel (Note 2)		NUCOR Steel	Note 6 composition
Concrete coupons	12"x12"X 2" structural concrete coupons, made with Portland cement type GU (ASTM C 1157), I, II (ASTM C-150); see note 7 for mixture.		Holcim (US) Inc. supplied Portland Cement. EPRI fabricated the coupons.	Note 8, Portland cement composition

Table B-5, ICET Test Material Information				
Material	**Specifications or Composition**	**Preparation or Pre-Test Treatment**	**Source or Supplier**	**Additional Remarks**
Particulate debris material	For each test run: Concrete particulate, 21.2 gm Surrogate latent debris (sand and clay) 63.7 gm	Concrete particulate was prepared by grinding material chipped from the corner/side of an extra concrete coupon.	LANL supplied the surrogate latent debris.	

Table B-5 note (1): Calcium Silicate Preparation:

Submerged and non-submerged volumes of insulation:

The Test Plan specifies the following:

i. Insulation material, fiberglass or calcium silicate value of ratio tested=0.137ft^3/ft^3
ii. Submerged %=75, non-submerged %=25
iii. Runs 3 & 4 insulation mix, 80% calcium silicate, 20% fiberglass

The test plan specifies a volume of 0.137ft^3/ft^3 of fluid. The 250 gallons is 33.42 ft^3. Therefore, the total volume of cal-sil and fiberglass should be 4.58 ft^3.

Material	Total	Non-submerged	Submerged
All Insulation	4.58 ft3	1.14 ft3 (25%)	3.43ft3 (75%)
Fiberglass, volume (20% of all)	0.92 ft3	0.23 ft3	0.69ft3
20% Fiberglass, weight @ 2.4 lb/ft3	2.20 lb	0.55 lb	1.65 lb
Cal-sil, volume (80% of all)	3.66 ft3	0.92 ft3	2.75 ft3

Because of the measured variability in density from that specified in the ASTM standard, it is recommended that the calcium silicate addition be based on a volumetric measurement of the original formed pieces. Subsequent apportionment by weight, if used, should be based on the initial volumetric measurement and average as-found density.

Size and area distribution of Calcium Silicate Insulation

It was agreed to use the size distribution of Table 2 of Ontario Power Generation Report N-REP-34320-10000, "Jet Impact Tests – Preliminary Results and Their Application". The distribution between the submerged and non-submerged regions is

given as 75% and 25% respectively by the Test Plan (Appendix C, Table 3), which also accounts for washdown, e.g., the 75% includes material washed down. Therefore, the location and size distribution was determined as follows:

Size	> 3 in	1- 3 in	< 1 in	dust	total
Percentile distribution from OPG	13.9	18.5	5.1	62.5	100
Submerged, % of total (total fraction 75%)	4.6	6.2	1.7	62.5	75
Non-submerged	9.3	12.3	3.4	0	25

Heat treatment of calcium silicate:
~37.2% volume of the Calcium silicate should be heated to ~500^{0}F for at least 72 hours. This is performed to simulate service conditions of calcium silicate so as to account for minor chemical changes in the iron oxide, rayon and pulp constituents of the insulating material. Yellow iron oxide will dehydrate into red iron oxide at temperatures above 400 ^{0}F, releasing water vapor. Heat transfer calculations indicate that about 37.2% of 4 inch thick insulation on a 30 inch OD pipe will be at temperatures > 400 ^{0}F.

Table B-5 note (2): Metallic Coupons:
12"x12"x1/16", except for coupons to be coated with IOZ, which will be 3/32" thick
Coupons may be formed by shearing.
Coupons shall be cleaned to remove foreign material. Gentle cleaning with a mild organic solvent is recommended.
Aggressive cleaning that could alter or remove oxide films from the material surface shall not be employed.

Table B-5 note (3): Inorganic Zinc Primer Application shall meet material and application requirements for DBA qualified nuclear coatings:
Surface preparation shall be in accordance with SSPC-SP 10, near-white metal blast, surface profile 1-3 mils.
Coating material: Carboline CARBOZINC 11 SG and shall be applied in accordance with the latest edition of the manufacturer's data sheet.
Cure at ambient conditions for 2 hours, minimum.
Using steam or water mist, keep coated surfaces wet for a minimum of 8 additional hours until the coated surfaces achieves a 2H pencil hardness per ASTM D6633.

Table B-5 note (4) Aluminum Mill Report, composition:

Element	Si	Fe	Cu	Mn	Mg	Cr	Zn	B	Ti
% min	0.2	0.62	0.11	1.12	0.005	0.001	0.005	0.0018	0.005
% max	0.22	0.7	0.13	1.25	0.014	0.002	0.005	0.0036	0.160

Table B-5 note (5): After fabrication and cleaning, copper coupons shall be artificially aged to achieve an oxide film by baking in an oxidizing atmosphere for at least 72 hours at 350-400 ^{0}F.

Table B-5 note (6) Carbon Steel Mill Report, Chemistry certification, %

Heat	C	Mn	P	S	Si	Cu	Ni	Cr	Mo	Sn	Al	V	Nb	N	Ti	B	Ca
1317337	0.040	0.250	0.011	0.005	0.020	0.09	0.030	0.030	0.010	0.006	0.032	0.001	0.003	0.006	0.003	0.00	0.002
2317334	0.030	0.270	0.010	0.003	0.020	0.09	0.030	0.030	0.010	0.006	0.037	0.002	0.004	0.007	0.003	0.00	0.002

Table B-5 note (7), Concrete Mixture: Portland cement: 26 lbs; stone: 68 lbs; sand: 44 lbs; water: 1.4 gallons

Table B-5 note (8) Portland Cement Chemical properties:

Compound	SiO_2	Al_2O_3	Fe_2O_3	CaO	MgO	SO_2	Loss on ignition	Insoluble residue	Equivalent alkalies
Analysis Result, %	20.5	5.1	3.7	62.7	1.1	2.8	1.7	026	0.42

Appendix C

Test Plan

Prepared by:

Westinghouse Electric Corporation, LLC under contract to the Pressurized Water Reactor Owners Group (formerly the Westinghouse Owners Group or "WOG") for the U. S. Nuclear Regulatory Commission and the Electric Power Research Institute (EPRI).

Test Plan:
Characterization of Chemical and Corrosion Effects Potentially Occurring Inside a PWR Containment Following a LOCA

Prepared By: /Original Signed By/
Timothy S. Andreychek

Organization: Westinghouse Electric Company, LLC

Date: July 20, 2005

Approved By:	/Original Signed By/	/Original Signed By/
	John M. Gisclon	B. P. Jain
Organization:	Electric Power Research Institute	U. S. Nuclear Regulatory Commission
Date:	July 20, 2005	July 20, 2005

Acknowledgement

This Test Plan was prepared for the Nuclear Energy Institute Sump Performance Task Force and U. S. Nuclear Regulatory Commission with input from the Westinghouse Electric Company, LLC, U. S. Nuclear Regulatory Commission and the Electric Power Research Institute (EPRI). The support of the Westinghouse Owners Group and the Babcock & Wilcox Owners Group in soliciting information, and the participation of individual plants in providing information to support the development of the Test Plan and is gratefully acknowledged.

TABLE OF CONTENTS

LIST OF ADDENDA

Revision Designation	Date	Affected Pages	Description
12	8/26/04	All	Initial release of the test plan.
12.a	10/6/04	Page 12	Amended text to correctly refer to "lithium concentration" rather than "LiOH". Amended upper limit of lithium concentration in primary coolant to be 3.5 ppm.
		Page 14	Added requirement for a single (1) side stream filter to be installed in the loop piping.
		Page 15	Amended chemistry parameters to specify LiOH concentration to be as required to reach 0.7 ppm lithium as LiOH.
		Page 18	Added text setting limits on the flow rate and total flow to be passed through the side filter.
		Page 22	Added text describing minimum inspection requirements associated with side filter.
12.b	2/8/05	Page 16	Added text clarifying process for considering minor changes or additions to confirmatory tests.
		Page 17	Added text describing the dimensions of concrete coupons.
		Pages 17	Added text describing the preparation and addition of latent debris to test run.
		Pages 17 through 21	Amended section on test guidelines including: • Added text under Section 4.4.3, "Test Operation," to note a summary of test operation guidelines is given in the following section. • Identified "Test Guidelines" as Section 4.4.3.1. • Revised presentation of the "Test Guidelines" section from bullet format to numbered format. • Added text clarifying frequency of taking test samples. • Added text describing guidance on analyzing sediment.
		Page 21	Added text describing guidance on adding TSP to test facility as Section 4.4.3.2.
12.c	3/30/05	Page 16	Swapped test sequence (3 → 4 and 4 → 3) to accommodate Industry request.

13	7/12/05	Page 10	Amended Section 4.1.31, including Table 4, "pH Levels of Sump Solutions," to include Sodium Tetraborate as a buffering agent in the ICET program. Identified that the pH of the test would be determined by mixing a Boric Acid solution having 2800 ppm Boron with a Sodium Tetraborate solution having 2100 ppm Boron to obtain a mixture Boron concentration of 2400 ppm.
		Page 11	Added explanatory text describing that the initial test fluid will contain Sodium Tetraborate buffering agent; no attempt will be made in the test to simulate the ice melt of an ice condenser plant. (Also see page 38, amended Section 5.5.1.)
		Page 14	Corrected a typographical error in Item 14.
		Page 15	Amended "Chemistry Parameters" to include Sodium Tetraborate
		Page 16	Amended Table 5, "Test Run Conditions," to include Sodium Tetraborate as the buffering agent for Test 5.
		Pages 19 and 20	Amended Item 4.4.3.1.5.3 to include a 4-hour spray duration at the initiation of Test 5.
		Page 21	Corrected a typographical error in Item 4.4.3.2.1.
		Page 22	Added Section 4.4.3.3, "Additional Guidance for Sodium Tetraborate Tests."
		Page 37	Amended the last sentence of Section 5.4, "Test Temperature," to identify 60° C (140° F) as being representative of long term pool temperatures for ice condenser containments.
		Page 38	Amended Section 5.5.1, "Spray Fluid pH," to identify that the test will be initiated with Boric Acid/Sodium Tetraborate mixture having an initial Boron concentration of 2400 ppm.
		Page 38	Amended Section 5.5.2, "Sump Fluid pH," to identify the pH of the simulated containment pool is derived from mixing Boric Acid and Sodium Tetraborate solutions to obtain a resulting mixture having a Boron concentration of 2400 ppm.

1 BACKGROUND

Pressurized Water Reactor (PWR) containment buildings are designed to both contain radioactive materials releases and to facilitate core cooling in the event of a Loss of Coolant Accident (LOCA). The cooling process requires water from the break and from containment spray to be collected in a sump and recirculated. The sump contains a screen that protects system structures and components in the Containment Spray and Emergency Core Cooling flow paths from the effects of debris that could be washed into the sump. There has been concern that fibrous insulation could form a mat on the screen that would obstruct flow. The flow through the fibrous mat would be further impeded if particles collect on the mat forming a dense filter cake.

Concerns have been raised about the potential for corrosion products to significantly block a fiber bed and increase its head loss. Among the materials that are found inside containment and are susceptible to corrosion and degradation by the post-LOCA solution, one can name aluminum, zinc, carbon steel, copper and non-metallic materials such as paints, thermal insulation and concrete.

A number of studies have been completed on the subject of zinc and aluminum corrosion in containment with regard to hydrogen generation. However little information is available on corrosion product release with representative post-LOCA conditions, and no studies have explored the possible interaction between the corrosion products (e.g. formation of gelatinous material, of agglomerates etc.) and the effects of those products on filtration. Further study is needed.

2 OBJECTIVE

This test plan addresses two (2) objectives:

- Determine, characterize and quantify the chemical reaction products that may develop in a representative post-LOCA containment sump environment.

- Determine and quantify any gelatinous material that develops during testing.

If gelatinous material is observed to develop in significant quantities during testing, the amount and location will be reported to the NRC and industry project managers for consideration for future debris bed head loss testing. Discovery of gelatinous material in quiescent flow zones may not be an issue as the likelihood of transport to sump screens is small. It is not intended that

this series of chemical effects tests be interrupted to conduct debris bed head loss tests if gelatinous material is found.

3 FUNDAMENTAL BASES FOR TEST PLAN DEVELOPMENT

This test plan is developed using the following as the bases for the plan:

1. The chemical corrosion codes identified by NRC (OLI Systems Inc., 2002a and 2002b) may be used, where applicable, to extend test data to plant conditions that may be beyond those explicitly covered in the test program.

2. The evaluation of the data collected will be directed at:

   2.1. First, determining if corrosion products form and/or if leaching of materials (from fiberglass, calcium silicate, concrete, etc.) occurs in a representative post-accident sump fluid inventory, and,

   2.2. If formed, characterizing and quantifying the corrosion products and leached solids to support evaluation of their impact on post accident sump head loss.

3. Epoxy-based protective coatings (paints) will not be included in the testing described in this test plan.

4. Measurement of head loss across a fiber bed is not considered as part of this test plan.

5. The test loop will be operated within a time-temperature-chemistry profile representative of PWR post-LOCA operation, except that the loop will be operated at a constant temperature of 60° C (140° F).

4 GENERAL APPROACH

This test plan addresses the following four (4) topical areas:

1. Definition of test parameters
2. Definition of the test loop
3. Test Performance
4. Characterization of test samples

4.1 Identification of Test Parameters

Tests will be conducted using justifiable proportions of non-metallic, metallic, and cementitious materials exposed to the warm, slightly basic pH liquid of the containment pool and spray environment. The specific parameters identified in the test plan are based on a review of readily available documentation and the results of surveys of U. S. nuclear power plants. The test plan logic is to conduct testing with representative material surface areas and sump volumes and chemical constituents to provide test conditions simulating the post-LOCA sump environment. Further justification for specific test parameters can be found in Section 5 to this document.

A limited number of test runs will be performed. For each test run, the parameters will be set to realistic levels that represent the conditions prevailing in containment after a LOCA. The test parameters and the bases for their selection are developed below.

4.1.1 Tested materials

The materials to be included in the test are:

- Zinc (in galvanized steel and in zinc-based protective coatings)
- Aluminum (valve actuator components, scaffolding)
- Copper (containment fan cooler fins)
- Carbon steel (untopcoated structural components)
- Concrete(representing exposed concrete surfaces and concrete dust particles)
- Insulation material (fiberglass, calcium silicate)

The amounts of each material are described below in the form of material surface areas to water volume ratios, with the exception of concrete dust, which will be represented as a mass to water volume ratio, and fiberglass and calcium silicate, which will be represented as a fiberglass or calcium silicate volume to water volume ratio. The bases for the values presented in Table 1 below are detailed in Section 5 of this document.

Table 1: Material Quantity/Sump Water Volume Ratios Planned to be Tested

Material	Value of Ratio Tested (ratio units)
Zinc in Galvanized Steel	8.0 (ft^2/ft^3)
Inorganic Zinc Primer Coatings (non-top coated)	4.6 (ft^2/ft^3)[1]
Inorganic Zinc Primer Coatings (top coated)	0.0 (ft^2/ft^3)[2]
Aluminum	3.5 (ft^2/ft^3)
Copper (including Cu-Ni alloys)	6.0 (ft^2/ft^3)
Carbon Steel	0.15 (ft^2/ft^3)
Concrete(surface)	0.045 (ft^2/ft^3)
Concrete(particulate)	0.0014 (lbm/ft^3)
Insulation material[3] (fiberglass or calcium silicate)	0.137 (ft^3/ft^3)

[1] This value addresses both untopcoated zinc-rich primer applied as an untopcoated system as well as zinc-rich primer exposed as a result of delamination of topcoat.

[2] Topcoated inorganic zinc coatings are protected against exposure to both containment spray and the liquid inventory of the containment pool by the topcoat. Therefore, they do not contribute to the development of corrosion products. Also, epoxy-based protective coatings provide for small quantities of leachable material, typically less than 200 ppm of the applied coating. Therefore, epoxy topcoats are judged to not contribute to the corrosion product mix post-accident and are not included in this test program.

[3] Two tests are to be conducted using 100% fiberglass as the insulation material. Two additional tests are to be run with 80% calcium silicate and 20% fiberglass as the insulation material. In both cases, the same ratio of insulation material-to-sump liquid inventory will be used.

4.1.2 Physical Parameters

4.1.2.1 Simulated Sump Temperature

Previous studies have demonstrated the importance of temperature in the corrosion process of aluminum and zinc (References 1 and 2):

- Corrosion rate quickly increases with temperature, and,
- While the solubility of oxidized Al increases with temperature, the solubility of oxidized Zn decreases with temperature.

The predicted temperature history in the sump post-accident depends on the accident scenario, the operation of the plant, and the input values assumed for the calculation. A representative predicted temperature versus time profile for a large break LOCA gives the following:

- A maximum expected sump temperature of about 130° C (266° F), achieved less than 1 minute after the break.
- A cool-down of liquid temperatures in the sump such that, within 1 hour, the temperature decreases to approximately 65° C (149° F), and,
- Within 24 hours, a steady state value of 55° C (131° F) is predicted.

See Section 5.4, "Test Temperature," for additional discussion and Figures 2 through and including 7 for representative design basis sump water temperature calculations. These calculations use input assumptions designed to maximize containment sump temperature calculations.

Performing the tests in a high temperature, high-pressure facility is not proposed. This is based on a thermodynamic simulation study conducted using Environmental Simulation Program (ESP) Version 6.6® (OLI Systems, Inc., 2002a) and StreamAnalyzer Version 1.2® (OLI Systems, Inc., 2002b) (Reference 12). The calculations performed indicated the amount of corrosion and leaching products that might be expected is dominated by the 14day low temperature phase rather than the 30 minute high temperature phase of the LOCA.[4]

[4] Corrosion and leaching rates used in the study were based on open literature data and selected based on conservative values obtained between a pH 7 and 10 in borated water. The influence of pressure, temperature, and pH on chemical speciation was studied by speciating a fixed amount of each component based on its corrosion rate. The simulation study assumed certain corrosion and leaching rates of the metallic, concrete, and insulation materials as a function of temperature in a borated alkaline solution. An experimental study is being conducted to validate the corrosion and leaching rates used in the study.

The time of containment high-temperature operation post-accident approximately corresponds to the post-LOCA injection phase. The high temperature (> 100° C) portion of the transient is over at the time recirculation from the containment sump is initiated. This is typically 20 to 30 minutes after the accident. The pH conditions during the injection phase differ from those during the recirculation phase (see section on pH below). The effect of high temperatures and a different pH on the resulting corrosion and leachant products were estimated for individual materials using the OLI systems, Inc. thermodynamic modeling suite of programs (Reference 12). The resultant calculations indicated that an elevated temperature effect is not expected to reduce the potential formation of silica-based gelatinous solids.

However, exposure of some materials to a high pH fluid which may be present during the initial spray injection for plants using NaOH buffering agent may significantly affect amount of corrosion and leachant products in the sump water, and hence affect the chemical evolution of the water. Therefore, the NaOH test will include a high pH spray injection phase to simulate this condition as described later in this document. In other words, this high pH spray injection phase will aid in the corrosion and leaching process, and potentially accelerate the formation of solid species, which may include gels, that may be formed after reaching their solubility limit.

4.1.2.2 Simulated Containment Temperature

Containment transient analysis results show that containment temperature is normally slightly below the sump temperature. Based on engineering judgment, it is estimated that the small difference in temperature between the containment vapor space and sump will have a very minor impact on the test results. Therefore the containment vapor space temperature will not be simulated independently of the sump temperature.

4.1.2.3 Simulated Sump Recirculation Flow

Velocities over samples shall be representative of post-LOCA fluid velocity conditions in PWR containment pool – which range from near zero to 3 cm/sec. A velocity profile map of the submerged portion of the test chamber will be developed so that the approximate velocity that a metallic or concrete coupon, fiberglass or calcium silicate sample is subjected to in the test can be ascertained. However, the volume of the test tank and test loop beyond the coupon samples shall be constructed so as not to allow corrosion product particulates to settle. The corrosion product particulates, if they exist, are to be collected from the grab sample line, as shown in Figure 1.

4.1.2.4 Simulated Containment Spray Flow

The ratio of spray flow to containment cross section area will be used as a simulation parameter. The value of containment spray flow and the containment cross-sectional diameter are plant specific parameters. However, a preliminary evaluation suggests that values in the table below are representative for PWR designs and are recommended for use in the test program. The suggested duration for simulating containment spray is given in Section 4.1.2.6.

Table 2: Ratio of Spray Flow to Containment Cross Sectional Area

Spray Flow (ft3/Hr)	Containment Diameter (ft)	Flow/Area Ratio (ft/Hr)
25,000	135	1.75

4.1.2.5 Submergence of Test Samples

The amount of material that will be submerged long term post-accident during the operation of the ECCS and CSS in the recirculation mode is a plant specific value that is dependent on the post-accident flood-up level for each plant. Based on a preliminary assessment of several representative PWRs, the split between submerged and non-submerged samples as shown in Table 3 is recommended for this test.

4.1.2.6 Test Duration

The high pH phase for NaOH spray injection testing is to last 30 minutes. The spray portion of the test will last for 4 hours including the aforementioned 30 minutes. (Note: The range of time for spray termination based on pressure control for a large dry Westinghouse 4-loop reactor is generally an hour or less. It is acknowledged that some plants continue spray operation to control dose. The 4 hours of spray operation is conservatively representative of the extended spray operation for dose control.)

Maximum duration of any test is limited to 30 days. Duration of subsequent test runs following the initial run will be determined after evaluating the results of the first run, and will consider establishing steady state conditions.

It is recommended that, metallic test specimens will be aged to allow a thin (μm thick) air oxide film to form, however, due to time constraints this may not be possible in all cases, less than

complete aging will result in samples being more susceptible to corrosion because of the absence of a protective oxide film and yield "conservative" results in this testing.

Table 3: Percentage of Surface Areas Above and Below Containment Flood Levels

Material	Submerged %	Non-Submerged %	Comment
Zinc Galvanizing	5	95	• The submerged value accounts for grating and duct work that might be submerged.
Zinc Coatings (topcoated)	0	0	• Epoxy-based topcoats preclude interaction of the zinc primer with containment sump inventory and containment spray. Exposure of zinc primer to containment sump and containment spray fluids due to local failures of epoxy-based topcoats is accounted for in the untopcoated zinc coatings.
Zinc Coatings (untopcoated)	4	96	• Addresses both untopcoated zinc primer applied as an untopcoated system as well as zinc primer exposed as a result of delamination of topcoat.
Aluminum	5	95	• Aluminum is generally not located at elevations inside containment where it may be submerged.
Copper	25	75	• Majority of surface from CRDM coolers and instrument air lines.
90-10 Cu/Ni	25	75	• Majority of surface present in containment fan coolers.
Concrete	34	66	• The submerged value accounts for limited damage to floor and wall surface areas that will be submerged due to primary RCS piping being elevated above the containment floor.
Carbon Steel	34	66	
Fiberglass	75	25	• The submerged value accounts for most of the fiberglass to remain in areas where it will wash down into the sump pool.
Calcium silicate	75	25	• The submerged value accounts for most of the cal-sil to remain in the areas where it will wash down into the sump pool.

4.1.3 Chemical Parameters

4.1.3.1 pH

The pH of the sump solution and containment spray solutions will have a large effect on corrosion and precipitation reactions. Hydrated trisodium phosphate (TSP) ($Na_3PO_4.12H_2O$) and sodium hydroxide (NaOH) are the standard chemicals used for pH control in post-LOCA solutions. For plants using TSP, the TSP is stored in baskets on the containment floor and is dissolved by the post-LOCA solution within a certain time. For plants using sodium hydroxide, the NaOH is injected and mixed directly with the containment spray flow. During the approximately 30 minute initial NaOH injection into the spray stream, pH values in this stream can be as high as 12. Typical values of sump solution pH are shown in Table 4 below[5].

Table 4: pH Levels of Sump Solutions

Sodium Hydroxide (NaOH)	Trisodium Phosphate	Sodium Tetraborate
10	7	T. B. D. (See explanation below.)

For tests using NaOH as a buffering agent, the maximum pH of the recirculation solution is 10 when pH adjustment is made with sodium hydroxide and the Boron concentration in the RWST is low (2300 ppm). When TSP is used, its required quantity is calculated to reach a minimum pH of 7.0 at high boric acid concentration in the RWST. For the test using Sodium Tetraborate, the pH is a consequence of achieving a target Boron concentration as described below.

Therefore three sets of pH conditions will be simulated:

- pH = 10, with NaOH.
- pH = 7.0, with TSP.
- pH = Initial pH will be determined by combining and mixing appropriate quantities of Boric Acid solution having a Boron concentration of 2800 ppm and Sodium Tetraborate solution having a concentration of 2100 ppm Boron to produce an initial test solution having a Boron concentration of 2400 ppm.

[5] pH of a post-LOCA containment pool is initially determined by the pool constituents. For ice condenser plants, this includes the ice-sodium tetraborate solution (2100 ppm Boron), the reactor coolant system (variable, depending on time in core life), and the ECCS/RWST (boric acid) Boron concentrations. An initial pH of ~ 8.1-8.5 in the test

No adjustment of the initial pH will be made after the commencement of the test.

At a pH range of 6.5 to 7.0, corrosion of aluminum is minimal. It is known that corrosion of aluminum increases with increasing pH (References1 and 2).

Similarly, zinc corrosion reaches a minimum at a pH range of 7.0 to 8.0 and increases outside that range (References 2, 7 and 8). It is noted that Reference (2) shows this minimum corrosion to be in the pH range of 8.5 to 9.5.

It should also be noted that the solubility of aluminum oxides increases with pH while the solubility of zinc oxides decreases with pH (Reference 1).

pH conditions during the injection phase are different from those during the recirculation phase.

- For plants with TSP as pH control agent, the minimum pH during injection (pH ranging from 4.7 to 5) corresponds to the boric acid concentration in the RWST (2000-2800 ppm boron). It is noted that sump pH will not reach a steady state until the TSP is completely dissolved (one to two hours). For the pre-conditioning of test coupons, a conservatively low value of 4.7 is selected corresponding to a concentration of 2800 ppm boron in the RWST.

- For plants with NaOH addition, the spray pH can be higher – up to 12 – during the injection phase, when sodium hydroxide is mixed with the spray water.

- Plants that use sodium tetraborate as a pH control agent are ice condenser plants. For these plants, the minimum pH during injection (pH ranging from about 4.7 to 5) corresponds to the boric acid concentration of the RWST (2000-2800 ppm boron). Sodium tetraborate is added to the sump liquid inventory as the ice condenser ice bed melts. Thus, the sump pH will not reach its final value until the ice bed is completely melted (generally within about one hour after initiation of the large break LOCA).

For tests using NaOH as a buffering agent, the short operating period in plants with a high pH value (about 30 minutes of containment spray) will be simulated. For the tests using TSP as the buffering agent, a gradual introduction of the buffering agent over an hour will be simulated. For the test using Sodium Tetraborate as a buffering agent, the test will be initiated with a solution

---

loop is expected when the Sodium Tetraborate and Boric Acid solutions are mixed, not considering other effects such as CO_2 ingestion or reactions with the sample materials.

representing the boron concentration at the completion of ice bed melt. That is, no attempt will be made to simulate the addition of Sodium Tetraborate due to the phenomena of ice melting. See Section 5.5.1 for additional discussion on this approach.

Hydrochloric acid (HCl) can be formed from the degradation of cable insulation material (Reference 5). The test will provide for the conservative treatment of this degradation by having an initial concentration of 100 ppm of HCl in the fluid simulating the sump inventory.

4.1.3.2 Aeration

Dissolved oxygen is known to accelerate corrosion. Therefore, all tests will be conducted in fully aerated (e.g., air saturated) conditions. It is also recognized that some reduction of pH may result from entrainment of CO_2 in the fluid. No attempt will be made to increase or maintain pH beyond the initial value of ~10 for NaOH injection tests to compensate for this effect.

4.1.3.3 Other

Several chemical species will be set at the same initial value from test to test. Specifically, this pertains to boric acid, lithium hydroxide and pre-existing surface corrosion.

- For boric acid, a maximum boron concentration of 2800 ppm is selected. This value is chosen in recognition of the current trend to increase boron concentration in the RWST as core designs move to more reactive cores. (It is noted that some plants in the US already operate with 2900 ppm boron in the RWST). The initial boron concentration of 2800 ppm will be used during all test runs as this value is set largely by the RWST tank boron concentration and does not vary significantly from plant to plant.

- The lithium cation will affect zinc and aluminum corrosion primarily through an indirect pH effect. Lithium concentration typically varies between 0 and 3.5 ppm in the RCS, so its concentration would be less than 0.7 ppm in the post-LOCA recirculation solution. The impact is obviously negligible when compared to the NaOH concentration (more than 2500 ppm). However, to preclude the possibility of this assumption being challenged after the testing has been completed, this minimal concentration (0.7 ppm Li as LiOH) will be incorporated into the Test Plan for completeness.

4.2 Applicable ASTM Standards and Standard Practices

The following ASTM Standards and Standard Practices should be used, as applicable, in conjunction with the specific instructions offered below.

- G 1-90 (1999), Practice for Preparing, Cleaning, and Evaluating Corrosion Test Specimens
- G 4-01, Guide for Conducting Corrosion Coupon Tests in Field Applications
- D 3370-95a (1999), Standard Practices for Sampling Water from Closed Conduits
- G 16-93 (1999), Guide for Applying Statistics to Analysis of Corrosion Data
- G 31-72 (1999), Standard Practice for Laboratory Immersion Corrosion Testing of Metals

To minimize the number of individual coupons used in testing, the coupon sizing may depart from those specified in the procedures above. This is considered acceptable as determination of corrosion rate data is considered to be of secondary importance to the stated test objectives.

4.3 Test Loop Functional Requirements

The functional requirements for the test loop are described in this section. A schematic of a suitable test loop is shown in Figure 1

1. The central component of the system is a test tank. The test tank shall be designed to preclude the formation of sedimentation in the test tank.

2. The test tank shall be capable of maintaining both a liquid and vapor environment as would be expected in containment post-LOCA.

3. The test loop shall be capable of temperature control of the liquid phase to within ± 5° F.

4. The system shall be capable of circulating water at flow rates that simulate spray flow rate per unit area of containment cross section. Pump required flow and head will be determined later.

5. The test tank shall provide for water flow over submerged test coupons that will simulate the range of sump fluid velocities that may be related to conditions expected at plants.

6. Piping and related isolation valves are to be provided such that the parallel stream can be isolated during performance of the test.

7. The pump discharge line shall split in two: one branch being directed to the spray ramp located in the vapor space inside the reaction tank, the other branch returning to the liquid side of the tank. Each branch will be provided with an isolation valve and flow meter.

8. A flow meter shall be provided in the recirculating piping.

9. The pump circulation flow rate shall be controlled at the pump discharge to be within ± 5 per cent of the flow required to simulate fluid velocities in the test article. Flow control may be either automated or manual. The ability to manually control flow at the levels identified for testing is to be demonstrated prior to initiating testing.

10. The tank shall accommodate a rack of immersed sample coupons including the potential reaction constituents identified previously.

11. The tank shall also accommodate a rack of sample coupons that may be exposed to spray of liquid that simulates the chemistry of a containment spray system. Provision is to be made for visual inspection of the spray rack.

12. The tank shall provide for sufficient space between the test coupons as to preclude galvanic interactions[6] among the coupons. As a minimum, different metallic test coupons shall be electrically isolated from each other and the test stand to prevent galvanic effects resulting from metal-to-metal contact between specimens or between the test tank and the specimens as outlined in procedures ASTM G4 and G31.

13. The fluid volumes and sample surface areas shall be based on scaling considerations to relate the test conditions to plants.

14. A cartridge or analytical filter shall be provided for in a side stream from the loop piping. The cartridge or analytical filter shall be capable of retaining particulates having a dimension of 0.45 microns or larger. The cartridge or analytical filter shall be constructed of material that will not chemically interact with the test fluid.

15. All components of the test loop shall be made of corrosion resistant material (for example, stainless steel for metallic components).

[6] Galvanic reactions are local corrosion effects, occurring between two or more electrically coupled dissimilar metals with an electrolyte path between the metals. Due to the small scale of the test, the potential influence of the tank and the potential variable effects from possible metallic coupon arrangements, there is a concern that electrically coupling coupons could yield non-typical results. To preclude this occurrence, test coupons are to be electrically isolated from one another.

4.4 Test Performance: Program and Guidelines

The practices that govern the testing outlined below are given in ASTM G4 and G31.

4.4.1 Test Program

Based on the evaluation of parameters identified in Table 3, the liquid volume of the test facility used to perform the test will fix the specific values for each of the materials and the following test parameters:

Physical parameters:

- Water volume in the test tank: 949 l (250 gal.)
- Circulation flow: 0 – 200 l/min (0 – 50 gpm)
- Spray flow: 0 – 100 l/min (0 – 25 gpm)
- Sump temperature: 60° C (140° F)

Chemistry parameters:

- Boron concentration: 2800 ppm
- $Na_3PO_4.12H_2O$ concentration: as required to reach pH 7 in the simulated sump fluid — approximately 2 g/l
- NaOH concentration: as required to reach pH 10 in the simulated sump fluid — approximately 6g/l
- Sodium tetraborate concentration: as required to reach a Boron concentration of 2400 ppm in the simulated sump fluid — approximately 15 g/l
- HCl concentration: 100 mg/l
- LiOH concentration: as required to reach 0.7 ppm lithium as lithium hydroxide

The test program defined by this test plan includes five (5) test runs. The parameters of each run are described in Table 5.

An objective of Test 5 is to provide information regarding the chemical effects with a Sodium Tetraborate buffer, including evaluating resulting products of chemical reactions. The initial pH for Test 5 is expected to be between that achieved for Test 1, which used Sodium Hydroxide as a buffering agent, and for Test 2, which used Trisodium Phosphate as a buffering agent. Other test parameters for Test 5 (fluid temp, number and type of coupons, and insulation tested) are similar to those of Test 1 and Test 2.

Table 5: Test Run Conditions

Run	Temp (° C)	Buffering Agent	pH	Boron (ppm)	Note
1	60	NaOH	10	2800	100% Fiberglass insulation test. High pH, NaOH concentration as required by pH. (See Notes 1 and 2)
2	60	TSP ($Na_3PO_4.12H_2O$)	7	2800	100% Fiberglass insulation test. Low pH, Trisodium Phosphate concentration as required by pH.
3	60	TSP ($Na_3PO_4.12H_2O$)	7	2800	80% Calcium silicate / 20% fiberglass insulation test. Low pH, Trisodium Phosphate concentration as required by pH.
4	60	NaOH	10	2800	80% Calcium silicate / 20% fiberglass insulation test. High pH, NaOH concentration as required by pH. (See Note 2)
5	60	Sodium Tetraborate	8.0 to 8.5 (est.)	2400	100% fiberglass insulation test with sodium tetraborate buffer. The sump solution is to be targeted to simulate the solution mixture of a representative ice condenser plant after melting of the ice beds. (Note 3).

Notes:

(1) The duration of Test 1 will be 30 days.

(2) During the first 30 minutes of Tests 1 and 4, NaOH will be injected in the spray fluid. The quantity of NaOH injected in the spray solution is subject to the following constraints:

a. The pH of the spray fluid shall not exceed a value of pH = 12 during this initial 30 minute injection phase, and,

b. The target pH of the simulated sump fluid inventory at the termination of the of containment spray simulation (e.g., after the 30 minute NaOH injection phase), not considering pH effects due to CO_2 absorption and other chemical effects which may be occurring during NaOH injection, is a value of pH = 10.

(3) For Test 5, the planned test loop solution is to be a mixture of Boric Acid solution having a Boron concentration of 2800 ppm and Sodium Tetraborate solution having a concentration of 2100 ppm to achieve a resulting Boron concentration of 2400 ppm. To the extent practicable the remaining run parameters will be consistent with those of Test 1 and Test 2. This includes the temperature of the test solution, number and types of coupons, and insulation samples. Spray will be initiated at the commencement of the test and continue for 4 hours, but no additional buffering chemical will be added to the spray stream.

4.4.2 Test Coupon Preparation

The following guidance is given for the preparation of coupons to be used in the tests identified in this test plan.

4.4.2.1 Metallic Coupons

Test coupons should be prepared using the recommended practices outlined in ASTM G1, as applicable. This practice describes accepted procedures for and factors that influence laboratory immersion corrosion tests, particularly mass loss tests. These factors include specimen preparation, apparatus, test conditions, methods of cleaning specimens, evaluation of results, and calculation and reporting of corrosion rates. This practice also emphasizes the importance of recording all pertinent data and provides a checklist for reporting test data. As noted previously, to minimize the number of individual coupons used in testing, the coupon sizing may depart from those specified in the procedures above. This is considered acceptable practice as determination of corrosion rate data is considered to be of secondary importance to other stated test objectives. However, exceptions and deviations from ASTM G1 are to be documented and justified by the test performer.

4.4.2.2 Fiberglass and Calcium Silicate

For fiberglass and calcium silicate, retention in multiple sample baskets fabricated from fine (~1/16-inch stainless steel mesh) screens with small, removable sample containers, is recommended. Most of the submerged fiberglass and calcium silicate should be inserted below the metallic coupons where flow can pass through it. Some of this material should be placed in areas of the test tank that are expected to be quiescent as well.

4.4.2.3 Concrete Samples

Concrete coupons are to be located in both the submerged and non-submerged region. To facilitate placement of the 12" x 12" x 2" concrete coupon only one coupon will be placed in the submerged rack. The area of this coupon will exceed the surface area requirement for submerged concrete (.51 ft^2) and non-submerged concrete (.99 ft^2). Since it is all submerged, it is conservatively exposed to the sump fluid for the entire duration of the test run versus the 4 hour spray interval.

4.4.2.4 Aging

It is recommended that, metallic test specimens will be aged in air under ambient conditions to allow a thin (μm thick) air oxide film to form. Due to time constraints this may not be possible in all cases. However, less than complete aging will result in samples being more susceptible to corrosion because of the absence of a protective oxide film. This will allow for greater corrosion of the test coupons and samples and yield "conservative" results in this testing.

4.4.2.5 Latent Debris

Particulate material simulating 200 lb_m of latent containment debris is to be added to the fluid in the test tank as follows:

- Concrete particulate [simulating 50 lb_m]: 21.2 grams (0.75 ounces)
- Surrogate particulate debris (sand and clay) [simulating 150 lb_m]: 63.7 grams (2.25 ounces)

The basis for the above amounts of debris identified above is as follows:

- The test plan assumed 50 lbs of concrete particulate debris in a representative containment, and provides a factor of 0.0014 lbs (test material) / ft^3 of system volume.
- The mass of the concrete particulate sample is then calculated as

  $$0.0014 \times 250 \text{ gallons} / 7.48 \text{ gal/ft}^3 = 0.0467 \text{ lbs} = 0.75 \text{ oz} = 21.2\text{gms}$$

- Assuming a total latent particulate loading in containment of 200 lbs, including the concrete particulate, the mass of the surrogate particulate would then correspond to 150 lbs or three times that for the concrete particulate or 2.25 oz or 63.7 gms.

The particulate material should be shaken into the test tank after all of the chemical additions have been completed and the tank temperature has reached 60 °C, but before insertion of the fiberglass and sample coupons.

Note: The concrete particulate matter is to be obtained by chipping off one corner of one of the concrete test coupons and grinding it into a fine powder, about the size of the surrogate particulate debris. Chipping and grinding shall be performed in a manner so as not to contaminate the concrete with extraneous material such as iron oxide or glass.

4.4.3 Test Operation

The general practices for testing given in ASTM G4 and G31 should be used, as applicable, to perform the test. Detailed test procedures or instructions shall be developed. Such procedures and instructions shall be approved by the NRC and EPRI project managers/test program leads prior to use. A summary of test operation guidelines are given below:

4.4.3.1 Test Guidelines

The following general sequence of events is to be followed for the testing:

4.4.3.1.1 The cleanliness of the test loop shall be verified. Between test runs the loop shall be cleaned in accordance with applicable portions of ASTM A 380-99, Standard Practice for Cleaning, Descaling, and Passivation of Stainless Steel Parts, Equipment, and Systems. No observable scale or sediment shall be present in the test tank or loop piping, and the loop water conductivity (after cleaning) shall be < 50 μS/cm and turbidity shall be < 0.3NTU.

4.4.3.1.2 The test loop shall be filled with demineralized water and chemicals added and adjusted as required for the initial test run conditions.

4.4.3.1.3 The temperature of the system shall be adjusted to the normal test run operating temperature.

4.4.3.1.4 The sample coupons and other test material (insulation, debris) shall be placed into the test sample racks and inserted into the test loop in a preplanned manner consistent with scaling and other pertinent information.

4.4.3.1.5 Operation of the test loop shall be performed with conditions representative of postulated post-LOCA conditions, including:

4.4.3.1.5.1 A temperature of 60C (140F), +/- 2C

4.4.3.1.5.2 Fluid velocities over samples between 0 and 3 cm/sec (0.1ft./sec), except where specifically exempted (e.g., fiberglass samples near the drain line will be subjected to significantly higher velocities).

4.4.3.1.5.3 For all tests (Tests 1, 2, 3, 4 and 5), spray duration is 4 hours.

For tests using NaOH as a buffering agent, the initial high pH phase of the spray simulation will last 30 minutes. This high pH phase is intended to simulate containment spray with NaOH addition during the initial injection phase of a LOCA sequence. The remaining 3 ½ hours simulate spray on recirculation.

For the Sodium Tetraborate test, the containment spray duration will last 4 hours. The test will be initiated with a solution having a Boron concentration of 2400 ppm that is achieved from mixing a Boric Acid solution having a Boron concentration of 2800 ppm and a Sodium Tetraborate solution having a Boron concentration

of 2100 ppm. Spray will be conducted with recirculated sump fluid with no additional chemicals added to the spray stream

4.4.3.1.5.4 Nominal duration of each test run is 30 days, however, this may be shortened if chemical equilibrium is observed. Any reduction in duration shall be approved by the project managers/test program leads.

4.4.3.1.6 Sampling shall be performed at frequencies necessary to obtain necessary information regarding the behavior of the test loop and for characterization of chemical reaction products which may occur:

4.4.3.1.6.1 For all grab samples, the observable physical properties of the sample shall be noted as soon as possible after the sample is taken from the test loop. The properties include color, suspended solids, and kinematic viscosity.

4.4.3.1.6.2 Samples shall be obtained at appropriate times and frequencies during each test run, and particularly before and after significant changes are made in loop operations and frequently when parameters are expected to be changing rapidly. For example, samples should be obtained before adding debris, after adding debris, before initiating spray, after terminating a spray phase and frequently during the first day or so of the testing.

4.4.3.1.6.3 Characterization of particulate matter is particularly important. Where feasible, determination of the chemical constituency and compounds, size, density, specific surface area, and information relative to the microstructure of the material (crystalline or amorphous) shall be performed. Collection of samples for particulate characterization shall be performed at least following debris addition, 24 hours after test commencement and at weekly intervals thereafter unless sample analysis indicates that particulate inventory is stable at a low value.

4.4.3.1.6.4 If potentially gelatinous material is observed or identified, the project manager/test program leads shall be informed promptly with a description of the material and other pertinent information.

4.4.3.1.6.5 Analyses of fluids shall be performed to characterize dissolved material in the test loop and behavior of loop chemistry. For elements whose concentration is not expected to vary during the test such as B, Li, K, and Pb analyses shall be performed at the beginning, end, and mid-point of a test run. For elements whose concentration may vary during a test run, frequent analyses shall be performed. These elements include Al, Ca, Cu, Fe, Ni, Si, Na, and Zn. Collection of samples for these analyses shall be performed at least before coupon and insulation addition, after 30

minutes, after spray termination, at 2,4,8, and 24 hours, and at a nominal daily frequency thereafter. Sampling and analysis frequencies may be changed if a sufficient basis exists, subject to project manager/test program lead approval.

4.4.3.1.6.6 Post-run examinations include sediment characterization and examination of, weighing, photographing and storage of sample coupons and insulation samples. Except for samples undergoing detailed and possibly destructive examination, adherent deposits and/or corrosion products shall not be removed. Coupons and samples shall also be preserved in appropriate sealed storage containers for possible future examinations. Ultimate disposition of samples and material generated during testing shall be governed by instructions jointly issued by the NRC and EPRI project managers/test program leads.

4.4.3.1.6.7 Sediment characterization includes, as appropriate and feasible determining the mass and volume collected, determination of constituents (e.g., fiberglass, latent particulate, precipitate, etc.), determination of density and specific surface area, whether amorphous or crystalline, elemental composition and speciation. Specific direction concerning characterization shall be provided jointly by the NRC and EPRI project managers/test program leads.

4.4.3.1.7 The test matrix calls for four primary test runs and a confirmatory run. It is planned that one of the test runs will be repeated as a confirmatory test. However, minor changes or additions to the previous test run to be repeated may be made for the confirmatory test. The project managers/test program leads shall concur regarding which run will be repeated and any changes or additions to be made.

4.4.3.2 Additional Guidance for TSP Tests

The following clarify the requirements for TSP addition during appropriate test runs:

4.4.3.2.1 Benchtop analyses shall be performed to confirm the quantities, concentrations and pH values to be achieved with TSP buffer addition.

4.4.3.2.2 The initial 30-minute spray phase will not contain TSP, as this material will not be introduced into spray before commencing recirculation operations in a postulated post-LOCA sequence. TSP will dissolve gradually, and metered addition of TSP solution into the test loop during the remaining 3 ½ hour spray phase is appropriate.

4.4.3.2.3 HCl should be added toward the end of the TSP injection sequence, during the final two hours of spray operation. Adding HCl early in the sequence or before buffer addition would result in unrealistically low pH values in the test loop fluid.

4.4.3.3 Additional Guidance for Sodium Tetraborate Tests

The following clarify the requirements for sodium tetraborate addition during Test 5:

4.4.3.3.1 The target Boron concentration of the sodium tetraborate solution simulating the melting ice of an ice condenser is to be about 2100 ppm. During preparation and holding, the solution is to be maintained in constant recirculation to keep the borax in solution[7].

4.4.3.3.2 The target initial Boron concentration of the solution mixture in the test loop inventory is to be 2400 ppm. This concentration is to be achieved by mixing a Boric Acid solution having a Boron concentration of 2800 ppm with a Sodium Tetraborate solution having a Boron concentration of 2100 ppm.

4.4.3.3.3 Benchtop analyses shall be performed to confirm the quantities, concentrations and pH values to be achieved by mixing a Boric Acid solution with a Boron concentration of 2800 ppm and a Sodium Tetraborate solution with a Boron concentration of 2100 ppm to obtain a mixture having a Boron concentration of 2400 ppm.

4.4.3.3.4 Containment spray will be simulated for the first 4 hours of the test. This is conservative for ice condenser plants as there is little material in the ice condenser upper containment that containment spray solution can chemically interact with.

4.4.3.3.5 HCl is to be added during the final two hours of spray operation. This addition time is representative of the earliest time that HCl would be generated in the plant.

4.4.4 Test Termination Criteria

Based on the evaluation of the particulates captured on filtered grab samples, a decision will be made to continue or terminate the test. The criteria for termination are based on the following:

1. The first test will run for 30 days.
2. Maximum duration of any test is limited to 30 days. Duration of subsequent test runs following the initial run will be determined after evaluating the results of the first run, and will consider establishing steady state conditions.

[7] Achieving a super saturated solution of Sodium Tetraborate is not desired as it would be completely non-representative of the ice condenser chemistry. Moreover, this could produce precipitates or reaction products that would be test run artifacts not representative of a representative plant situation.

3. For subsequent tests, the following termination criteria will be used:
    a. The corrosion process achieves an equilibrium or steady-state condition in less than 30 days,
    b. The leaching of silica, should it occur, reaches a steady-state condition in less than 30 days,
    (Note: for criteria [a] and [b], the test sponsors will be consulted prior to termination of the test to determine whether the test should indeed be terminated.)
    c. The test duration reaches 30 days of continuous operation, or
    d. Alternate termination criteria, which will be discussed with the test sponsors prior to their implementation.

4.5 EVALUATION OF TEST SAMPLES

In general, ASTM G16-93 (1999) may be used to evaluate the corrosion data. Specific evaluation requirements are listed below.

4.5.1 Test Coupon Evaluation

Coupons used in the test should be weighed and photographed before and after testing. Prior to weighing, the coupons shall be dried to remove moisture from the attached corrosion products. These records and the coupons are to be retained for later use.

4.5.2 Fiberglass and Calcium Silicate Sample Evaluation

Similarly, the fiberglass and calcium silicate samples use in the test should be weighed and photographed before and after testing. Specific attention is to be given to possible collection of gelatinous material on the surface of the fiberglass or calcium silicate. Prior to weighing, the coupons shall be dried to remove moisture. These records and the fiberglass or calcium silicate samples are to be retained for later use.

4.5.3 Sampling and Grab Sample Analyses.

Given below are specific guidelines for collecting grab samples. See ASTM Standard D 3370-95a (1999), "Standard Practices for Sampling Water from Closed Conduits," for additional general guidance on collecting grab samples.

In preparation for collecting a grab sample, the sample line shall be flushed with a minimum volume equivalent to three sample line lengths. To assure a representative sample, the flow rate used during line flushing and sampling shall be sufficient to assure flow is sufficient to maintain all species in suspension in the sample line. Excess solution removed from the loop during sampling shall be collected and returned to the loop.

The volume of sample to be removed shall be sufficient to measure pH, turbidity and boron concentration on the unfiltered sample and to allow for filtration of an appropriate volume of solution through a 0.45 micron filter for collection of suspended material. A small amount of the grab sample fluid will be set aside for other analyses, and the remainder will be re-introduced to the test loop.

The sample for filtration should be filtered as rapidly as possible after collection to assure that precipitation of any material has not resulted from a decrease in sample temperature. The filtered material should be dried and weighed until reproducible results are obtained. The filtrate shall be collected and stored at ambient temperature in a sealed container and observed for at least 1 week to determine if precipitates form upon standing.

A sample should be evaluated as rapidly as possible after collection for the existence of gelatinous material in the grab sample fluid. One possible method of evaluation is to measure the viscosity of the sampled fluid.

At a later time, a representative portion of the filtered material shall be digested for the purpose of elemental composition. The filtrate shall be re-filtered using a 0.45 micron filter to remove for determination of elemental constituents any material that has settled from solution. The acidified filtrate shall also be analyzed to determine elemental constituents.

As a minimum, the filtered and non-filtered grab sample species shall be analyzed for the chemical species containing the following elements:

- Zinc
- Aluminum
- Silicon
- Copper
- Iron
- Nickel
- Calcium
- Magnesium
- Lead
- Sodium
- Potassium
- Chlorine

As stated in Section 2, an objective of the tests described in this test plan is to determine and characterize the chemical reaction products that may develop in a representative post-LOCA containment sump environment. The characterization of these corrosion products will be used as input parameters to the NUREG-6224 head loss correlation to determine the effect of corrosion products on resulting head loss across a fibrous debris bed that might form on the containment sump screen.

In addition to the chemical species identified above, particulate corrosion products shall be analyzed to determine;

- The total mass of particulates from the grab sample on the filter surface
- X-ray diffraction analysis to identify the major compounds
- Density or specific gravity of each type of particulate, if possible
- Particle size distribution of particulates, e.g.
  - 1-10 microns
  - 11-25 microns
  - 26-50 microns
  - 51-75 microns
  - 76-100 microns
  - > 101 microns
- Evaluate the specific surface area of the particulates of each corrosion product, if possible.

As a minimum, the side stream filter is to be viewed under an optical microscope with the objective of characterizing the material that may have collected on the filter.

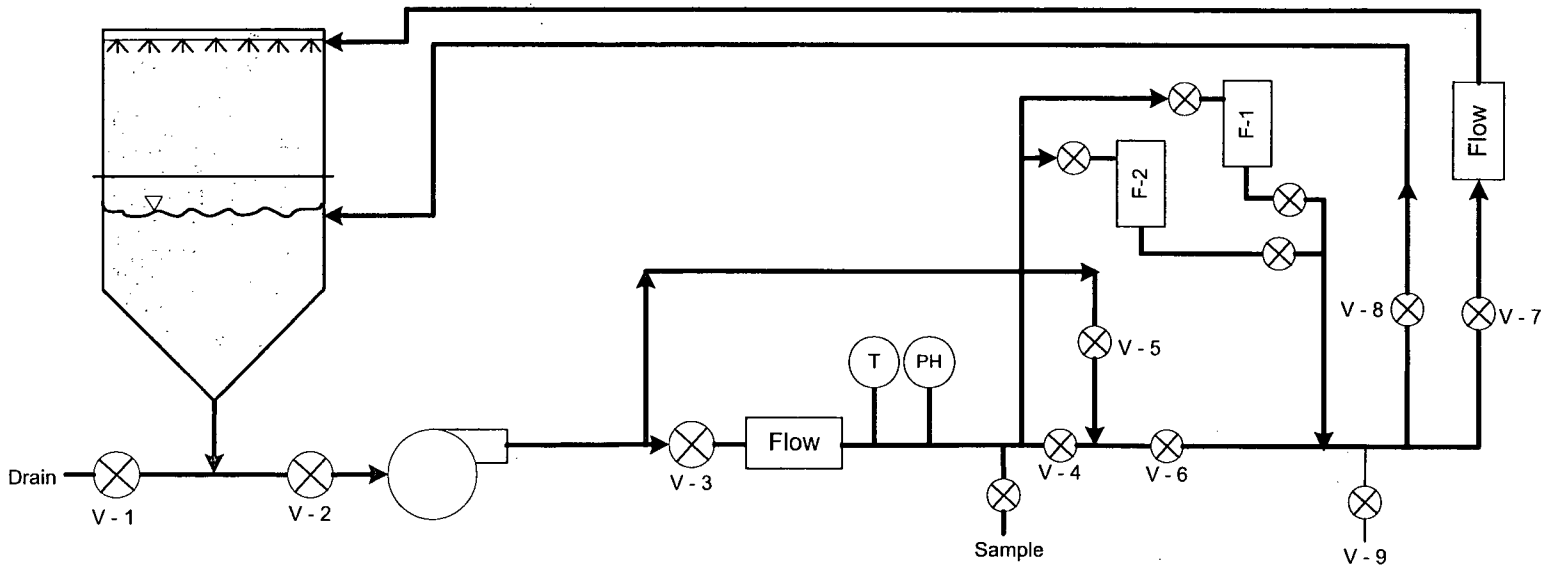

Figure 1 – Test Loop Process Flow Diagram

5 BASES FOR CONDITIONS INCLUDED IN THE GSI-191 POST-LOCA CORROSION TEST PLAN

5.1 Introduction

In order to develop the specific conditions, material types, and parameters to be included in a test program, and to assure that test results generated would be representative of all domestic PWRs, details of plant-specific conditions within containment (materials present, reactor coolant conditions, etc.) were necessary. To establish a representative set of detailed information, several sources of input were pursued. Westinghouse reviewed internally prepared plant-specific documents, such as Post-LOCA Hydrogen Generation Evaluations, other available plant documents (UFSARs) and issued survey questions to plant personnel. The plant survey responses formed the primary source of data for determining the parameters used to define the test conditions. The bases for selection of the parameters are discussed in this section.

5.2 Material Surface Areas

The primary concern for long-term corrosion in a post-LOCA environment is material that is submerged in reactor coolant water following containment flooding. Containment spray is actuated early during a design basis LOCA, but is terminated relatively early in the event (typically within 4 hours). Although some condensation may remain on equipment and material above the containment flood level, the amount of corrosion products contributed by this material is expected to be very small compared to the corrosion products generated by submerged materials. Therefore, the test parameters are primarily driven by the amount of material below the containment flood level at the point of switchover from injection to recirculation.

Representative values from the industry survey responses for material surface areas, with corresponding minimum post-LOCA sump volume of recirculation water, have been collected and are the basis for the material surface to sump water volume ratios identified in Table 1. Data that was collected from industry surveys and used to determine these values are shown later in Table 7. The surface area of each material type to be used in each test run will be the product of this ratio times the liquid volume in the tank of the test facility. The liquid volume of the test facility is 0.946 cubic meters (250 gallons). Although not expected at this time, if further refinement of the surface area to sump water volume ratio is warranted, based on additional information being made available prior to the start of testing, revised values should be substituted for those currently specified in Table 1.

Previous studies addressing post-LOCA corrosion (References 10 and 11) showed that aluminum and zinc, primarily in the form of galvanized carbon steel or as non-topcoated inorganic zinc based primer, will be the most corrosion susceptible materials in post-accident environment. Other less corrosion susceptible materials were also considered for this Test Plan. This was done because they were, in some cases, present in appreciable quantities (copper and copper based alloys), are known to be oxidants that can effect corrosion rates of other materials (copper ions), and may be sources of materials that may decrease the solubility of normally more soluble species when they are present (silica for fiberglass, calcium silicate and concrete). Table 7 contains the industry survey responses of exposed surface areas for a variety of materials within containment that would be susceptible to corrosion and/or chemical reaction when exposed to the post-LOCA chemical environment.

The goal in utilizing the collected data was to determine a representative area of individual material surfaces to be tested. These surface areas will then be exposed to a representative post-LOCA sump chemistry environment. This should result in a realistic quantity of dissolved and precipitated species in the simulated sump solution. These test results should be applicable to all PWRs.

For each material, Westinghouse attempted to determine a realistic upper bound estimate of the surface area to sump water volume ratio.

As discussed in Section 4.4.2, test coupons shall be prepared using the recommended practices outlined in ASTM G1. Exceptions or deviations to that guidance shall be documented and justified by the test performer.

5.2.1 Zinc

Zinc is present inside PWR containments in the form of both galvanized steel and zinc-based protective coatings. The following sections discuss the bases for the treatment of each of the two forms. The total area of zinc used in the test will be distributed among multiple coupons.

The surface area of zinc coupons to be used in each test run should be the product of the ratio of the surface area to liquid volume identified in Table 1, "Material Quantity/Sump Water Volume Rations Planned to be Tested," times the test facility liquid volume. It is recommended that the coupons be 0.0625 inches thick[8]. This coupon thickness for zinc should be followed for all tests performed using this test plan.

[8] Coupon thickness is to be 0.0625 (1/16) inches, except for those coupons to be coated with Inorganic Zinc (IOZ) primer, which are to be 0.0938 (3/32) inches thick.

5.2.1.1 Zinc in Galvanized Steel

Galvanized steel is present in the form of both electroplated and hot dipped.

A Westinghouse program to address Alloy 600 concerns calls for the addition of zinc acetate to the RCS. A preliminary assessment of the amount of zinc added under this program has determined that the amount of zinc added to the RCS inventory is small and is expected to have no impact on post-accident sump performance (Reference 10).

Zinc may be present in scaffolding stored in containment. However, since the scaffolding may be moved to an unsubmerged part of containment, or removed completely, the amount that may be present in scaffolding has not been accounted for in the surface to volume ratio used in the test.

5.2.1.2 Zinc Coatings

Generally, zinc coating has been topcoated with a DBA Qualified or "acceptable" epoxy, or a modified phenolic-epoxy topcoat. The industry survey returned very limited untopcoated zinc coatings in areas that could become submerged during a LOCA. However, untopcoated zinc will be included in the test to address concerns related to zinc primer exposed to post-accident conditions for those plants that reported having such coating systems inside containment.

The total surface area of zinc coatings inside containment available for reaction with the simulated sump solution does not reflect the surface area that is top coated with a qualified epoxy or modified phenolic epoxy based finish coat. These qualified topcoats protect the zinc primer from contact with reactive solutions and will reduce the surface area available for reaction with the simulated sump solution. Recently, however, NRC was made aware of the failure of coatings that were previously reported to be qualified. Therefore, a small amount of untopcoated zinc primer will be included in the test to account for the failure of coatings otherwise considered to be qualified.

5.2.2 Aluminum

Aluminum has been identified as the main contributor to hydrogen generation. Hence, the allowed quantity inside containment has typically been restricted (Reference 5) and tracked.

Aluminum may be present in scaffolding stored in containment. However, since the scaffolding may be moved to an unsubmerged part of containment, or removed completely, the amount that may be present in scaffolding has not been accounted for in the surface to volume ratio used in the test.

The surface area of aluminum coupons to be used in each test run should be the product of the ratio of the surface area to liquid volume identified in Table 1, "Material Quantity/Sump Water Volume Rations Planned to be Tested," times the test facility liquid volume. It is recommended that the coupons be 0.0625 inches thick. This coupon thickness for aluminum should be followed for all tests performed using this test plan.

5.2.3 Copper and Copper Alloys

The major sources of copper inside containment are the containment fan coolers and CRDM coolers. Other potential, albeit smaller, sources are instrument air lines. The surface area of the latter is insignificant compared to the former. In some plants, such as ice condenser plants, the fan coolers are isolated during a LOCA; therefore, they are not considered to be a potential contributor of corrosion products for the post-LOCA sump solution. At other plants, the coolers may be partially submerged following an event.

In early testing (Reference 9), it was demonstrated that copper and its alloys corroded at low rates in a simulated post-LOCA environment. This testing also pointed out that alloying of copper with nickel further significantly lowered measured corrosion rates. Therefore, the Test Plan will conservatively test only Copper. Values for Copper-Nickel alloys were collected, and are combined with the values for Copper in Table 7 for the purpose of determining the surface to volume ratio for the test.

The surface area of copper coupons to be used in each test run will be the product of this ratio times the liquid volume in the tank of the test facility. ASTM G31 typically calls for coupons that are either 0.125 inch or 0.25 inch thick. However, 0.0625 inch (1/16 inch) thick coupons should be used for all tests performed using this test plan.

5.2.4 Carbon Steel

The value for carbon steel surface areas (both submerged and non-submerged in a postulated post-LOCA sequence) given in the test plan are representative of the US PWR fleet and are appropriate for use in chemical effects testing for the following reasons:

- Generally, carbon steel components and structures inside containment are either:
  - Protected by qualified coatings for protection (structural steel),
  - Located in portions of the containment that do not actively participate in the flow path for recirculating liquid from the sump (reactor vessel), or,
  - Encased in insulation not affected by the postulated pipe break (reactor vessel, components removed from and / or protected by cubicles and barriers).

- For B&W and CE design primary systems, primary system piping is constructed of inconel-clad carbon steel piping, encased in insulation. (Westinghouse design NSSS plants are constructed of stainless steel primary piping.) Also, steam generators are constructed of a carbon steel outer shell. For a postulated break, the insulation on primary system piping of B&W and CE NSSS designs, and on steam generators of all NSSS designs, would be removed within the Zone of Influence (ZOI), exposing the carbon steel outer surface. Depending upon the containment design, these surfaces may be exposed to containment spray during the active spray period (some containment designs will limit exposure of the carbon steel surface of these components).

  Primary system piping and steam generators are not submerged post accident (they are above the post-accident flood-up level.) Therefore, these components are not subject to corrosion due to submergence in the containment pool. The duration of the exposure of the carbon steel piping to post-LOCA fluids is limited to the containment spray period. As noted above, some containment designs limit the direct exposure of primary system piping and steam generator shell surfaces to containment spray (for example, containments that are compartmentalized). The time duration of containment spray is short by comparison to the overall duration of the test (several hours versus several days), and both the corrosion rates and total corrosion are small (see the test plan for predicted containment steam space (non-submerged) temperature histories - time at temperatures above 200° F is relatively short). Moreover, examination of representative surfaces of components such as steam generators during in-service inspections indicates that there is practically no residual corrosion film on these components.

Therefore, carbon steel corrosion products are evaluated to not be a major contributor to the corrosion product mix in the post-accident sump of a PWR. This conclusion is supported by and consistent with the experimental results reported by Griess and Bacarella (Reference 9).

While being evaluated as a small contributor, the test plan does call for the inclusion of some bare, uncoated carbon steel surfaces. The surface area called for in the test plan ($0.15 ft^2/ft^3$, 34%

submerged) is based on actual plant input obtained from a survey conducted of the PWR plants. Based on the discussion above, this value has been evaluated as an appropriate amount of carbon steel for use in the chemical effects test.

5.2.5 Concrete

A protective coating (paint) is generally applied to most concrete surfaces in containment. This protective coating is generally qualified for Design Basis Accidents (DBA's). A very small portion of concrete inside containment is expected to be untopcoated.

However, it is recognized that concrete will be eroded from the surfaces impacted by the jet around the initiating break location. For the purpose of the test, an assumed corrodible surface area will be defined as follows:

It will be assumed that a jet pressure of 10 psi is needed to erode concrete surfaces. A break diameter of 32 inches is assumed. Using the ANSI58.2-1988 jet expansion model, at the 10 psi isobar of the jet, the volume of the jet is calculated to be about 133,800 ft^3. The radius of a sphere having the equivalent volume as the jet at the 10 psi isobar is calculated to be about 9.7 meters (31.7 feet). The surface area of this equivalent sphere is then calculated to be about 1174 m^2 (12,630 ft^2). This approach provides for a realistically conservative approach to calculating the concrete surface area exposed due to the action of a jet from a postulated pipe break. As noted in Attachment A to the PWR Containment Sump Baseline Evaluation Method, protective coatings are observed to withstand pressures in excess of 1000 psi. If the coatings remain intact, the concrete beneath the coatings also remain intact. The approach taken in this test plan is to use a 10 psi isobar to determine a spherical ZOI. Then, the full surface area of the 10 psi isobar ZOI is taken to be the maximum area of the concrete surface that is exposed due to the action of the jet.

The actual area of concrete that comes into contact with the expanding jet depends on the configuration of the containment and the break location. The value of 1174 m^2 (12,630 ft^2) is taken as a maximum surface area of concrete that will be exposed to erosion and will be used to set the concrete surface area to water volume ratio for the test.

In addition to the exposed concrete surface area resulting from the break, there may be initial quantity of concrete dust particulates in containment. The volume of this source of material will be accounted for as an initial mass of 22.7 kg (50 lbm) of concrete dust. This mass is based on an evaluation of current containment conditions. This ratio will apply to all plant types.

5.2.6 Insulation Material

Debris is generated within the Zone of Influence (ZOI) by the fluid escaping from the postulated break. Typical insulation materials include reflective metallic insulation (RMI), fiberglass and calcium silicate. In addition to deposition of the debris on the screen of a containment sump, this debris may be a potential source for nucleation of precipitants. Fiberglass and calcium silicate insulation debris may react at high pH values and release silica. Therefore, the tests will provide for the study of the possible interaction of insulation debris with the recirculation solution by chemical reaction.

The amount of fiberglass or calcium silicate inside containment depends on the specific plant design. Some plants use primarily reflective metallic insulation in the area that might be affected by a postulated large break in the primary piping. These plants have effectively no fiberglass or calcium silicate debris.

The largest component that may have fiberglass or calcium silicate insulation in the area that might be affected by a postulated large break is the steam generator. Based on the dimensions of a steam generator and accounting for a conservatively large ZOI volume, a preliminary calculation of the volume of fiberglass or calcium silicate insulation to be used to set the fiberglass to water ratio of this test has been estimated to be 141.6 m^3 (5,000 cubic feet). This number is representative for a PWR that uses fiberglass or calcium silicate insulation in general and will be used for the test.

The fiberglass or calcium silicate inside containment will be either blown onto the containment floor by the jet, or upward into upper containment.

- Large pieces of fiberglass or calcium silicate insulation blown into upper containment may not be transported back to lower containment due to curbs and gratings. This insulation will be subjected to containment spray flow, but will not undergo long-term submergence.
- All fiberglass or calcium silicate insulation that is blown onto the containment floor, and fiberglass or calcium silicate insulation that is washed onto the containment floor due to the action of containment spray, will be submerged in or floating on the liquid on the containment floor.

The test will provide for fiberglass or calcium silicate insulation that is both subjected to containment spray, and submerged long term.

As noted above, the same ratio approach may be applied to calcium silicate as was applied for fiberglass.

5.2.7 Protective Coatings

Epoxy-based protective coatings (paints) will not be included in the testing described in this test plan. In the event of an accident such as a LOCA, epoxy-based protective coatings on structures, systems and components in Pressurized Water Reactor (PWR) containments may be exposed to severe chemical environments. Recognizing this, the US nuclear industry issued ANSI N5.9-1967, later replaced by ANSI N5.12-1974, "Protective coatings (paints) for the nuclear industry," which is a screening methodology for candidate reactor containment coatings. Section 5 of ANSI N5.9/5.12, entitled "Chemical-Resistance Tests" provides, "...a common basis for methods and procedures for the evaluation of the resistance of coating systems to chemical environments." Candidate epoxy-based protective coating samples, for consideration for use in "severe" exposures such as reactor containment, are immersed for 5 days in 5% solutions of nitric acid, sulfuric acid, hydrazine, sodium hydroxide, ammonium hydroxide, and/or sodium borate as appropriate (see Subsection 5.3 of ANSI N5.12-1974). The samples are visually examined at 24 hour intervals during testing and again at 5 days, the completion of testing. Test samples are evaluated based on the following test standards or criteria:

- ASTM D772, "Standard Method of Evaluating Degree of Flaking (Scaling) of Exterior Paints" -
  Delamination - none permitted

- ASTM D714, "Standard Method of Evaluating Degree of Blistering of Paints" -
  Discoloration - will be permitted

- Other effects - noted for evaluation on an individual basis

Evaluation results are documented in writing (test reports). These test reports are retained and are available for the various coating manufacturers and plant licensees. Only epoxy-based protective coatings which have been screened in accordance with ANSI N5.9/N5.12 are subsequently DBA tested in accordance with ANSI N101.2, "Protective Coatings (Paints) for Light Water Nuclear Reactor Containment Facilities" for potential designation as "DBA qualified."

Epoxy coatings have been testes for leachable materials. These tests have shown that the amount of leachable material, primarily chlorides and fluorides, resulting in concentrations in the order of parts per million or less.

For plants to be licensed in the future, the chemical effects testing provisions of ANSI N5.9/N5.12 have been replaced by ASTM D 3912, "Test Method for Chemical Resistance of Coatings Used in Light-Water Nuclear Power Plants." ASTM D 3912 is identical in function and requirements to the chemical effects testing provisions of ANSI N5.9/N5.12. As with epoxy-based protective coatings DBA qualified for earlier plants, only coatings which have been screened in accordance with ASTM D 3912 are subsequently DBA tested in accordance with ASTM D 3911, "Test Method for Evaluating Coatings Used in Light-Water Nuclear Power Plants at Simulated Design Basis Accident (DBA) Conditions" for potential designation as "DBA qualified."

It is also noted that epoxy-based protective coatings are used in highly basic and highly caustic environmental commercial applications where leaching of protective coating material is undesirable. Examples of specific applications include direct contact with food, potable and non-potable water, sanitation applications and BWR torus coatings. Epoxy coatings have been tested by coatings manufacturers for leachable materials. These tests have demonstrated that the amount of leachable material in epoxy coatings, primarily chlorides and fluorides, is small and results in leached concentrations in the order of parts per million or less[9] of the applied coating. Therefore, epoxy-based coatings are not considered as a source of leachable materials and are not included in this test program.

The above discussion pertains to DBA qualified coatings. The Electric Power Research Institute (EPRI) is performing testing on representative unqualified coatings used in nuclear power plants to determine if these coatings fail. The information from those tests will be combined with information from this test. Therefore, inclusion of coatings in the current test program is either not warranted for qualified or DBA qualified coatings, or is redundant for unqualified coatings.

5.2.8 Other Materials

Other materials have been identified and evaluated for contribution to corrosion products in a post-LOCA environment inside containment.

[9] Testing for leachable materials is performed using ASTM Standard D1179, ASTM Standard F1277 and ANSI NSF-61. A typical upper limit of leachable materials from epoxy-based coatings is 200 ppm of the applied coating.

- Nickel is bound inside non-corrodible stainless steel. Nickel is also a constituent of crud that forms on fuel. Based on plant measurements, the average nickel release for a Westinghouse 4-loop PWR is 3500 grams, or 7.7 pounds, which equates to a concentration of about 0.16 ppm in the sump fluid inventory. This concentration is judged to be sufficiently small that it may be ignored for this test.
- Calcium, magnesium and silicon will be present from concrete and insulation material dissolution. Their levels will not be controlled directly, but will be allowed to evolve as dictated by the variables that effect concrete dissolution such as temperature and pH.
- Likewise, a variety of corrosion products may be added to solution from the corroding aluminum and zinc coatings and the corrosion of underlying exposed steel. These concentrations will be measured but will be controlled only by chemical and physical conditions that effect corrosion.

5.3 Material Surface Submerged and Exposed to Spray

Table 3 contains estimates of the percentages of each material that would be submerged and exposed to spray at maximum post-accident sump volume. In each case, material not submerged was assumed to be exposed to spray. The values in the Test Plan were established based on observations and experienced judgments of knowledgeable senior members of the Westinghouse engineering staff, as well as from responses to the industry survey.

As with the surface area to sump water volume ratio values, additional verification will be requested of the responding utility personnel that were outside the Test Plan value. The percent submerged value for these materials may be further refined prior to the start of testing.

For concrete and fiberglass the percent submerged values were based on the Zone of Influence calculation described in the Test Plan.

5.4 Test Temperature

Figures 2 through 7 are calculated post-LOCA temperature profiles for various PWR containment types.

These temperature profiles are based on LOCA Containment Integrity analyses performed to demonstrate that the containment heat removal systems are adequate. These analyses usually appear in FSAR Chapter 6.2 and are based on the Westinghouse LOCA M&E model described in WCAP-10325-P-A. Since these analyses assume the operation of a single train of

Containment Spray and Emergency Core Cooling Systems, these assumptions provide for the calculation of a conservatively high containment pressure, containment atmospheric temperature, and sump water temperature. Therefore, use of the attached curves, developed for the most limiting break, Double Ended Pump Suction break assuming a loss of offsite power and failure of the Diesel Generator to start, will provide a conservatively high estimate of the sump water temperature post-LOCA.

A comparison of Figures 2 through 7 shows that these calculated temperature profiles vary considerably with containment design. However, they all show the same initial temperature elevation early in the accident, followed by a gradual downward trend in temperature with time. From the figures, it is noted that some plants, like those with the ice condenser design, drop below 60° C (140° F) very rapidly. Others, such as the 4-loop designs, drop to 62° C (150° F) in approximately 4 days, reach 60° C (140° F) in less than 9 days, and continue to decrease thereafter. Still others like the small three loop designs seem to remain at elevated temperature much longer.

There are general "rules of thumb" that state that for every 10° C increase in reaction temperature the rate of reaction will double. From solubility considerations, it is known that while the solubility of aluminum oxides increase with increasing temperature the reverse is true for zinc oxides. So, it is evident that selecting a temperature for the testing will have a significant impact on test results.

A constant temperature of 60° C (140° F) was selected for the test. The rationale for the specific value is that the temperature profiles shown in Figures 2 through 7 are conservatively large values, as described above. Realistic analysis assumptions will provide for the calculation of lower values earlier in the transient for both the 3-loop and 4-loop plants. The use of a single representative, but conservative, value simplifies test operation. Thus, considering these factors and the effects of temperature on chemical reaction rates, a constant temperature of 60° C (140° F) is chosen to be representative of long term sump flood conditions across the fleet of PWRs, including ice condenser plants, for the purposes of this test.

5.5 pH

The following sections identify the pH requirements for the containment spray simulation and the sump pool simulation of this test.

5.5.1 Spray Fluid pH

The pH of containment spray for plants using TSP as a buffering agent is the pH of the RWST tank and has been calculated to vary from about 7 to about 8.5. For preconditioning test coupons and fiberglass samples, a pH of 7 is selected to represent plants using TSP as a buffering agent because at the lower pH, the potential for forming precipitants is greater than with a pH of 8.5. Thus, using a lower pH will increase the probability of the formation of precipitants.

The pH of containment spray for plants using NaOH as a buffering agent is calculated to be about 12 during the NaOH injection phase. Therefore, to simulate conditions for plants using NaOH, the initial 30 minutes of containment spray simulation will have a maximum pH of 12. See Section 4.1.3.1, "pH," and Note (2) to Table 5, "Test Run Conditions," for additional discussion on the pH of the NaOH spray simulation.

Containment spray will include the Sodium Tetraborate buffering agent mixed into the test loop inventory at the start of test. No attempt is made in the test to simulate the ice melting process of an ice condenser containment, which would require the gradual introduction of Sodium Tetraborate into the recirculating fluid. Not performing this gradual introduction results in the non-submersed coupons being subjected to a spray solution having a pH associated with the complete dissolution of the buffering agent in the recirculating flow at the start of test.

5.5.2 Sump Fluid pH

The initial pH of containment sump water for plants using TSP as a buffering agent has been calculated to vary from about 7 to about 8.5. A pH of 7 was selected to represent plants using TSP as a buffering agent because at the lower pH, the potential for forming precipitants is greater than with a pH of 8.5. Thus, using a lower pH will increase the probability of the formation of precipitants.

An initial pH of containment sump water for plants using NaOH as a buffering agent has been calculated to vary from about 8 to 11. A pH for 10 was selected to represent plants using NaOH as a buffering agent.

The pH of for the Sodium Tetraborate test will be determined from achieving a Boron concentration of 2400 ppm from mixing a Boric Acid solution having a Boron concentration of 2800 ppm with a Sodium Tetraborate solution having a Boron concentration of 2100 ppm. This Boron concentration is representative of the containment pool inventory at the time of the ice bed melt and will yield a pH representative of ice condensers at that time in the postulated LOCA event.

6 REFERENCES

1. R.Burchell and D.Whyte, WCAP-8776 "Corrosion Study for Determining Hydrogen Generation from Al and Zn During Post Accident Conditions" (1976)
2. J.Piippo et al., "STUK-YTO-TR 123 Corrosion behaviour of zinc and aluminum in simulated nuclear accident environments", Finnish Center for Radiation and Nuclear Safety, February 1997.
3. Westinghouse CN-CDME-03-13, "Impact of Zinc Addition on Containment Sump Performance Under Post-LOCA Conditions", (2003)
4. Westinghouse Standard Information Package 5-1 Chemistry Criteria and Specifications, Part II, Sections 1 and 3, March 1977.
5. H.Hermansson, S.Erixon SKI Report 98:12: "Chemical Environment for Strainers at LOCA Conditions in a PWR", February 1997.
6. P.Gauthier Westinghouse WB-CN-ENG-03-06: "Almaraz 1&2 Maximum pH in the Containment Sump", January 2003.
7. NUREG/CR-2812 "The relative importance of temperature, pH and boric acid concentration on rates of H2 production from galvanized steel corrosion", January 1984.
8. NUREG/CR-3803 "The effects of post-LOCA conditions on a protective coating (paint) for the nuclear power industry", March 1985.
9. J. Griess and A. Bacarella, "Design Considerations of Reactor Containment Spray Systems – Part III. The Corrosion of Materials in Spray Solutions.", ORNL-TM-2412 Part III, December 1969.
10. WCAP-8776, "Corrosion Study for Determining Hydrogen Generation from Aluminum and Zinc During Post Accident Conditions, R. C. Burchell and D. D. Whyte (1976).
11. ORNL-TM-2412, Part III, "Design Considerations of Reactor Containment Spray Systems – Part III. The Corrosion of Materials in Spray Solutions, J. C. Griess and A. L. Bacarella, December 1969.
12. V. Jain et al., CWNRA 2004-07, "Chemical Speciation, Using Thermodynamic Modeling, During a Representative Loss-of-Coolant Accident Event", Center for Nuclear Waste Regulatory Analyses, July 2004.

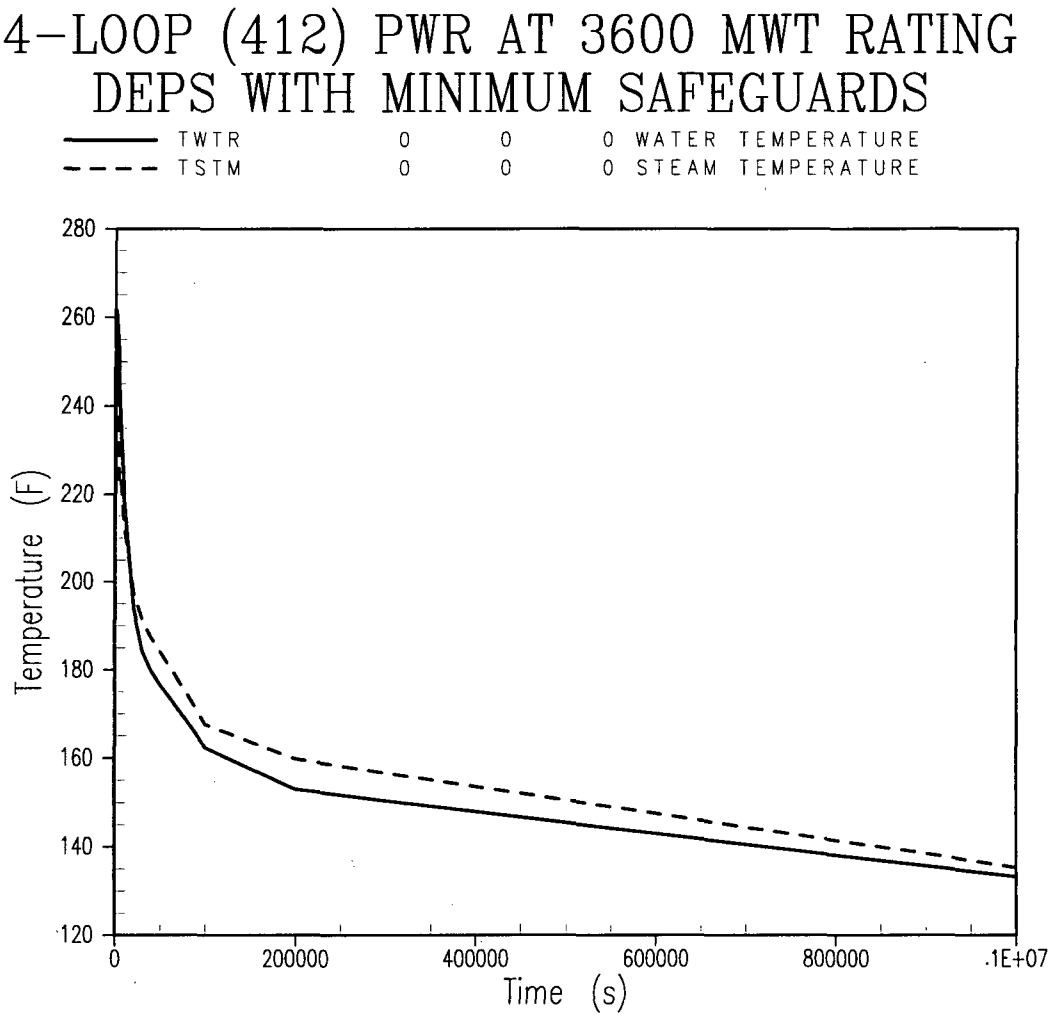

Figure 2: Four Loop Post-LOCA Temperature Profile (Linear Time Scale).

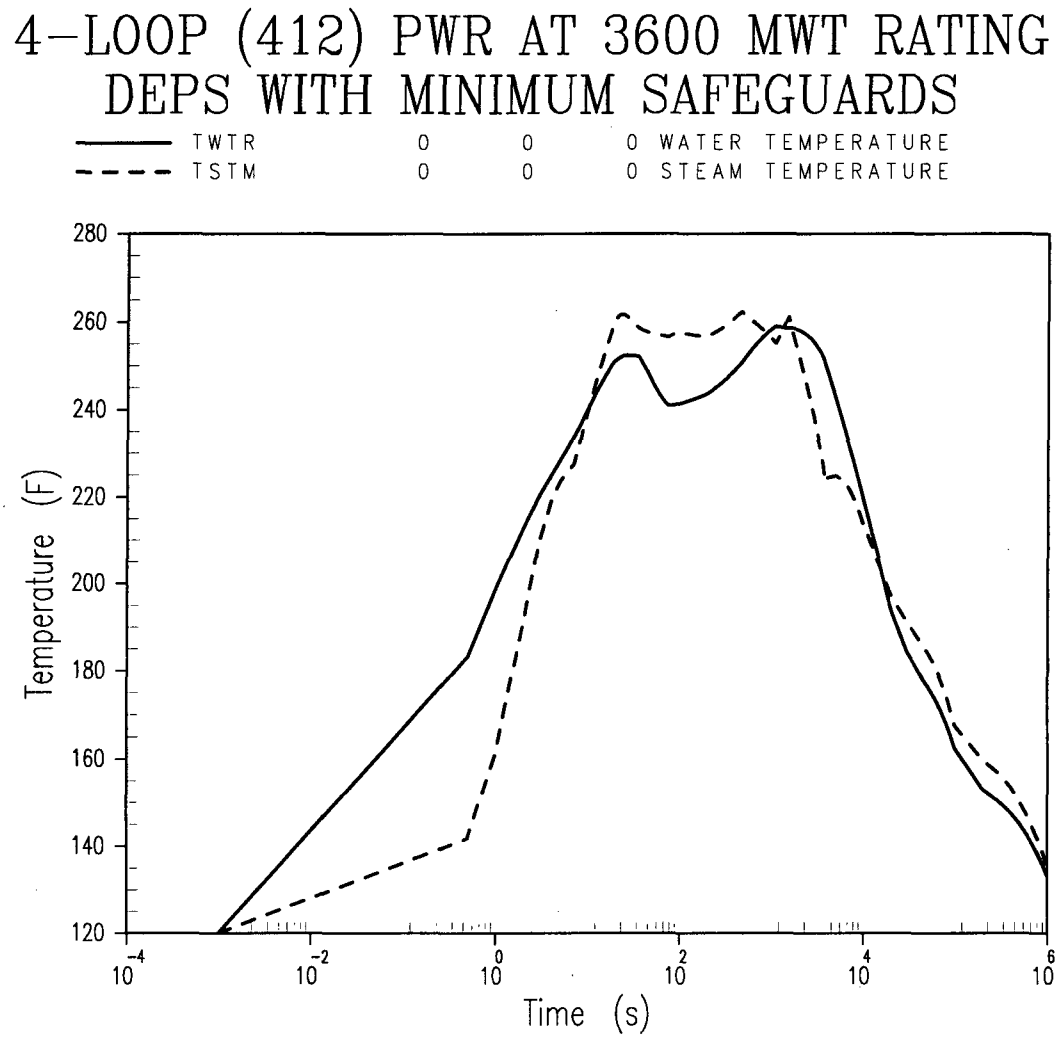

Figure 3: Four Loop Post-LOCA Temperature Profile (Logarithmic Time Scale).

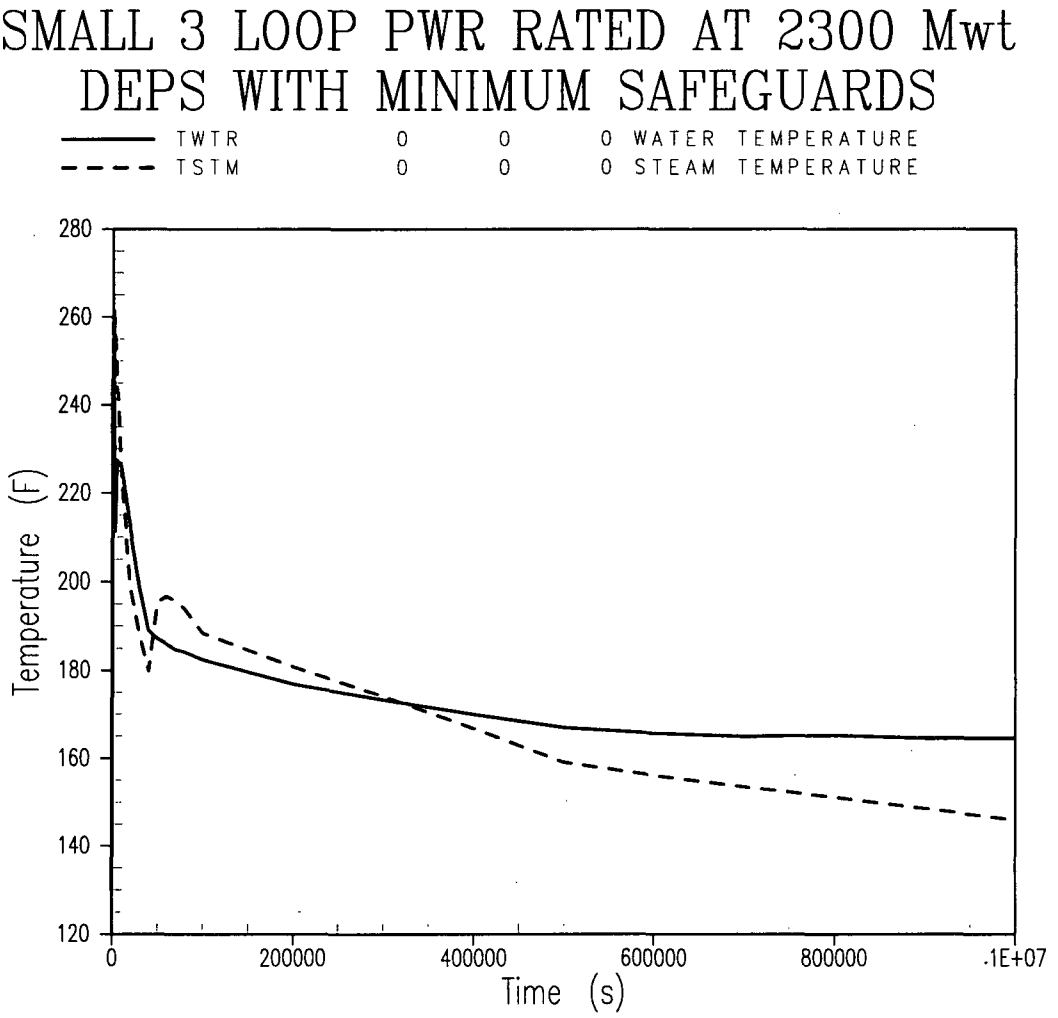

Figure 4: Three Loop Post-LOCA Temperature Profile (Linear Time Scale).

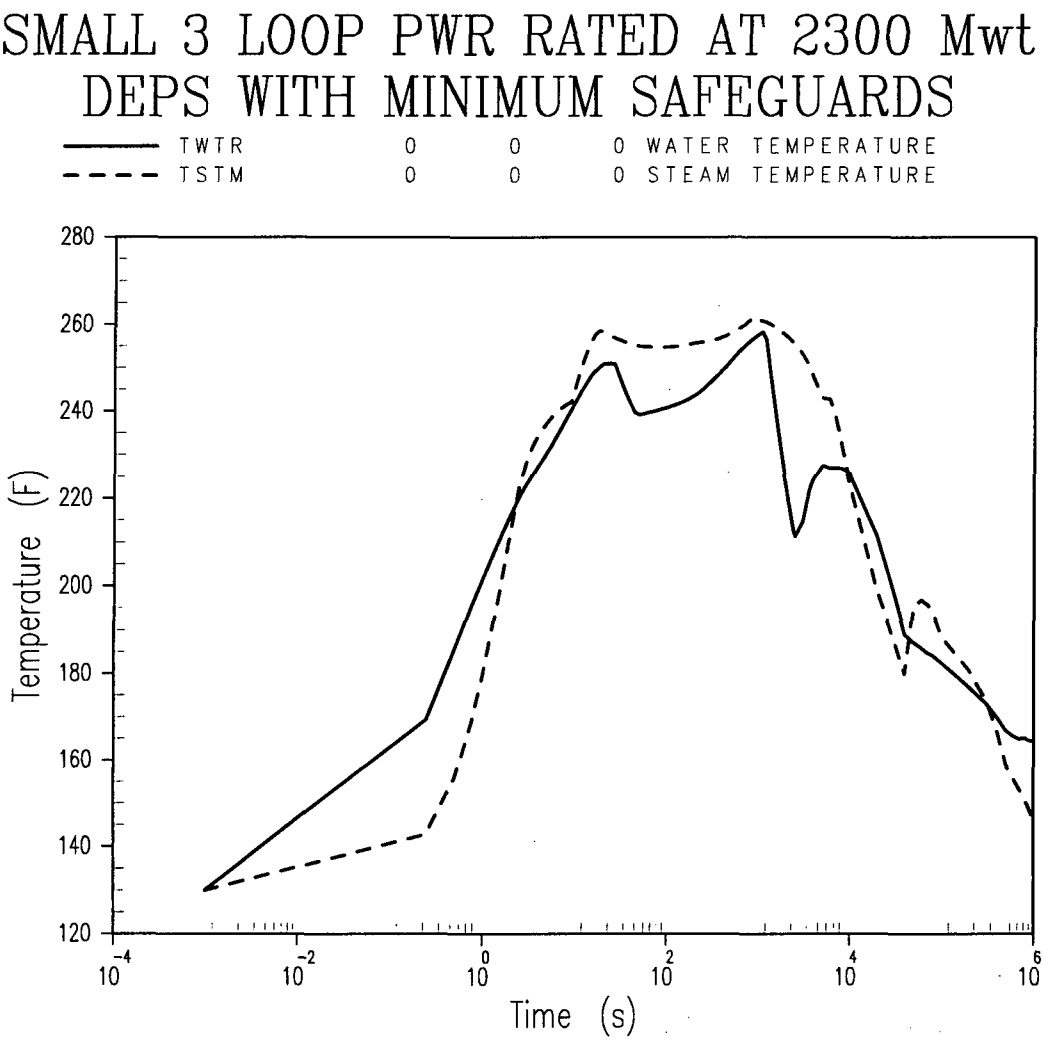

Figure 5: Three Loop Post-LOCA Temperature Profile (Logarithmic Time Scale).

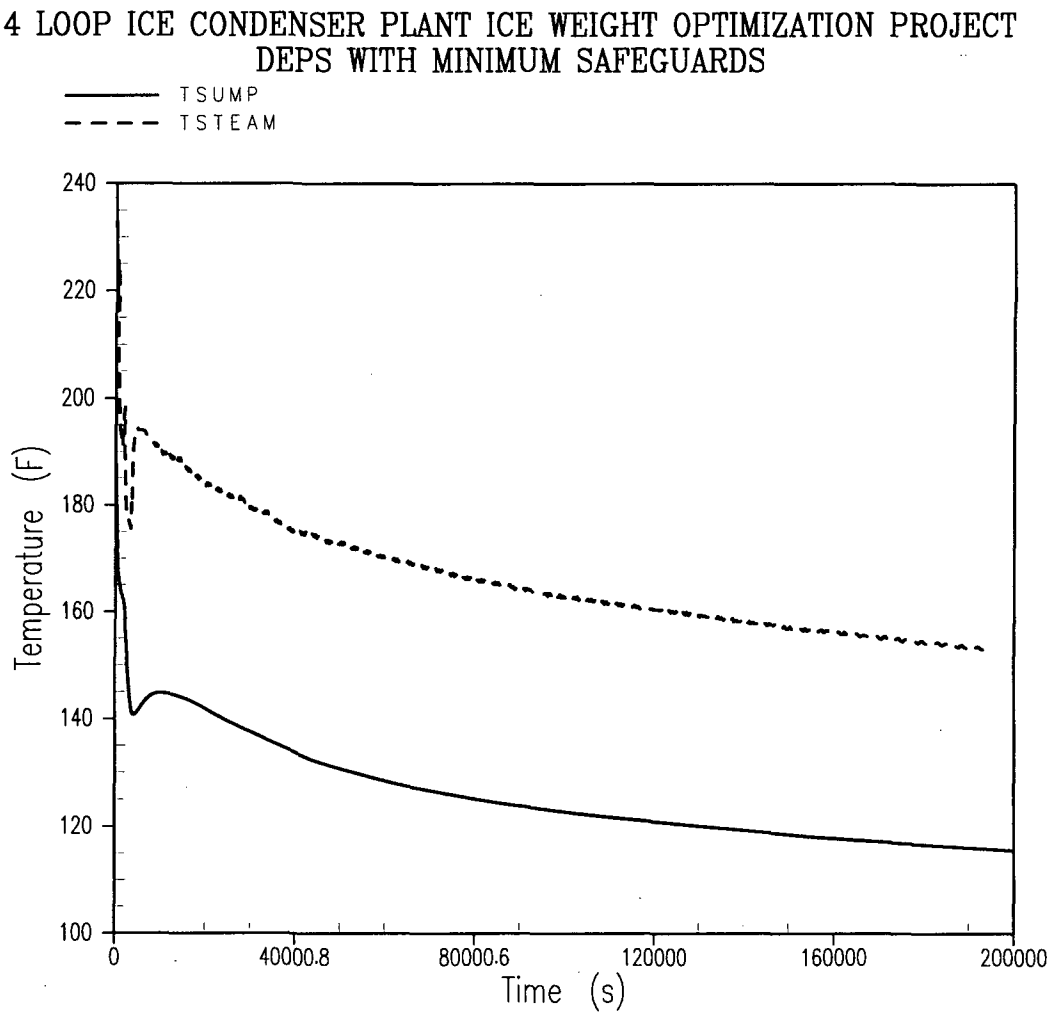

Figure 6: Four Loop Ice Condenser Plant Post-LOCA Temperature Profile (Linear Time Scale).

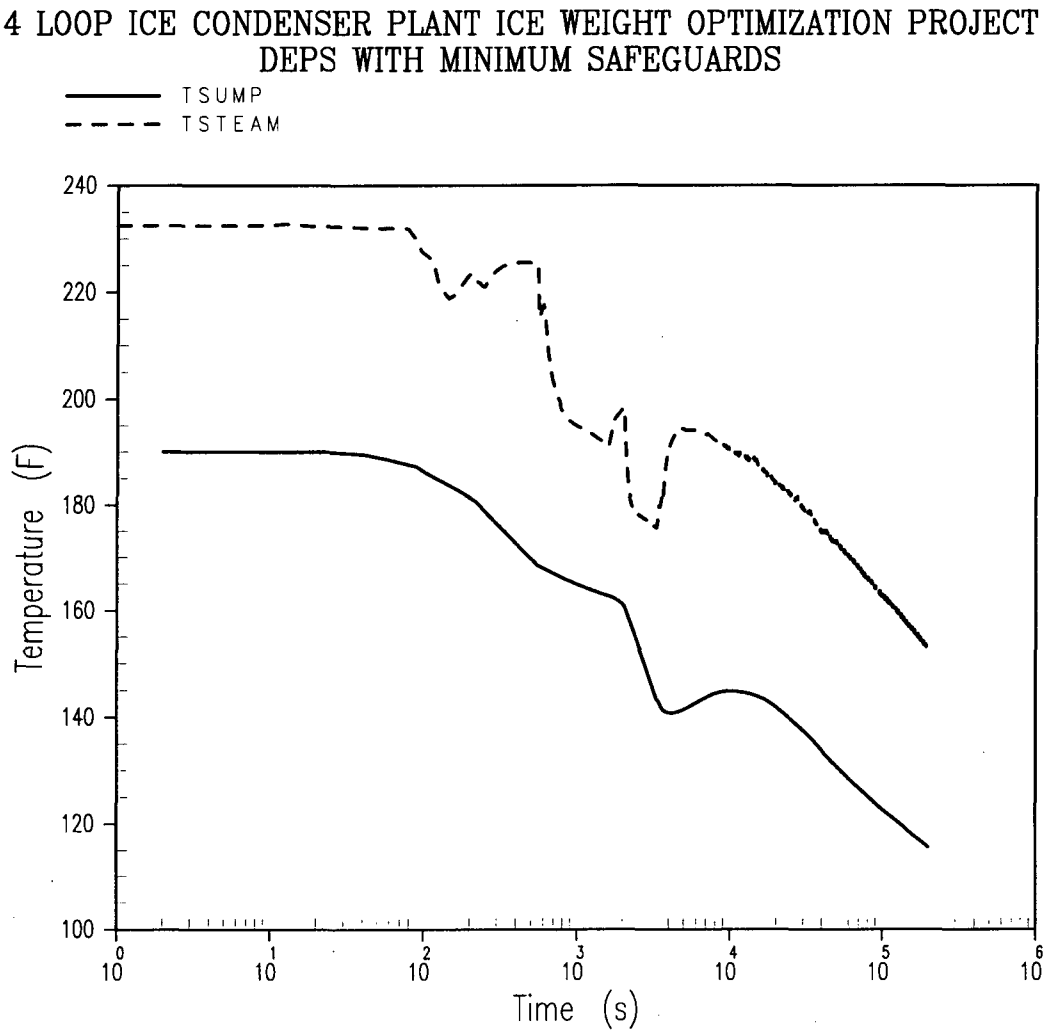

Figure 7: Four Loop Ice Condenser Plant Post-LOCA Temperature Profile (Logarithmic Time Scale).

Table 7: Industry Survey Response Data

Plant	Plant Type	Containment Type	Min Sump Vol (ft^2)	Total Mat'l (ft^2)	Submerged %	Submerged Mat'l	Mat'l Exposed to Spray	Ratio (Total)	Ratio (Submerged)	Ratio (Sprayed)
Galvanized Zn										
T	B&W	Dry	37,100.00	65,000.00	1	650.00	64,350.00	1.75	0.02	1.73
U	CE	Dry	55,000.00	105,979.00	1	1,059.79	104,919.21	1.93	0.02	1.91
J	3 Loop	Small Sub-Atm	68,809.00	128,845.00	N/A					
K	3 Loop	Small Sub-Atm	126,472.00	176,257.00	N/A					
Q	4 Loop	Large Dry	50,418.28	106,300.00	5	5,315.00	100,985.00	2.11	0.11	2.00
BB	B&W	Dry	36,682.00	8,000.00	1	80.00	7,920.00	0.22	0.00	0.22
N	2 Loop	Small Dry	41,073.00	63,596.00	5	3,179.80	60,416.20	1.55	0.08	1.47
JJ	4 Loop	Large Dry	159,740.00	325,215.00	3.5	11,382.53	313,832.48	2.04	0.07	1.96
S, KK, LL	B&W	Dry	52,600.00	43,970.00	N/A			0.84		
R	CE	Dry	40,758.00	74,540.00	5	3,727.00	70,813.00	1.83	0.09	1.74
O, P	2 Loop	Small Dry	44,200.00	60,000.00	10	6,000.00	54,000.00	1.36	0.14	1.22
RR	4 Loop	Large Dry	42,131.00	355,000.00	3	10,650.00	344,350.00	8.43	0.25	8.17
QQ	3 Loop		35,134.00	24,859.39	0	0	24,859.39	0.71	0.00	0.71
X	4 Loop	Large Dry	61,209.00	127,520.00	3	3,825.60	123,694.40	2.08	0.06	2.02
							Max Ratios	**8.43**	**0.25**	**8.17**
Topcoated Zn Coatings										
T	B&W	Dry	37,100.00	N/A						
U	CE	Dry	55,000.00	N/A						
J	3 Loop	Small Sub-Atm	68,809.00	85,099.00	N/A			1.24		
K	3 Loop	Small Sub-Atm	126,472.00	263,163.00	N/A			2.08		
Q	4 Loop	Large Dry	50,418.28	131,443.00	1	1,314.43	130,128.57	2.61	0.03	2.58
BB	B&W	Dry	36,682.00	N/A	N/A					
N	2 Loop	Small Dry	41,073.00	139,555.00	5	6,977.75	132,577.25	3.40	0.17	3.23
JJ	4 Loop	Large Dry	159,740.00	11,886.00	5	594.30	11,291.70	0.07	0.00	0.07

Plant	Plant Type	Containment Type	Min Sump Vol (ft^2)	Total Mat'l (ft^2)	Submerged %	Submerged Mat'l	Mat'l Exposed to Spray	Ratio (Total)	Ratio (Submerged)	Ratio (Sprayed)
S, KK, LL	B&W	Dry	52,600.00	374,500.00	N/A			7.12		
R	CE	Dry	40,758.00	129,797.00	15	19,469.55	110,327.45	3.18	0.48	2.71
O, P	2 Loop	Small Dry	44,200.00	146,900.00	5	7,345.00	139,555.00	3.32	0.17	3.16
RR	4 Loop	Large Dry	42,131.00	4,000.00	3	120.00	3,880.00	0.09	0.00	0.09
QQ	3 Loop		35,134.00	0	0					
X	4 Loop	Large Dry	61,209.00	289,200.00	1	2,892.00	286,308.00	4.72	0.05	4.68
							Max Ratios	**7.12**	**0.48**	**4.68**
Untopcoated Zn Coatings										
T	B&W	Dry	37,100.00		1					
U	CE	Dry	55,000.00		1					
J	3 Loop	Small Sub-Atm	68,809.00	N/A	N/A					
K	3 Loop	Small Sub-Atm	126,472.00	30,326.00	N/A			0.24		
Q	4 Loop	Large Dry	50,418.28	228,657.00	0.1	228.66	228,428.34	4.54	0.00	4.53
BB	B&W	Dry	36,682.00	100.00	10	10.00	90.00	0.00	0.00	0.00
N	2 Loop	Small Dry	41,073.00	7,345.00	5	367.25	6,977.75	0.18	0.01	0.17
JJ	4 Loop	Large Dry	159,740.00	N/A	N/A					
S, KK, LL	B&W	Dry	52,600.00	0	N/A					
R	CE	Dry	40,758.00	N/A	N/A					
O, P	2 Loop	Small Dry	44,200.00	N/A	N/A					
RR	4 Loop	Large Dry	42,131.00	N/A	N/A					
QQ	3 Loop		35,134.00	0	0					
X	4 Loop	Large Dry	61,209.00	76,500.00	0.05	38.25	76,461.75	1.25	0.00	1.25
							Max Ratios	**4.54**	**0.01**	**4.53**
Aluminum										
T	B&W	Dry	37,100.00	10,750.00	1	107.50	10,642.50	0.29	0.00	0.29
U	CE	Dry	55,000.00	1,206.00	1	12.06	1,193.94	0.02	0.00	0.02
J	3 Loop	Small Sub-Atm	68,809.00	1,559.00	N/A			0.02		
K	3 Loop	Small Sub-	126,472.00	1,559.00	N/A			0.01		

Plant	Plant Type	Containment Type	Min Sump Vol (ft^2)	Total Mat'l (ft^2)	Submerged %	Submerged Mat'l	Mat'l Exposed to Spray	Ratio (Total)	Ratio (Submerged)	Ratio (Sprayed)
Q	4 Loop	Atm Large Dry	50,418.28	2713.39 lbm	5					
BB	B&W	Dry	36,682.00	3,000.00	1	30.00	2,970.00	0.08	0.00	0.08
N	2 Loop	Small Dry	41,073.00	203.20	1	2.03	201.17	0.00	0.00	0.00
JJ	4 Loop	Large Dry	159,740.00	18,979.00	1	189.79	18,789.21	0.12	0.00	0.12
S, KK, LL	B&W	Dry	52,600.00	27,800.00	N/A			0.53		
R	CE	Dry	40,758.00	136,818.00	25	34,340.00	102,478.00	3.36	0.84	2.51
O, P	2 Loop	Small Dry	44,200.00	900.00	10	90.00	810.00	0.02	0.00	0.02
RR	4 Loop	Large Dry	42,131.00	1,800.00	3	54.00	1,746.00	0.04	0.00	0.04
QQ	3 Loop		35,134.00	670.00	0	0.00	670.00	0.02	0.00	0.02
X	4 Loop	Large Dry	61,209.00	854.00	5	42.70	811.30	0.01	0.00	0.01
							Max Ratios	**3.36**	**0.84**	**2.51**
Cu/Cu Alloys										
T	B&W	Dry	37,100.00	191,400.00	1	1,914.00	189,486.00	5.16	0.05	5.11
U	CE	Dry	55,000.00	191,400.00	1	1,914.00	189,486.00	3.48	0.03	3.45
J	3 Loop	Small Sub-Atm	68,809.00	4,754.00	N/A			0.07		
K	3 Loop	Small Sub-Atm	126,472.00	4,824.00	N/A			0.04		
Q	4 Loop	Large Dry	50,418.28	116,207.60	0	0	116,207.60	2.30	0.00	2.30
BB	B&W	Dry	36,682.00	0	N/A			0.00		
N	2 Loop	Small Dry	41,073.00	60,844.00	0	0	60,844.00	1.48	0.00	1.48
JJ	4 Loop	Large Dry	159,740.00	35,495.00	N/A		35,495.00	0.22		
S, KK, LL	B&W	Dry	52,600.00	102,728.00	0	0	102,728.00	1.95	0.00	1.95
R	CE	Dry	40,758.00	66,526.00	25	16631.5	49,894.50	1.63	0.41	1.22
O, P	2 Loop	Small Dry	44,200.00	80,000.00	0	0	80,000.00	1.81	0.00	1.81
RR	4 Loop	Large Dry	42,131.00	2,618.00	0	0	2,618.00	0.06	0.00	0.06
QQ	3 Loop		35,134.00	7,610.00	0	0	7,610.00	0.22	0.00	0.22
X	4 Loop	Large Dry	61,209.00	162,051.00	0	0	162,051.00	2.65	0.00	2.65
							Max Ratios	**5.16**	**0.41**	**5.11**

NRC FORM 335
(9-2004)
NRCMD 3.7

U.S. NUCLEAR REGULATORY COMMISSION

BIBLIOGRAPHIC DATA SHEET

(See instructions on the reverse)

1. REPORT NUMBER
(Assigned by NRC, Add Vol., Supp., Rev., and Addendum Numbers, if any.)

NUREG/CR-6914, Volume 1

2. TITLE AND SUBTITLE

Integrated Chemical Effects Test Project: Consolidated Data Report

3. DATE REPORT PUBLISHED

MONTH	YEAR
December	2006

4. FIN OR GRANT NUMBER

Y6999

5. AUTHOR(S)

J. Dallman, B. Letellier, J. Garcia, J. Madrid, W. Roesch; Los Alamos National Laboratory

D. Chen, K. Howe; University of New Mexico

L. Archuleta, F. Sciacca, Omicron Safety& Risk Technologies, Inc.

6. TYPE OF REPORT

Final

7. PERIOD COVERED *(Inclusive Dates)*

May 2004 - September 2006

8. PERFORMING ORGANIZATION - NAME AND ADDRESS *(If NRC, provide Division, Office or Region, U.S. Nuclear Regulatory Commission, and mailing address; if contractor, provide name and mailing address.)*

Los Alamos National Laboratory
PO Box 1663
Los Alamos, NM 87545

University of New Mexico
Department of Civil Engineering
Albuquerque, NM 87110

Omicron Safety & Risk Technologies, Inc.
2500 Louisiana Blvd. NE, Suite 410
Albuquerque, NM 87199-3065

9. SPONSORING ORGANIZATION - NAME AND ADDRESS *(If NRC, type "Same as above"; if contractor, provide NRC Division, Office or Region, U.S. Nuclear Regulatory Commission, and mailing address.)*

Division of Fuel, Engineering, & Radiological Research
Office of Nuclear Regulatory Research
U.S. Nucelar Regulatory Commission
Washington, DC 20555-0001

10. SUPPLEMENTARY NOTES

B. P. Jain, NRC Project Manager; prepared in cooperation with Electric Power Research Institute

11. ABSTRACT *(200 words or less)*

Five tests conducted in the Integrated Chemical Effects Test (ICET) project attempted to simulate the chemical environment present inside a pressurized-water-reactor containment water pool after a loss-of-coolant-accident. A representative chemical environment was established in the tests, including prototypical buffering agents. The tests were conducted for 30 days at a constant temperature of 60°C. The materials tested within this environment included representative amounts of submerged and unsubmerged metals and insulation. Test solution chemistry varied from test to test, depending on the starting conditions and amount of material corrosion or leaching. Either particulate, flocculent, or film (webbing) deposits were observed in the insulation after each test. Visible changes were also seen on the metal coupons in each test. Corrosion was evident on both submerged and unsubmerged coupons. Test #3 sediment contained a gel-like material found on top of the sediment. Precipitates were present in the test solution in Tests #1 and #5 when the solution was cooled to ambient temperature. Test solution from those two tests also exhibited non-Newtonian behavior when the solution was cooled to ambient temperature.

12. KEY WORDS/DESCRIPTORS *(List words or phrases that will assist researchers in locating the report.)*

Chemical effects, ICET, GSI-191, PWR, ECCS recirculation

13. AVAILABILITY STATEMENT

unlimited

14. SECURITY CLASSIFICATION

(This Page)
unclassified

(This Report)
unclassified

15. NUMBER OF PAGES

16. PRICE

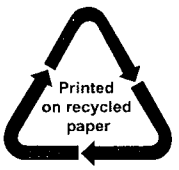

Federal Recycling Program